UNIVERSIDAD MICHOACANA DE SAN NICOLÁS DE HIDALGO

INSTITUTO DE INVESTIGACIONES QUÍMICO BIOLÓGICAS

PROGRAMA INSTITUCIONAL DE DOCTORADO EN CIENCIAS BIOLÓGICAS OPCIÓN: BIOLOGÍA EXPERIMENTAL

TESIS:

"Participación de las proteínas Grx5p, Isa2p e Iba57p, en el ensamble del centro [2Fe-2S] en la subunidad Rip1p y su impacto en la formación de los supercomplejos respiratorios en *Saccharomyces cerevisiae*"

PARA OBTENER EL GRADO DE DOCTOR EN CIENCIAS BIOLÓGICAS

M. en C. LUIS ALBERTO SÁNCHEZ BRIONES

TUTOR:

D. en C. JESÚS CAMPOS GARCÍA

MORELIA, MICHOACAN, MÉXICO, ABRIL, 2021

INSTITUTO DE INVESTIGACIONES QUÍMICO-BIOLÓGICAS

Participación de las proteínas Grx5p, Isa2p e Iba57p en el ensamble del centro [2Fe-2S] en la subunidad Rip1p y su impacto en la formación de los supercomplejos respiratorios en *Saccharomyces cerevisiae*

Dedicatoria

A mis padres Juana y José Luis:

Quienes me han brindado su apoyo en todo momento y que sin este, no habría logrado esta meta en mi vida profesional, gracias por sus palabras, consejos y total confianza, pero sobre todo gracias porque, a pesar de la distancia, nunca me siento solo. LOS AMO.

A mi hermana Emma:

Quien también me ha apoyado incondicionalmente, gracias por la convivencia, por tus locuras y por tu confianza. Espero que este trabajo te sirva de ejemplo para que sigas adelante, siempre podrás contar conmigo, también quiero que sepas que gran parte de mi inspiración es el motivarte a seguir adelante.

A Elizabeth:

Mi compañera que me alentó a seguir en este periodo de preparación, gracias por tus palabras, tu comprensión y por apoyarme personal y profesionalmente, gracias por convertirte en un ejemplo de persona, siempre tendrás mi cariño, amor y admiración.

A mi abuelo Pablo Q. E. P. D:

Siempre te llevare en mis pensamientos, donde quiera que te encuentres, sé que sigues creyendo en mí, gracias por todos los momentos inolvidables, tus historias, tus risas y todo tu cariño.

Agradecimientos

Al Dr. Jesús Campos García, por permitirme haber sido parte de su equipo de trabajo, por las enseñanzas, consejos y apoyo. Además de ámbito académico, siempre le estaré agradecido por el apoyo en momentos difíciles, por lo mismo considero que no solo se construyó un lazo profesional, también de amistad que espero nunca perder.

A mi comité sinodal la Dra. Rocío del Carmen Montoya Pérez, Dr. Mauro Manuel Martínez Pacheco, Dr. Christian Cortes Rojo y Dr. José Salud Rodríguez Zavala, gracias por sus comentarios y aportaciones que enriquecieron este trabajo.

A las técnicas del laboratorio: Alma por su amistad, sus recomendaciones y consejos para el desarrollo de experimentos importantes que se incluyen en este trabajo. A Lore por hacer tan ameno el ambiente del laboratorio con su repertorio de buena música y ocurrencias, por su amistad y por su apoyo en el trabajo experimental.

A mis amigos compañeros de posgrado, Omar por su compañerismo, amistad y todos los buenos ratos que compartimos. A Sharel por su cariño, sinceridad, su calidad como persona, y por todas las ocurrencias que compartimos. A Laura, por su cariño, confianza, su leal amistad y apoyo incondicional, además, debo reconocer que las alumnas superaron al maestro. Siempre contaran con un servidor, espero y deseo nunca perder el lazo de amistad que se construyó en este periodo de tiempo tan especial e inolvidable.

A mis amigos, Cuauhtémoc, Héctor, Maximiliano, Hugo, Alejandro, Iván, Carlos y Nereida, por los gratos y no tan gratos momentos, por alentarme a seguir superándome y principalmente por su valiosa y sincera amistad,

A la Universidad Michoacana de San Nicolás de Hidalgo, casa de toda mi formación académica.

Al Instituto de Investigaciones Químico Biológicas, lugar donde realicé mi servicio social de licenciatura, tesis de licenciatura, maestría y ahora doctorado.

A CONACyT por la beca otorgada.

Índice

Participación de las proteínas Grx5p, Isa2p e Iba57p en el ensamble del centro [2Fe-2S] en la subunidad Rip1p y su impacto en la formación de los supercomplejos respiratorios en *Saccharomyces cerevisiae*

Resumen

Los centros [Fe-S] son cofactores encontrados en proteínas que están involucradas en diversos procesos, la formación de estos grupos y su ensamble en las correspondientes proteínas son procesos conservados entre los organismos de todos los reinos. En eucariontes existen dos formas principales de centros [Fe-S]: el tipo rómbico [2Fe-2S] y el tipo cúbico [4Fe-4S]. La biogénesis de centros [Fe-S] mitocondrial, es un proceso que describe tres eventos principales, la síntesis de *novo* de centros [2Fe-2S] por el complejo ISU1, la traslocación de estos cofactores a proteínas blanco por el sistema de chaperona-cochaperona-glutarredoxina (Ssq1p-Jac1p-Grx5p) y la síntesis de centros [4Fe-4S] por el subsistema Fe-S-IBG (Isa1p, Isa2p, Iba57p y Grx5p). Sin embargo, a la fecha, no se ha descrito por completo esta vía de síntesis. En este trabajo se estudió en *Saccharomyces cerevisiae* el papel que juegan las proteínas Iba57p, Isa2p y Grx5p, miembros del subsistema Fe-S-IBG en el ensamble del centro [2Fe-2S] de la subunidad Rip1p del complejo III. Los resultados indicaron que las proteínas que constituyen el subsistema Fe-S-IBG en *S. cerevisiae,* además de participar en el ensamblaje de centros [4Fe-4S], también está involucrado en la maduración de la subunidad Rip1p-[2Fe-2S]. Se observó que en la ausencia de las proteínas Iba57p e Isa2p, el complejo III no presenta actividad por la ausencia de la subunidad catalítica Rip1p, adicionalmente se afecta la formación de los supercomplejos respiratorios (III-IV). Otro aspecto evaluado dependiente de la deficiencia de la proteína Rip1p fue el estrés oxidativo; encontrando que se desencadena la producción de especies reactivas de oxígeno de manera exacerbada, fenómeno observado de manera similar en mutantes en Iba57p e Isa2p. En conclusión, en *S. cerevisiae*, el subsistema Fe-S-IBG está implicado en la maduración de la proteína Rip1p, dicha subunidad es esencial para la formación y funcionalidad de los supercomplejos respiratorios III-IV.

Palabras clave: Mitocondria; Centros [Fe-S]; Glutarredoxina; Complejo III; Supercomplejos respiratorios.

Abstract

[Fe-S] clusters are cofactors found in proteins that are involved in various processes, the formation of these clusters and their assembly in their corresponding proteins are processes conserved among organisms of all kingdoms. In eukaryotes there are two main forms of [Fe-S] clusters: the rhombic type [2Fe-2S] and the cubic type [4Fe-4S]. The mitochondrial [Fe-S] cluster biogenesis pathway is a process that describes three main events, the de novo synthesis of [2Fe-2S] clusters by the ISU1 complex, the translocation of these cofactors to target proteins by the chaperone-cochaperone-glutarredoxin system (Ssq1p-Jac1p-Grx5p) and the synthesis of [4Fe-4S] clusters by the Fe-S-IBG subsystem (Isa1p, Isa2p, Iba57p and Grx5p). To date, this synthetic pathway has not been fully described. In this work, the role of Iba57p, Isa2p and Grx5p proteins, members of the Fe-S-IBG subsystem, in the assembly of the [2Fe-2S] cluster of the subunit Rip1p of the complex III was investigated. The results indicated that the Fe-S-IBG subsystem in S. cerevisiae, in addition to participate in the assembly of [4Fe-4S] centers, is also involved in the maturation of the Rip1p- [2Fe-2S] subunit. It was observed that in the absence of the Iba57p and Isa2p proteins, complex III does not present activity due to the absence of the catalytic subunit Rip1p, additionally affecting the formation of respiratory supercomplexes (III-IV). Another aspect dependent on Rip1p protein deficiency evaluated was oxidative stress; finding that the production of reactive oxygen species is exacerbated, a similarly phenomenon observed in mutants of Iba57p and Isa2p. In conclusion, in S. cerevisiae, the Fe-S-IBG subsystem is involved in maturation of Rip1p protein, a subunit essential for the formation and functionality of respiratory supercomplexes III-IV.

Keywords: Mitochondria; [Fe-S] clusters; glutarredoxin; complex III; respiratory supercomplexes.

1. Introducción

1.1 *Saccharomyces cerevisiae* como modelo biológico de estudio de la mitocondria.

Parte del conocimiento actual sobre las funciones celulares en eucariontes, provienen de estudios que han utilizado a *Saccharomyces cerevisiae* como modelo biológico, esta levadura es una excelente herramienta para estudiar aspectos fundamentales de la biología celular y molecular de eucariontes. Una de las principales características es su metabolismo aerobio facultativo, que le permite fermentar azúcares en presencia de oxígeno siempre y cuando la concentración de azucares en el medio sea por encima del 1%, a lo cual se le conoce como efecto Crabtree. Así, esta levadura puede sobrevivir incluso con mitocondrias disfuncionales (Pfeiffer y Morley, 2014).

Las mitocondrias son orgánulos que contienen dos membranas, una membrana interna y una membrana externa que rodean dos compartimentos, la matriz mitocondrial y el espacio intermembranal, respectivamente. La morfología de las mitocondrias se rige por los procesos de fisión y fusión, lo que permite adaptaciones metabólicas dependiendo de las condiciones del medio (Westermann, 2012). Las mitocondrias son conocidas como las fábricas de energía de las células debido a su papel en la síntesis de la mayor parte del ATP celular a través del ciclo de Krebs y la fosforilación oxidativa (Saraste, 1999). Sin embargo, las funciones mitocondriales se extienden a otros procesos metabólicos tales como el metabolismo de aminoácidos y lípidos (Galluzzi, 2012, Horvath y Daum, 2013), así como la síntesis de grupos hemo y de centros hierro-azufre (Lill, 2012). La mayoría de las funciones mitocondriales están conservadas entre las levaduras y organismos superiores, por lo que ha sido de utilidad para estudiar la biología y las enfermedades mitocondriales en humanos (Claypool, 2013). *S. cerevisiae* puede satisfacer sus requerimientos energéticos a través de la fermentación. Por lo tanto, puede tolerar mutaciones que afectan la fosforilación oxidativa, e incluso, soporta la pérdida completa de ADNmt, siempre que

haya fuentes de carbono fermentables; esto permite estudiar las mutaciones que causan disfunción mitocondrial, a diferencia de organismos superiores, que no soportan las deficiencias mitocondriales (Chen y Clark, 1999). Existe una amplia disponibilidad de herramientas para manipular los genomas nuclear y mitocondrial de *S. cerevisiae*, lo que permite modelar las mutaciones implicadas en los trastornos mitocondriales (Bonnefoy y Fox, 2007). Por otro lado, las poblaciones de levadura se vuelven homoplásmicas en pocas generaciones, lo que significa que todas las copias de ADNmt tendrán la misma secuencia de nucleótidos. Esto permite estudiar la gravedad y el impacto en la función mitocondrial de las mutaciones puntuales, que a menudo, son heteroplasmáticas en las mitocondrias humanas (Shibata y Ling, 2007). Por todo lo anterior, se utiliza a *S. cerevisiae* como modelo de estudio de mutaciones en el ADNmt, incluidos los genes que codifican para algunos de los componentes de los complejos de la cadena respiratoria (Meunier *et al*., 2013).

1.2 Cofactores [Fe-S] de las proteínas.

Los cofactores son moléculas de bajo peso molecular que se unen a motivos estructurales conservados que brindan propiedades específicas a las proteínas. Existen cofactores inorgánicos que incluyen varios iones metálicos como el Mg^{2+}, Zn^{2+}, Mn^{2+}, $Cu^{1+/2+}$, $Fe^{2+/3+}$ y los centros Hierro-Azufre [Fe-S] (Lill, 2009).

La disponibilidad de hierro y azufre, así como las condiciones climáticas en la tierra primitiva permitieron la síntesis y fusión de centros [Fe-S] con las proteínas, lo que les permitió adquirir nuevas funciones. Existen centros [Fe-S] de diferentes conformaciones, los comunes son el tipo rómbico [2Fe-2S], el tipo semicúbico [3Fe-4S], y el tipo cúbico [4Fe-4S], Sin embargo, también existen centros [Fe-S] como el de la enzima nitrogenasa, la cual cuenta con un centro [8Fe-7S] (Figura 1) (Py y Barras, 2010; Lill, 2009 y Fontecilla *et al.*, 2009). La principal función de los centros [Fe-S], es la transferencia de electrones, que se basa en la propensión del hierro a cambiar entre los estados de oxidación Fe^{+2} y Fe^{+3},

mientras que el azufre siempre se encuentra en el mismo estado de oxidación S^{2-}. Dentro de un entorno proteico dado, los centros [Fe-S] pueden adoptar potenciales redox de −700 mV a +300 mV. Por lo tanto, los centros [Fe-S] pueden servir como donantes y aceptores de electrones en reacciones biológicas diversas. (Johnson *et al.*, 2005 y Nanda *et al.*, 2016). Además, la versatilidad estructural y reactividad química de los centros [Fe-S] dotan a las proteínas con funciones bioquímicas tales como catálisis, como ácidos de Lewis y como reguladores genéticos ante diferentes tipos de estrés, principalmente causados por deficiencia o ausencia de hierro. El reclutamiento de estos cofactores por las proteínas ayudo significativamente al desarrollo de la vida (Beinert, 2000; Kiley y Beinert, 2003 y Fontecave, 2006). Sin embargo, los centros [Fe-S] también pueden desencadenar procesos negativos como la producción de especies reactivas de oxígeno (ERO), por la reacción de Fenton y/o un malfuncionamiento de enzimas transportadoras de electrones con centros [Fe-S] (Gómez *et al.*, 2014 y Wachnowsky, 2018).

En las últimas dos décadas se logró un avance importante en entender cómo se lleva a cabo la biogénesis de centros [Fe-S], estos pueden ser sintetizados en condiciones de laboratorio a partir de hierro y azufre inorgánico en condiciones anaeróbicas en ausencia de enzimas que catalicen la reacción (Rao, 2004). Sin embargo, la comprensión de su síntesis *in vivo* ha sido un reto para la comunidad científica. Organismos como *Escherichia coli, Sacharomyces cerevisiae, Arabidopsis thaliana, Azotobacter vinelandii, Erwinia chrysanthemi, Salmonella entérica, Synechocystis sp., Synechococcus sp.,* así como algunas líneas celulares de humanos, son ejemplos de los diferentes modelos de investigación para estos cofactores. Esto habla del grado de conservación en los diferentes reinos taxonómicos y la importancia que representan estos cofactores para la evolución y supervivencia de los seres vivos (Py y Barras, 2010).

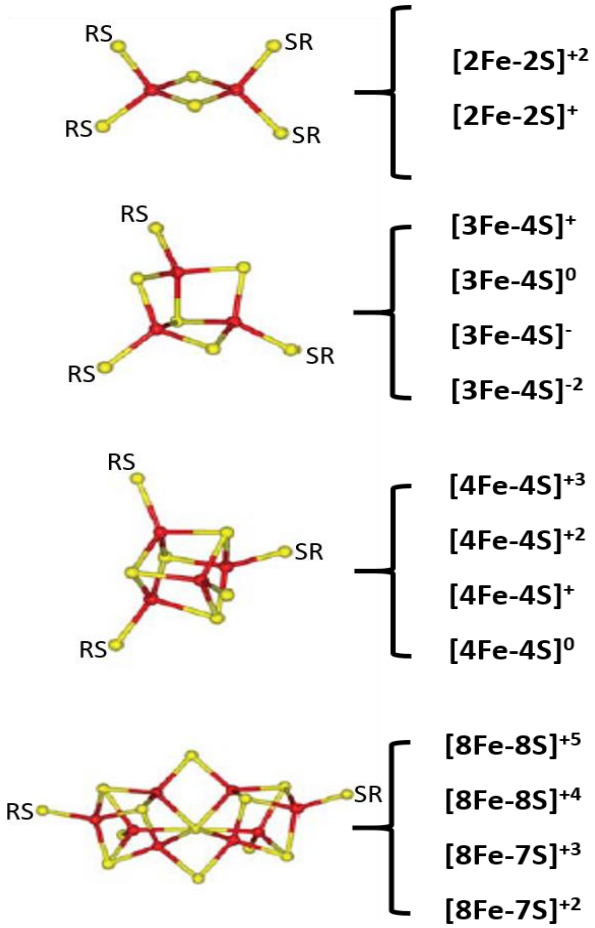

Figura 1. Estructura y estados de oxidación de los centros [Fe-S]. En rojo se muestran los átomos de hierro y en amarillo los átomos de azufre, el hierro del cofactor sirve como ligando al enlazarse con los grupos tiol de los residuos de cisteína en sus motivos proteicos. Los residuos como histidina, arginina, aspartato y serina también pueden servir como ligando de hierro (Modificado de Johnson *et al*., 2005).

1.3 Biogénesis de centros Fe-S.

En la década de 1980 creció el interés por comprender como las células regulan la absorción y distribución del hierro. Los primeros descubrimientos sugirieron que la ferritina era un mecanismo regulador postranscripcional crucial para la homeostasis del hierro en

los vertebrados. Se identificó la región de la transcripción de ferritina responsable de mediar su traducción y se denominó IRE, (por sus siglas en ingles *Iron-Responsive Element*) (Leibold y Munro, 1988). Posteriormente se identificaron las dos proteínas citosólicas Irp1p e Irp2p que se unen a la región IRE (Rouault *et al.,* 1990). Rápidamente se evidencio que la secuencia de aminoácidos de Irp1p era muy similar a la aconitasa mitocondrial, que presenta actividad de aconitasa citosólica al incorporar un centro [4Fe-4S] y que puede unirse con gran afinidad a las regiones IRE presentes en varios ARNm que codifican proteínas involucradas en homeostasis del hierro (Kaptain *et al.,* 1991). La unión de Irp1p a la región 5'-UTR del ARNm de la ferritina interfiere estéricamente con la traducción de la proteína, y por lo tanto, con su síntesis (Downey, 1991). Al descubrir el papel de un centro [Fe-S] en la regulación del metabolismo intracelular del hierro, las investigaciones comenzaron a centrarse en la cuestión de cómo las células sintetizan los centros [Fe-S]. La clave para dilucidar el mecanismo de la biogénesis de [Fe-S] en células vivas fue proporcionada por estudios en *Azotobacter vinelandii*, donde se encontraron tres operones dedicados a la biogénesis de centros [Fe-S], uno de los cuales es el operón Nif, especializado en codificar proteínas involucradas en el ensamblaje de centro [Fe-S] de la nitrogenasa (Jacobson, 1989). Más tarde se identificaron los operones Isc y Suf para la biogénesis de centros [Fe-S] de *Escherichia coli*. Estos operones se activan en diferentes condiciones, el operón Isc se expresa constitutivamente, mientras que el grupo de genes Suf se activa en condiciones de estrés oxidativo. Además, se han identificado genes ortólogos en levaduras, plantas y animales, lo que revela que la maquinaria central para la biogénesis de centros [Fe-S] está conservada evolutivamente (Barras, 2005 y Selbach, 2013). Sin embargo, los intensos estudios en la levadura *S. cerevisiae* son los protagonistas, al haber proporcionado la mayor parte de las ideas sobre el mecanismo del ensamblaje de los centros [Fe-S] en eucariontes.

En eucariotas existen dos sistemas de ensamblaje de centros [Fe-S]: la vía de biogénesis mitocondrial (ISC por sus siglas en inglés *Iron Sulfur Cluster*) y la vía citosólica (CIA por sus siglas en inglés *Cytosolic Iron Sulfur Cluster Assembly*). Los defectos en la biogénesis de centros [Fe-S], así como el ensamblaje de centros [Fe-S] en las proteinas, causan enfermedades con resultados a menudo fatales en humanos (Stehling, 2014). Gracias al metabolismo facultativo de *Sacharomyces cerevisiae,* estudios con mutaciones en los genes que codifican proteínas para la vía de biogénesis con centros [Fe-S] son posibles.

1.3.1 Síntesis *de novo* de centros [2Fe-2S].

La biogénesis de centros [Fe-S] implica la síntesis de *novo* de un centro [Fe-S] en el complejo ISU, este complejo consta de seis componentes diferentes: 1) Isu1p, como proteína de andamiaje; 2) Nfs1p, una cisteína desulfurasa que forma un subcomplejo con 3) Isd11p y 4) Acp1p, proteína portadora de acilo (Van Vranken *et al.*, 2016 y Wiedemann *et al.,* 2006); 5) Yah1p una ferredoxina; 6) Yfh1, una frataxina que también se une al subcomplejo Nfs1-Isd11 (Schmucker *et al.*, 2011; Shan *et al.*, 2007 y Webert *et al.*, 2014). La proteína de andamiaje Isu1p es muy dinámica, tiene la capacidad de formar diferentes complejos durante la formación del centro [Fe-S], su naturaleza permite que diferentes componentes participen en el proceso de biogénesis. Nfs1p se ensambla con la proteína LYR-Isd11p y la proteína portadora de acilo Acp1p, con una estequiometria 2Nfs1p:2LYR-Isd11p:2Acp1p. La proteína de andamiaje Isu1p se asocia para aceptar el ion persulfuro, producido por la remoción del azufre de una cisteína por Nfs1p. La frataxina Yfh1p media la transferencia del persulfuro a Isu1p. Mutaciones en el gen que codifica la frataxina humana han sido asociadas al desarrollo de ataxia de Freidreich en humanos, y la eliminación del gen homólogo en levaduras conduce a una acumulación excesiva de hierro mitocondrial (Babcock *et al.,* 1997). La frataxina tambien tiene la capacidad de unir Fe^{+2}, por lo que se postuló que la frataxina era el donante de hierro para la formación del cofactor

[2Fe-2S] en Isu1p, (Yoon y Cowan, 2003). Sin embargo, la sustitución de los aminoácidos candidatos a estar involucrados en la unión de Fe^{+2}, causaron defectos modestos en la formación de centros [Fe-S] (Correia *et al.*, 2010), por lo que aún se desconoce la procedencia del hierro para formar el cofactor. Por último la ferredoxina Yah1p proporciona los electrones que reducen el sulfato a iones sulfuro (Yan *et al.*, 2015). Una vez que se forma el centro [2Fe-2S] en Isu1p, la unión de Jac1p inicia la disociación del complejo y media la liberación del grupo (Figura 2).

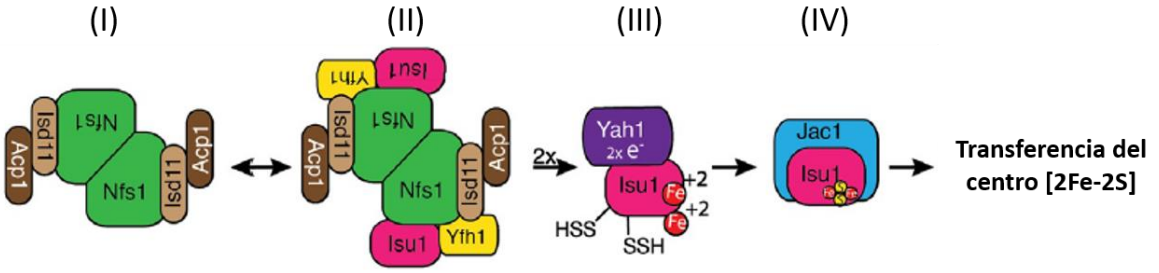

Figura 2. Biogénesis mitocondrial de centros [2Fe-2S]. (I) formación del subcomplejo desulfurasa de cisteína Nfs1-Isd11-Acp1. (II) La proteína de andamiaje Isu1p se asocia al complejo para aceptar el ion persulfuro con la ayuda de Yfh1p. (III) La ferredoxina ayuda a liberar la proteína de andamiaje y proporciona electrones para reducir el sulfato. (IV) Jac1p reconoce el complejo de andamiaje con el recién formado centro [2Fe-2S] e inicia el proceso de transferencia a apoproteínas. Modificado de Melber y Winge, 2018.

1.3.2 Translocación de centros [2Fe-2S] a las apoproteínas.

La liberación del centro [Fe-S] del complejo ISU está a cargo del sistema chaperona-cochaperona Ssq1p-Jac1p, Ssq1p es una proteína de la familia Hsp70 con actividad ATPasa, mientras que Jac1p pertenece a la familia de Hsp20, esta última reconoce a Isu1p-[2Fe-2S] provocando la disociación del subcomplejo Nfs1p-Isd11p (Dutkiewicz *et al.,* 2003; Majewska *et al.,* 2013 y Manicki *et al.,* 2014). Posteriormente, Ssq1p reconoce el complejo Isu1p-[2Fe-2S]-Jac1p. Para la liberación del centro [2Fe-2S] son necesarios dos factores:

(I) la hidrólisis del ATP por Ssq1p facilitada por el intercambiador de nucleótidos Mge1p, esto provoca cambios conformacionales en Ssq1p que desencadenan la liberación de Jac1p y el centro [2Fe-2S]; (II) dos glutarredoxinas (Grx5p) que se encargan de recibir el centro [2Fe-2S] recién liberado. En el dímero de Grx5p, el centro [2Fe-2S] es estabilizado con un segundo ligando de tiolato procedente de un glutatión unido a Grx5p (Banci *et al.,* 2014) (Figura 3). Las células que carecen de Grx5p tienen defectos en los centros [4Fe-4S] y [2Fe-2S] mitocondriales, así como en los centros [Fe-S] citosólicos (Uzarska *et al.,* 2013). Sin embargo, la importancia funcional de Grx5p no está del todo esclarecida, ya que todos estos defectos son modestos en relación con la naturaleza esencial de los componentes anteriormente mencionados en la ruta de biogénesis ISC (Gómez *et al.*, 2014).

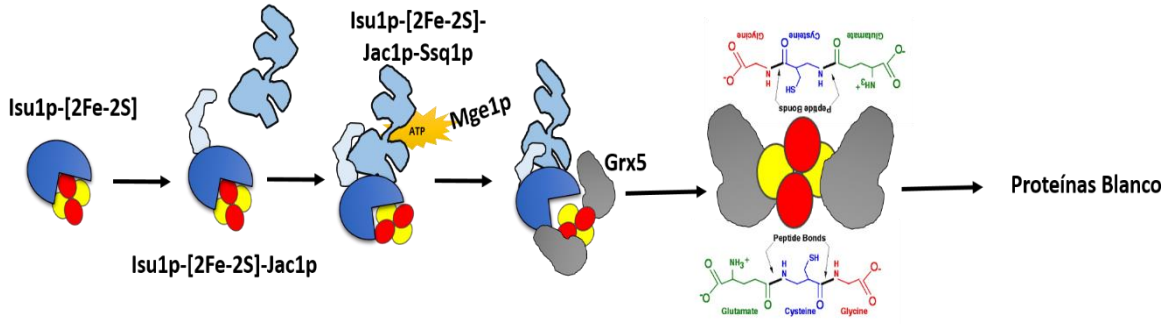

Figura 3. Transferencia del centro Fe-S a Grx5p. La transferencia de centro [2Fe-2S] a las proteínas blanco está mediada por el homodímero de Grx5 que coordina un centro [2Fe-2S]. Tomado y modificado de Lill *et al*., 2012 y Lill *et al*., 2015.

La evidencia establece el papel de Grx5p como agente de transferencia de centros [2Fe-2S] en las mitocondrias de levadura; sin embargo, se ha propuesto un modelo alternativo en mamíferos (Maio y Rouault, 2015). Este modelo postula que las apoproteínas mitocondriales humanas con centros [2Fe-2S] se unen a HSC20 (homologa de Jac1p) asociada con la proteína de andamiaje ISCU (homologa de Isu1p) para la transferencia directa de cofactor estimulada por HSPA9 (homologa de Ssq1p). Se encontró que las

subunidades que contienen [2Fe-2S] de los complejos respiratorios II (SDH) y III (proteína Rieske), interactúan con HSC20 y el sistema de andamiaje ISCU en células de mamífero. También se encontró que GLRX5 (Grx5p en levaduras) está presente en el sistema de andamio-chaperona-ISCU. Sin embargo, este modelo no ha sugerido una función alternativa para GLRX5 (Maio *et al.*, 2017).

Se ha descrito que proteínas accesorias interactúan con la glutarredoxina mitocondrial. Estudios recientes *in vitro* revelaron que la proteína Bol1p mitocondrial interactua con Grx5p en levaduras y en humanos. Se planteó la hipótesis de que un heterodímero Grx5p-Bol1p unido por un grupo [2Fe-2S], puede ser un agente de transferencia específico a cierta apo-proteína blanco aun no identificada dentro de las mitocondrias. También se planteó que este subsistema ayuda a la exportación del componente X, necesario para la biogénesis de centros [Fe-S] citosólicos; sin embargo, estas hipótesis aún no se han comprobado (Melber *et al.*, 2016; Uzarska *et al.*, 2016).

1.3.3 Síntesis *de novo* de centros [4Fe-4S].

Los centros [Fe-S] más abundantes en las células son los de tipo cúbico [4Fe-4S], la síntesis mitocondrial de estos cofactores la lleva a cabo un subsistema de la maquinaria ISC, conformado por las proteínas Isa1p, Isa2p e Iba57p (Gelling, 2008 y Muhlenhoff *et al.*, 2011). Por otro lado, los centros [4Fe-4S] nucleares y citoplasmáticos son sintetizados por la maquinaria CIA, pero requieren de un sustrato o componente X donado por la maquinaria mitocondrial ISC y exportado por el transportador Atm1 (Lill *et al.*, 2015), aunque existe controversia al respecto. La síntesis de centros cúbicos se lleva a cabo por las proteínas Isa1p e Isa2p, que comienza con la transferencia de dos centros [2Fe-2S] por parte del sistema de las glutarredoxinas mitocondriales hacia Isa1p e Isa2p, estas enzimas condensan los centros [2Fe-2S] para formar un centro [4Fe-4S] (Banci *et al.*, 2014; Brancaccio *et al.*, 2014). Un tercer componente en este proceso es Iba57p (Figura 4), esta

proteína no se considera como un factor de ensamblaje, como las proteínas involucradas en la maquinaria de biogénesis hasta al momento mencionadas. No obstante, Iba57p interactúa físicamente con las proteínas Isa1p e Isa2p. Células mutantes en cualquiera de estas proteínas muestran fenotipos similares, lo que sugiere que el complejo de estas tres proteínas forma la unidad funcional. Los fenotipos resultantes por la deficiencia de Isa1p, Isa2p o Iba57p, son disfuncionalidad en proteínas mitocondriales, como la aconitasa, la homoaconitasa y las sintasas de ácido lipoico y biotina, todas con centros [4Fe-4S], por consiguiente, estas mutaciones desencadenan pérdida parcial del ADN mitocondrial, acumulación de hierro en la mitocondria y auxotrofias a lisina y glutamato (Gelling, 2008 y Muhlenhoff *et al.*, 2011). Estas mutaciones en *Saccharomyces cerevisiae* no son letales, mientras que en humanos, las mutaciones o deficiencias en estas proteínas son severas, provocando enfermedades crónico - degenerativas que conllevan a una muerte temprana de los pacientes.

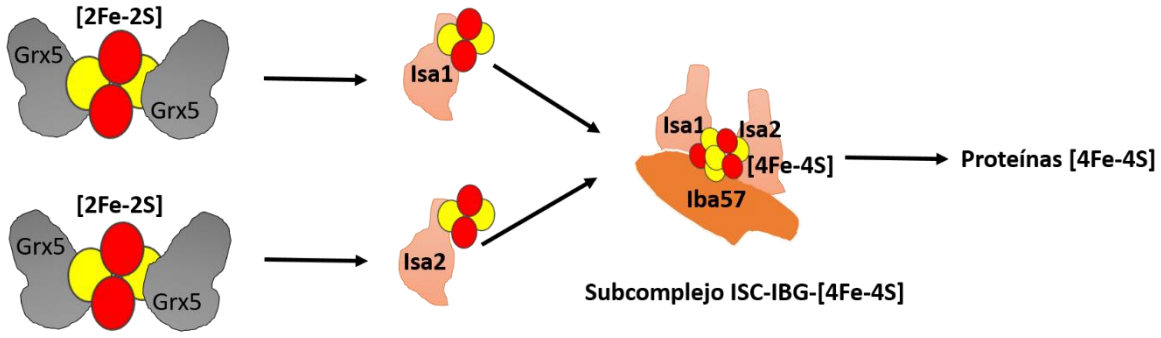

Figura 4. Síntesis de centros [4Fe-4S] por el subcomplejo IBG-[4Fe-4S] de la maquinaria de biogénesis mitocondrial ISC. Dos centros [2Fe-2S] son condensados por las proteínas Isa1p e Isa2p mediados por Iba57p. Modificado de Mühlenhoff *et al.*, 2011 y Brancaccio *et al.*, 2014.

1.3.4 Controversias de la biogénesis y ensamble de centros [Fe-S].

La biogénesis de proteínas con centros [Fe-S] es compleja, por lo que su mecanismo no ha sido elucidado por completo. Además de las proteínas esenciales de la vía ISC mitocondrial, existen factores de transferencia específicos para ciertas proteínas. Por ejemplo, la proteína Nfu1p transfiere los cofactores de las proteínas aconitasa y Sdh2 al unirse a centros [4Fe-4S], formados por las proteínas Isa1p e Isa2p (Cai *et al.*, 2016; Melber *et al.*, 2016). La ausencia o disfunción de Nfu1p provoca defectos menores en el desarrollo de levaduras cultivadas en condiciones aeróbicas, mientras que en condiciones fermentativas las células no muestran defectos en las enzimas con centros [4Fe-4S], lo que sugiere que Nfu1 es necesaria para proteger los grupos recién sintetizados del daño oxidativo, en la transferencia hacia las proteínas blanco. Otra proteína es IND1 de humanos, la cual está implicada en el ensamblaje del complejo I respiratorio (Bych *et al.*, 2008). La falta de IND1 en células de mamíferos conduce a una atenuación marcada en la actividad y una disminución de la abundancia de varias subunidades del complejo I con centros [4Fe-4S] (Sheftel *et al.*, 2009). Se desconoce si Nfu1 interacciona con Ind1 en el ensamblaje del complejo I; sin embargo, algunos de los pacientes con desordenes mitocondriales presentan mutaciones en el gen NFU1 y defectos en el complejo I (Ahting *et al.*, 2015; Navarro *et al.*, 2011). Las funciones potenciales de un sistema de transferencia tardío incluyen facilitar la liberación del centro [4Fe-4S] o estabilizar la interacción con las proteínas blanco (Melber *et al.*, 2016) por lo que son necesarios más estudios para esclarecer estas hipótesis.

1.4 Cadena de transporte de electrones.

Como se mencionó anteriormente, las mitocondrias son las plantas de energía de las células eucariotas, al producir la mayor parte del ATP necesario para el funcionamiento de la célula. El proceso se lleva a cabo mediante la fosforilación oxidativa, que consiste en que

cuatro complejos multiproteicos conectan el transporte de electrones al oxígeno con el establecimiento de un gradiente electroquímico en el espacio de intermembranal de la mitocondria. En este proceso la energía química de los productos del ciclo del ácido cítrico se transduce en un gradiente electroquímico de protones impulsado por los complejos respiratorios. Los protones fluyen de regreso a la matriz mitocondrial a través de canales de protones en el complejo F_1F_0-ATP sintasa e impulsan una rotación mecánica, provocando cambios conformacionales en los sitios de unión de nucleótidos del subcomplejo F_1, catalizando así la conversión del ADP y fosfato en ATP (Sousa *et al.*, 2018).

Los complejos de la cadena respiratoria se encuentran entre los complejos de proteínas de membrana más grandes de la célula. Transfieren electrones del NADH y $FADH_2$ al oxígeno molecular a través de una serie de cofactores redox, entre los que se incluyen flavinas, iones metálicos, grupos hemo y centros [Fe-S] (Kumari, 2018). Las bombas de protones son la NADH:ubiquinona oxidorreductasa o complejo I, que oxida el NADH y transfiere electrones a la ubiquinona con la translocación de cuatro protones a través de la membrana interna mitocondrial (Wirth *et al*., 2016). *Saccharomyces cerevisiae* no cuenta con este complejo; sin embargo, cuenta con tres NADH deshidrogenasas que suministran electrones a la ubiquinona supliendo la función del complejo I (Velázquez y Pardo, 2001 y Luttik *et al*., 1998). La ubiquinol:citocromo *c* oxidorreductasa o complejo III, transfiere electrones del ubiquinol al citocromo *c* y transloca 4 protones al espacio intermembranal (Trumpower y Gennis, 1994). Por último, la citocromo *c* oxidasa o complejo IV, transfiere electrones del citocromo *c* al oxígeno molecular y transloca cuatro protones (Wikstrom, 1977). Por otro lado, la succinato deshidrogenasa o complejo II, forma parte tanto del ciclo del ácido cítrico, como de la cadena de transferencia de electrones, aporta electrones adicionales a la ubiquinona que se originan a partir del succinato, este complejo no transloca protones (Sousa *et al.*, 2018).

1.4.1 Biogénesis de los complejos respiratorios en *Saccharomyces cerevisiae.*

La biogénesis de los complejos respiratorios es un proceso sofisticado, debido a la doble fuente genética de las subunidades que componen a la mayoría de los complejos de la cadena respiratoria. Su ensamblaje requiere una estrecha coordinación entre las maquinarias de expresión génica nuclear y mitocondrial. Además, los factores de ensamblaje coordinan minuciosamente la adición paso a paso de subunidades catalíticas y accesorias, así como la incorporación de los cofactores redox (Herrmann *et al*., 2013). Estudios en levadura han revelado los principios básicos de las vías de ensamblaje de los complejos. Sin embargo, día con día se descubren nuevos factores de ensamble accesorios, con funciones que recientemente se empiezan a comprender.

Los complejos respiratorios están compuestos de subunidades proteicas, a la vez, los complejos respiratorios se ensamblan en estructuras superiores nombradas supercomplejos (Vonck y Schafer, 2009). Incluso, se ha adoptado el nombre de "respirasomas" a la asociación de los complejos respiratorios I, III y IV (Schagger y Pfeiffer, 2000), lo que sugiere la posibilidad de canalización de electrones desde el NADH hacia el oxígeno por un solo supercomplejo (Genova *et al*., 2008; Vonck y Schafer, 2009). En *Saccharomyces cerevisiae* también se reportó la presencia de respirasomas, compuestos por las NADH deshidrogenasas y los complejos III y IV (Figura 5).

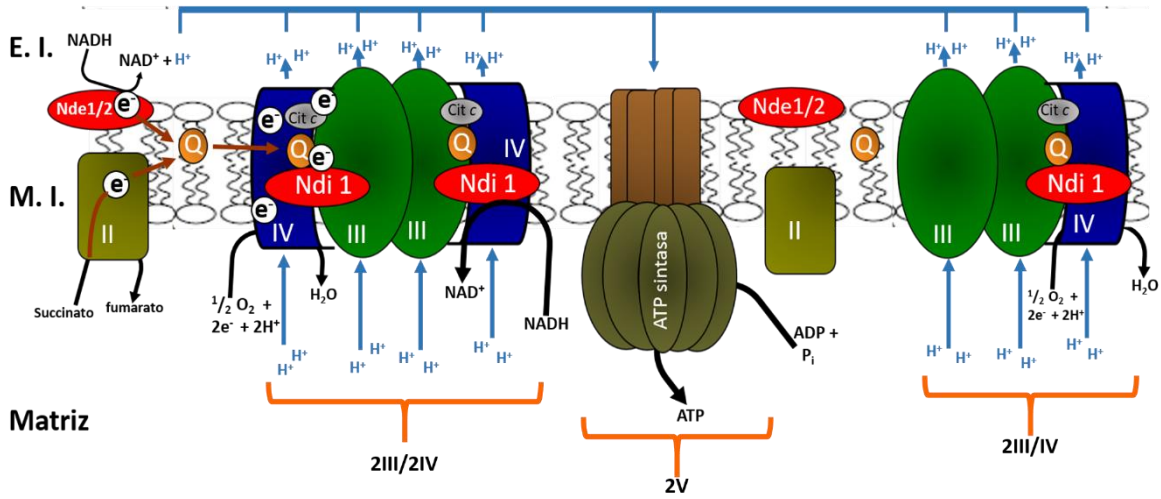

Figura 5. Cadena de transporte de electrones y síntesis de ATP. Modelo de mosaico sólido, en la figura se representan los supercomplejos respiratorios de *Saccharomyces cerevisiae* en sus diferentes proporciones. Modificado de Schägger y Pfeiffer, 2000 y Matus *et al*., 2015.

NADH deshidrogenasas mitocondriales en *S. cerevisiae:* Las tres NADH deshidrogenasas mitocondriales están codificadas en el genoma nuclear. *NDI1*codifica la NADH deshidrogenasa situada en la membrana interna mitocondrial, la enzima madura tiene una sola subunidad de 53 kDa con un FAD como único grupo prostético, cuyo dominio catalítico se encuentra orientado hacia la matriz mitocondrial. Esta enzima cataliza la transferencia de electrones del NADH intramitocondrial generado por el complejo piruvato deshidrogenasa y el ciclo de Krebs hacia la ubiquinona, sin translocar protones a través de la membrana interna mitocondrial (Velázquez y Pardo, 2001). El crecimiento respiratorio requiere la reoxidación continua del NADH citosólico y mitocondrial. Debido a que el NADH citosólico no puede atravesar la membrana mitocondrial interna, son necesarias NADH

deshidrogenasas encargadas de oxidar el NADH proveniente del citosol. *NDE1* y *NDE2* codifican para las NADH deshidrogenasas externas Nde1p y Nde2p de 62.7 y 61.6 kDa, respectivamente. Estas enzimas tienen gran similitud con Ndi1p; sin embargo, el sitio catalítico de ambas está orientado hacia el espacio intermembranal (Overkamp *et al.,* 2000). Estas enzimas oxidan el NADH con FAD, que a su vez reduce a la ubiquinona a ubiquinol, el cual transfiere los electrones al complejo III, generándose el gradiente de protones que estimula la síntesis de ATP (Figura 5) (Vries y Marres, 1987; Overkamp *et a*l., 2000 y Matus *et al*., 2015).

Succinato deshidrogenasa (complejo II): Este es el único complejo que interviene tanto en el ciclo de Krebs como en la cadena de transporte de electrones, la topología de la enzima le permite esta característica ya que las subunidades hidrofílicas se encuentran orientadas hacia la matriz mitocondrial, lo que permite oxidar al succinato y transferir los electrones mediante sus cofactores hacia la quinona, mediante las subunidades hidrofóbicas ancladas a la membrana interna mitocondrial. Esta enzima está conformada de cuatro subunidades codificadas en el genoma nuclear, Sdh1p, Sdh2p, Sdh3p y Sdh4p, que contienen un péptido señal mitocondrial en el extremo amino terminal, lo que permite que sean transportadas por las translocasas de importación de proteínas TOM (*translocase of the outer membrane*) y TIM (*translocase of the inner membrane*) (Vranken *et al*., 2014). El modelo de biogénesis del complejo II es un proceso coordinado entre la expresión de la proteína, el transporte de las subunidades a la mitocondria y el ensamble de sus cofactores para la formación de dos subcomplejos y finalmente el ensamble de la enzima completa (Figura 6). La maduración de Sdh1 y Sdh2 se lleva a cabo simultáneamente, Sdh1 adquiere un FAD dentro de la matriz mitocondrial gracias a la chaperona Sdh5p, posteriormente Sdh1-FAD es reconocido por otro factor, Sdh8p el cual permite el reconocimiento con la subunidad Sdh2p y evita la formación de anión superóxido por el FAD de Sdh1p. Sdh2p al

igual que Sdh1p se transloca a la matriz mitocondrial donde adquiere los centros [2Fe-2S], [4Fe-4S] y [4Fe-3S], mediante la maquinaria ISC. El complejo II requiere de otros dos factores de ensamble Sdh6p y Sdh7p y se propuso que estas proteínas son necesarias para proteger los centros Fe-S del daño oxidativo y también para reconocer a los integrantes de la maquinaria ISC que ceden los cofactores. El segundo subcomplejo de esta enzima está conformado por las subunidades Sdh3p y Sdh4p, estas subunidades son hidrofóbicas, por lo que son proteínas integrales de la membrana mitocondrial interna. Este subcomplejo tiene los sitios de unión a la quinona y a un grupo hemo (Vranken *et al*., 2014).

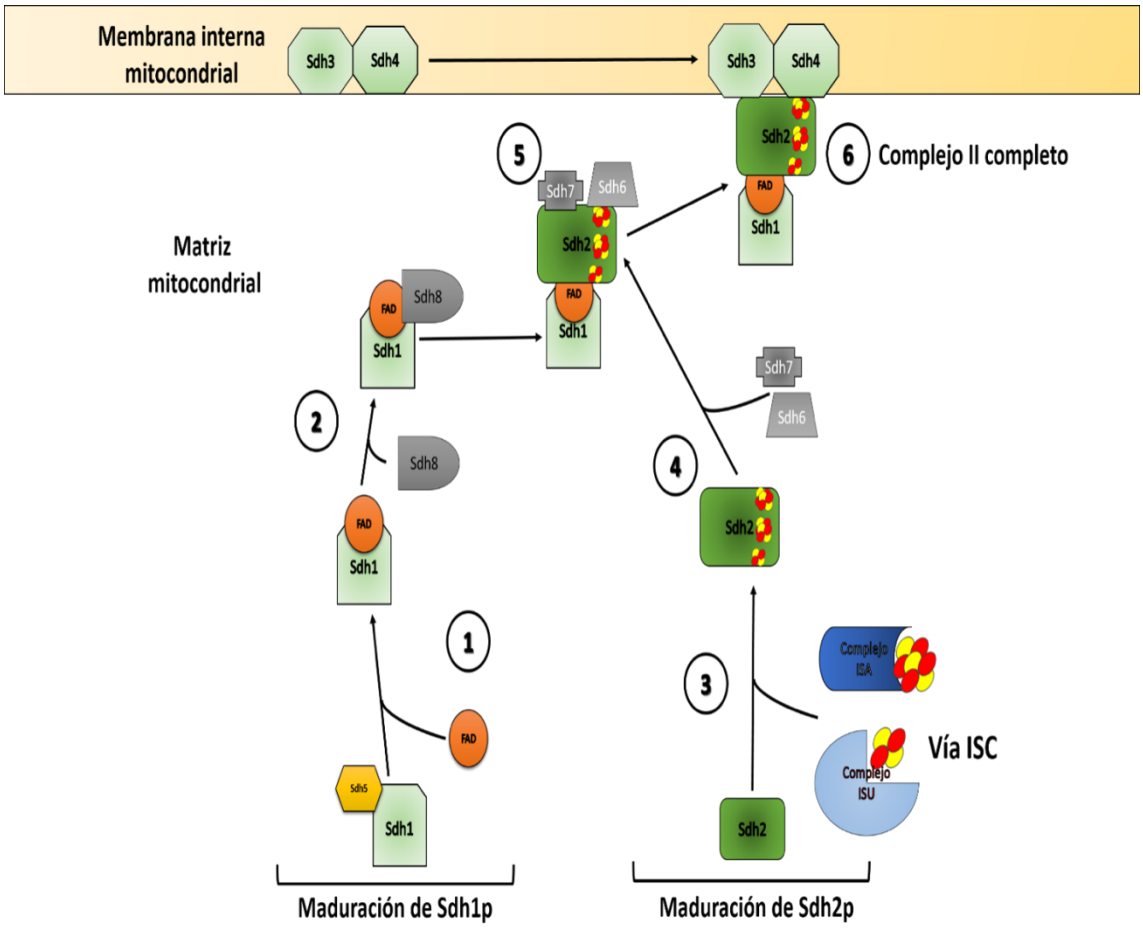

Figura 6. Biogénesis del complejo II (Tomado y modificado de Vranken *et al*., 2014).

Ubiquinol:citocromo *c* oxidorreductasa (complejo bc_1 o complejo III): Este complejo es un homodímero donde cada monómero está compuesto por 11 subunidades, tres de estas son consideradas como catalíticas y las ocho restantes como accesorias. Las subunidades catalíticas son el citocromo *b*, el citocromo c_1 y la proteína [2Fe-2S], Rip1p o proteína de Rieske. Las subunidades accesorias son Cor1p, Cor2p, Qcr6p, Qcr7p, Qcr8p, Qcr9p y Qcr10, todas ellas sin ningún tipo de cofactor (Conte *et al*., 2015). El ensamble de este complejo enzimático es un proceso de múltiples pasos en el cual se forman varios subcomplejos inmaduros. Un subcomplejo núcleo de 230 kDa se forma por la asociación del citocromo *b*, única subunidad de complejo III codificada por el ADNmt, y las subunidades accesorias Qcr7p y Qcr8p. Este se posiciona en la membrana interna mitocondrial. Subsecuentemente, el citocromo c_1 forma otro subcomplejo con las subunidades Cor1p y Cor2p, se asocia con el subcomplejo núcleo y forma un complejo inmaduro de 500 kDa. A este complejo inmaduro se asocian las subunidades Qcr6p y Qcr9p. Como resultado se obtiene un monómero inmaduro que forma dímeros con capacidad de formar asociaciones con 1 o 2 monómeros del complejo IV de la cadena de transporte de electrones (Zara *et al*., 2007 y 2009). Finalmente, para la maduración completa del complejo III se asocian las subunidades Qcr10 y Rip1p (Conte *et al*., 2015), esta última subunidad es importada a la matriz mitocondrial donde incorpora un centro [2Fe-2S] por la maquinaria mitocondrial ISC (Wagener *et al*., 2011). Posteriormente, la subunidad Rip1p es estabilizada por la chaperona Mzm1 y luego translocada de la matriz mitocondrial al complejo inmaduro en la membrana interna por la chaperona Bcs1p. La mutación de cualquiera de estas chaperonas moleculares causan disfunción en la actividad del complejo III (Conte *et al*., 2011 y Cui *et al*., 2012), debido a que Rip1p es la subunidad encargada de la reacción limitante del complejo (Denke *et al*., 1998) y posiblemente también estabiliza al dímero, debido a que el dominio globular que contiene el sitio catalítico de Rip1p interactúa con un monómero del complejo III,mientras que el amino terminal interactúa con el monómero adyacente (Conte

et al.,2015).Entre las cuestiones por investigar está el esclarecimiento de como Rip1p incorpora su cofactor por la maquinaria ISC mitocondrial (Figura 7).

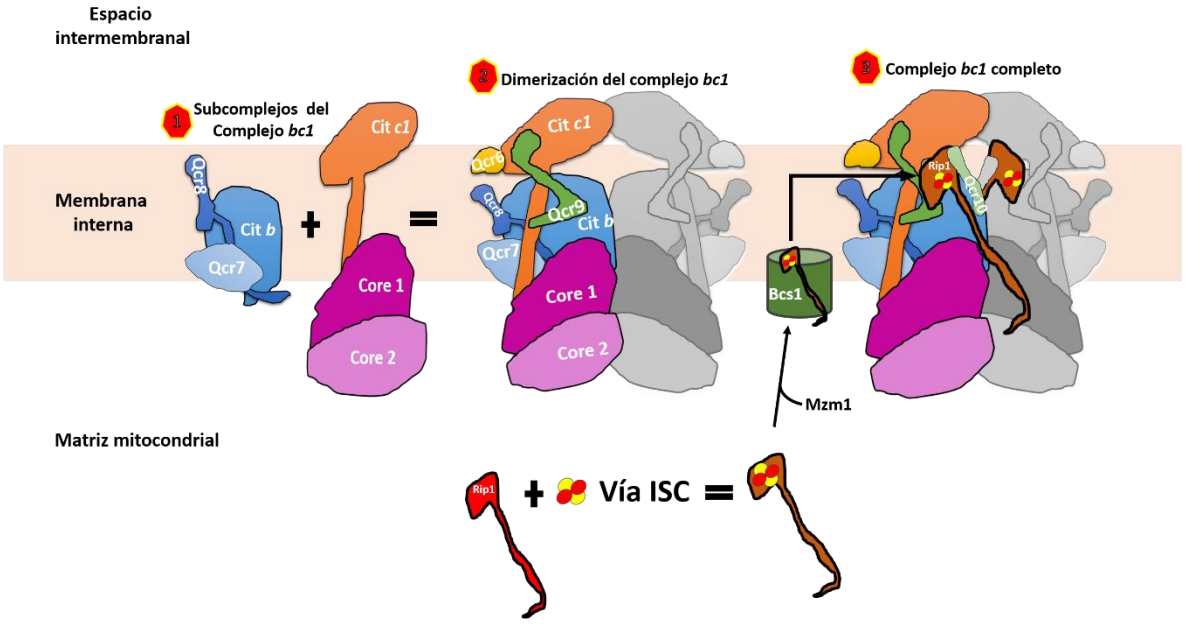

Figura 7. Biogénesis del complejo III. Adaptado de Zara *et al*., 2007 y 2009; Conte *et al*., 2015 y Wagener *et al*., 2011.

Citocromo-*c*-oxidasa o complejo IV: Este complejo es una proteína integral de la membrana interna mitocondrial. En la levadura está compuesto por las subunidades Cox1p, Cox2p, Cox3p, Cox4, Cox5ap, Cox5b^{2}p, Cox6p, Cox6ap, Cox6bp, Cox7ap, CoxVIIbp y Cox8p. Este complejo también se ensambla de manera multimodular y coordinadamente entre los genomas nuclear y mitocondrial. Las subunidades principales son Cox1p, Cox2p y Cox3p las cuales están codificadas en el ADNmt. La subunidad Cox1p tiene un centro de cobre nombrado CuB y dos grupos hemo *a* y a_3, en esta subunidad es donde se produce la reducción del oxígeno molecular a agua. En Cox2p se encuentra un centro de cobre denominado CuA el cual es el aceptor inicial de electrones provenientes del citocromo *c* (Ferguson y Babcock, 1996 y Wikström *et al*., 2015). Cox3 no contiene centros redox, pero se cree que estabiliza el núcleo catalítico del complejo (Sharma *et al*., 2015).

La formación del subcomplejo Cox1 se lleva a cabo en 5 pasos mediante la formación de intermediarios nombrados D1 a D5 (Mcstay *et al*., 2013).Primeramente D1 se forma por la interacción de Cox1p recién traducida con Cox14p y el factor de ensamble Coa1p. Posteriormente, a D1 se agrega Mss51p y la subunidad Cox5ap para formar D2, que se convierte en D3 mediante la adición de Cox6p y Cox8p. El subcomplejo D4 aún no está bien caracterizado; sin embargo, se ha identificado la adición de Cox4p. Finalmente para la formación de D5 se agrega Shy1p la cual ha sido implicada en la maduración de los centros hemo *a* de COX (Smith *et al*., 2005; Khalimonchuk *et al*., 2010). El segundo subcomplejo es Cox2, este no cuenta con ninguna subunidad estructural del complejo IV (Franco *et al*., 2018). Sin embargo, se ha demostrado la formación de varias interacciones con proteínas que ayudan a su maduración. Cox18p es una proteína de andamiaje específica de Cox2p necesaria para la inserción de la hélice alfa N-terminal en la membrana, Cox20p es la segunda proteína específica de Cox2, esencial para la inserción de la membrana y la transferencia del dominio C-terminal hidrófilo de Cox2 al espacio intermembranal (Hell *et al*., 2000 y Elliot *et al*., 2012). Además, en este subcomplejo se han identificado las proteínas Sco1 y Coa6 necesarias para la maduración del sitio CuA de Cox2p (Soto *et al*., 2012). El subcomplejo de Cox3p, se ensambla independientemente de los otros dos módulos. El intermediario más pequeño contiene Cox7p, Cox13p y comparte Cox4 con el módulo Cox1. Este subgrupo después interactúa con Rcf1p, una proteína que ha sido implicada en la formación de supercomplejos y moduladora de la actividad del complejo IV (Strogolova *et al*., 2012; Strogolova *et al*., 2019; Dawitz *et al*, 2020). No se sabe si existe un orden obligatorio en el que los tres módulos de Cox interactúan entre sí, y de ser así, cuál podría ser la secuencia (Figura 8).

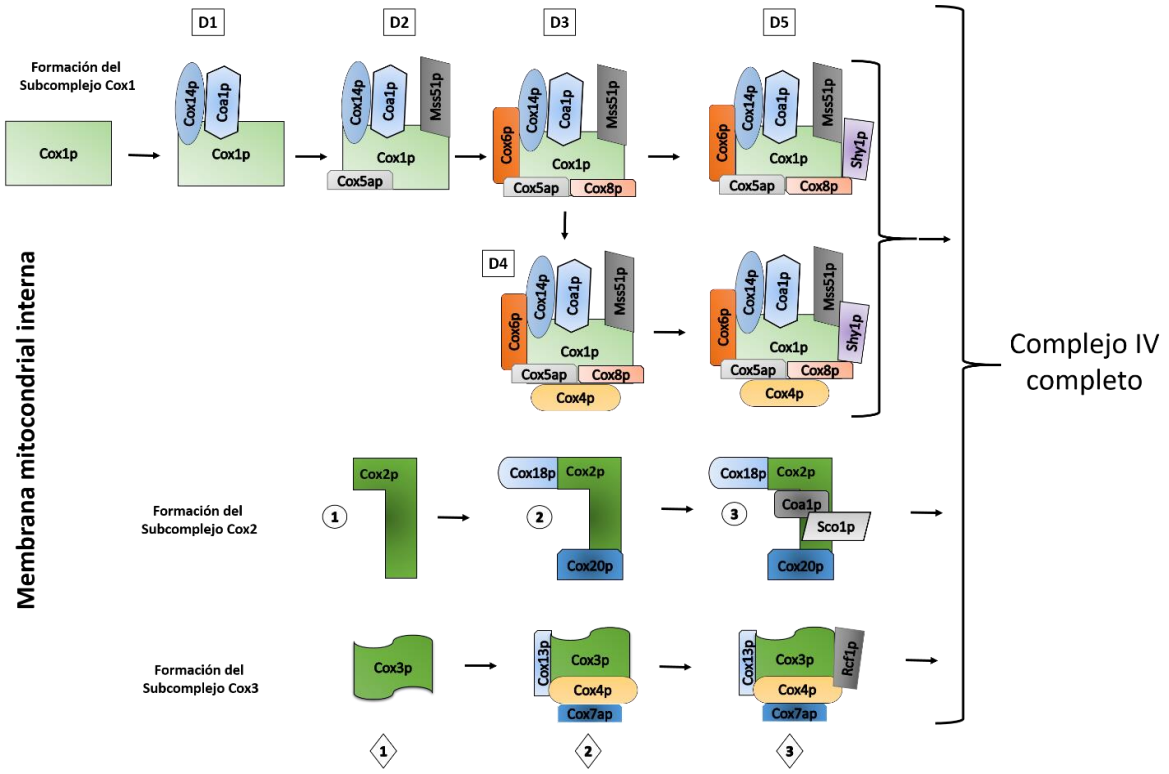

Figura 8. Biogénesis del Complejo IV. Modificado de Mcstay *et al*., 2013 y Franco *et al*., 2020.

ATP sintasa F_1-F_0. La biogénesis de la ATP sintasa se ha estudiado en levaduras, bacterias, y recientemente, en células humanas. En cada caso, los diferentes sectores de la enzima se pre ensamblan como unidades o subcomplejos separados (Figura 9): 1 el subcomplejo ATPasa F1 orientado hacia la matriz mitocondrial y 2, el subcomplejo F0 en la membrana interna (Kagawa y Racker, 1966 y Franco *et al*., 2020). F_1 contiene cinco subunidades diferentes α, β, γ, δ y ε, en una estequiometría de 3: 3: 1: 1: 1. Las tres copias de las subunidades α y β se alternan para formar un barril hexámero que rodea un tallo central que contiene una copia de la subunidad γ (Boyer, 1997; Stock *et al*., 2000). Tres de las seis interfaces formadas por las subunidades α y β contienen los tres sitios catalíticos de unión a nucleótidos donde se sintetiza o hidroliza ATP. El tallo central se conforma con las subunidades γ, δ y ε, y proporciona el vínculo físico entre F_1 y F_0. La unidad F_0 de

membrana en levadura consta de 8 polipéptidos, tres de los cuales (Atp6, Atp8 y Atp9) están codificados por el ADNmt (Macreadie *et al*., 1983). Atp6 y Atp8 están presentes en una sola copia, mientras que diez copias de Atp9 se oligomerizan en una estructura en forma de anillo. Atp9 consta de dos α-hélices transmembranales que interactúan con las subunidades δ, γ y ε del tallo central F_1 para constituir el rotor de la ATP sintasa (Fillingame *et al*., 2002 y Stock *et al*., 1999). El tallo o estator periférico está compuesto por las subunidades Atp4p, Atp7p, Atp14p y OSCP (por sus siglas en inglés *Oligomycin Sensitivity Conferral Protein*). Las tres subunidades periféricas del tallo (Atp7p, Atp14p y OSCP) están ubicadas completamente fuera de la membrana, mientras que la cuarta subunidad Atp4p es una hélice α extendida, un extremo de la cual está incrustado en la bicapa de fosfolípidos y puede considerarse como un componente de la membrana. Las cuatro subunidades del tallo periférico actúan como un estator que evita que el cilindro α3β3 periférico de F_1 gire, lo que permite que la subunidad γ se ponga en contacto secuencialmente con cada uno de los tres sitios catalíticos α/β internos de F_1 durante el ciclo catalítico (Walker *et al*., 2006). La ATP sintasa forma dímeros con un ángulo de 86º entre ellos (Davies *et al*., 2012). Los dímeros están dispuestos en filas formando cintas de ATP sintasa dimérica en las crestas de la membrana interna. El ángulo de 86º entre los monómeros de ATP sintasa es responsable del plegamiento de la membrana interna en crestas (Davies *et al*., 2011; Blum *et al*., 2019).

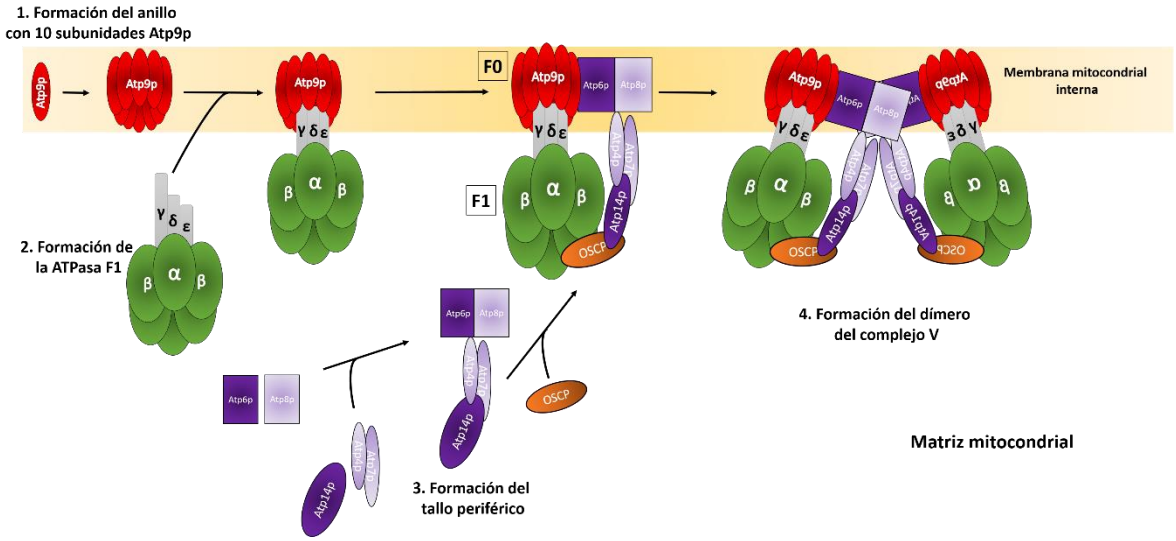

Figura 9. Biogénesis de la ATP sintasa mitocondrial. Tomado y modificado de Davies *et al*., 2012 y Franco *et al*., 2020

1.5 Regulación de la función mitocondrial por la biogénesis de centros Fe-S.

La biogénesis de los centros [Fe-S] juega un papel importante en los mecanismos de la homeostasis del hierro y está relacionada con la función mitocondrial. En este sentido, estudios recientes indican que la generación de ERO causada por H_2O_2, la menadiona o el etanol, se asocian con una pérdida de la homeostasis del hierro que es exacerbada por la disfunción del sistema ISC, lo cual contribuye a aumentar la toxicidad de estos compuestos a través de una mayor generación de ERO, provocando el agotamiento de la respuesta antioxidante y la muerte celular (Pérez-Gallardo *et al*, 2013). La concentración de hierro intramitocondrial durante la biogénesis de los centros [Fe-S] tiene que ser finamente regulada para evitar un aumento perjudicial en la concentración de hierro lábil, puesto que el hierro ferroso (Fe^{2+}) y el férrico (Fe^{3+}) catalizan la formación del radical hidroxilo ($OH^{\bullet}$) en presencia de H_2O_2 y O_2^- a través del ciclo de Habber-Weiss. En las mitocondrias, estas ERO se producen fisiológicamente como subproductos de la actividad de la cadena de transporte de electrones a nivel del complejo III. La homeostasis no controlada del hierro mitocondrial

causa daño oxidativo en el ADN, lípidos y proteínas a través de la generación de ERO, que a su vez deteriora aún más la función de la CTE y conduce a la muerte celular (Turrens, 2010; Pérez-Gallardo *et al*, 2013; Gómez *et al*, 2014).

Estudios previos (Pérez-Gallardo *et al,* 2013; Gómez *et al,* 2014) sugieren que las proteínas Isa1/Iba57 consideradas como donantes de centros [4Fe-4S], también son capaces de ensamblar centros [2Fe-2S] en apoproteínas como la succinato deshidrogenasa (Sdh2p) y la proteína Rieske (Rip1p) del complejo II y III de la CTE, respectivamente, ya que la mutación en los genes *ISA1* e *IBA57* anula la actividad de los complejos II, III y IV de la CTE. Lo que sugiere que la generación de ERO en las mutantes ISC podría estar asociada con la disfuncionalidad de la CTE a nivel de la transferencia de electrones, por proteínas que contienen [Fe-S]. Estos hallazgos sugieren que la acumulación de centros [Fe-S] pre-ensamblados debido a un fallo en su inserción, por la interrupción de los genes ISC o la ausencia de la apoproteína receptora (es decir, succinato deshidrogenasa, aconitasa o proteína Rieske), conducen a un incremento del hierro lábil, provocando un desequilibrio en la respuesta celular antioxidante.

Para el caso de la mutante *rip1Δ*, el hierro destinado a la proteína Rieske y la incapacidad para transferir los electrones en la CTE, pueden estar relacionados con el incremento exacerbado de ERO. Como se ha mencionado, las mutantes *isa1Δ* e *iba57Δ* mostraron una pérdida casi total de la actividad de los complejos II y III de la CTE, sugiriendo que probablemente el ensamble de proteínas que contienen grupos [Fe-S] en estos complejos, pueden ser asistidos también por las proteínas de ensamblaje Isa1p, Isa2p e Iba57p.

2. Justificación:

En *S. cerevisiae* se ha reportado que el subgrupo de la maquinaria *ISC* mitocondrial integrado por las proteínas Isa1p, Isa2p e Iba57p, son exclusivas en el proceso de síntesis y transferencia de centros [4Fe-4S]. Sin embargo, estudios previos sugieren que estas proteínas adicionalmente están involucradas en la maduración de la proteína Rip1p o Rieske del complejo respiratorio III, cuyo grupo prostético es un centro [2Fe-2S]. Por lo que se debe corroborar si las proteínas del subsistema tardío de la vía ISC mitocondrial están involucradas en la maduración de Rip1p, lo cual podría dar lugar a plantear que este subsistema es esencial para el correcto funcionamiento de la cadena de transporte de electrones de *S. cerevisiae* al influenciar la formación de supercomplejos mediado por el correcto ensamble del centro [2Fe-2S] de Rip1p.

3. Hipótesis

El subsistema [Fe-S-IBG] de la maquinaria ISC mitocondrial transfiere el centro [2Fe-2S] a la subunidad Rip1, la cual participa en la estabilización de los supercomplejos respiratorios en *S. cerevisiae*.

4. Objetivo general

Determinar la participación del subsistema [Fe-S-IBG] en la inserción del centro [2Fe-2S] en la subunidad Rip1p y su impacto en la formación de supercomplejos III/IV de *S. cerevisiae*.

4.1 Objetivos específicos

- Evaluar el funcionamiento de la cadena de transporte de electrones mitocondrial en la deficiencia del subsistema Fe-S-IBG en *S. cerevisiae.*
- Evaluar la estabilidad de los supercomplejos respiratorios en la ausencia del subsistema Fe-S-IBG en *S. cerevisiae*.
- Determinar la interacción entre el subsistema Fe-S-IBG y la subunidad Rip1p de *S. cerevisiae*.

5. Resultados

5.1 Capítulo 1

Mitochondrion 44 (2019) 75–84

Contents lists available at ScienceDirect

Mitochondrion

journal homepage: www.elsevier.com/locate/mito

Iba57p participates in maturation of a [2Fe–2S]-cluster Rieske protein and in formation of supercomplexes III/IV of *Saccharomyces cerevisiae* electron transport chain

Luis A. Sánchez[a,1], Mauricio Gómez-Gallardo[a,1], Alma L. Díaz-Pérez[a], Christian Cortés-Rojo[b], Jesús Campos-García[a,*]

[a] Lab. de Biotecnología Microbiana, Instituto de Investigaciones Químico Biológicas, Universidad Michoacana de San Nicolás de Hidalgo, Morelia, Michoacán, Mexico
[b] Lab. de Bioquímica, Instituto de Investigaciones Químico Biológicas, Universidad Michoacana de San Nicolás de Hidalgo, Morelia, Michoacán, Mexico

ARTICLE INFO

Keywords:
Saccharomyces cerevisiae
Mitochondria
Iron–sulfur cluster
Rieske protein
Supercomplexes
Iron homeostasis
Reactive oxygen species

ABSTRACT

The [Fe-S] late-acting subsystem comprised of Isa1p/Isa2p, Grx5p, and Iba57p proteins (Fe–S-IBG subsystem) is involved in [4Fe-4S]-cluster protein assembly. The effect of deleting *IBA57* in *Saccharomyces cerevisiae* on mitochondrial respiratory complex integration and functionality associated with Rieske protein maturation was evaluated. The *iba57*Δ mutant showed decreased expression and maturation of the Rieske protein. The loss of Rieske protein caused by *IBA57* deletion affected the structure of supercomplexes III_2IV_2 and III_2IV_1 and their integration into the mitochondria, causing dysfunction in the electron transport chain. These effects were correlated with decreased cytochrome functionality and content in the *iba57*Δ mutant. These findings suggest that Iba57p participates in maturation of the [2Fe–2S]-cluster into the Rieske protein and that Rieske protein plays important roles in the conformation and functionality of mitochondrial supercomplex III/IV in the electron transport chain.

1. Introduction

The enzymatic complexes forming the electron transport chain (ETC) in the mitochondria of both mammals and yeast are organized as supramolecular structures and are known as supercomplexes. In yeast, supercomplexes are formed by interactions between the bc_1 complex (complex III) and cytochrome *c* oxidase complex (complex IV) in a stoichiometric ratio of two is to one (III_2/IV_1) or two is to two (III_2/IV_2) (Schagger and Pfeiffer, 2000). Supercomplex formation has been found to be essential for channeling of substrates, structural stabilization of individual ETC complexes, and modulation of reactive oxygen species (ROS) generation (Vartak et al., 2013). Thus, disruption of supercomplex formation may be detrimental to cell survival because of energy deficiency, enhanced oxidative stress, and/or inability to adapt to environmental changes (Gutierrez-Cirlos et al., 2002).

In yeast, supercomplex formation has been suggested to depend on the iron-sulfur protein (Rip1p) subunit of complex III (Conte et al., 2015; Cui et al., 2014; Zara et al., 2009). Rip1p (Rieske protein) is one of the three catalytic subunits of complex III and disruption of either its assembly or insertion of the Rip1p prosthetic group into the complex, a [2Fe–2S] cluster, severely alters both its structure and function (Gutierrez-Cirlos et al., 2002). The [Fe–S] clusters of the cytosolic and mitochondrial compartments are mainly synthesized by the mitochondrial iron–sulfur cluster (ISC) machinery (Braymer and Lill, 2017; Lill, 2009; Lill et al., 2012; Lill and Muhlenhoff, 2006), which is encoded in *Saccharomyces cerevisiae* by the genes *SSQ1*, *JAC1*, *NFS1*, *ISU1*, *ISU2*, *YAH1*, *YFH1*, *ISA1*, *ISA2*, *GRX5*, and *IBA57* (Lill, 2009; Schilke et al., 2006).

In contrast, the insertion and maturation of [4Fe–4S] clusters into target proteins such as aconitase, lipoic acid synthase, and homoaconitase are carried out by a specialized, late-acting Fe-S subsystem comprised of Isa1/Isa2, Iba57, and Grx5 proteins (Schilke et al., 2006), named as the Fe–S-IBG subsystem (by Isa1/2, Iba57, and Grx5 proteins). Fe–S-IBG subsystem components are not considered as essential for the maturation of mitochondrial [2Fe–2S] proteins (Muhlenhoff et al., 2011; Sheftel et al., 2012). Deletion of Isa1p, but not of Isa2p and Grx5p, is essential for [4Fe–4S] cluster assembly into target proteins. However, the essential role of Iba57p has not been demonstrated.

* Corresponding author at: Lab. de Biotecnología Microbiana, Instituto de Investigaciones Químico Biológicas, Universidad Michoacana de San Nicolás de Hidalgo, Edif. B-3, Ciudad Universitaria, 58030 Morelia, Michoacán, Mexico.
E-mail address: jcgarcia@umich.mx (J. Campos-García).
[1] Both authors contributed equally to this work and share first authorship.

https://doi.org/10.1016/j.mito.2018.01.003
Received 5 June 2017; Received in revised form 20 October 2017; Accepted 10 January 2018
Available online 16 January 2018

Previous studies indicated that the Fe S-IBG subsystem can also act in [2Fe 2S]-cluster protein maturation (Banci et al., 2014; Beilschmidt et al., 2017; Nasta et al., 2017). Thus, altered [2Fe–2S] cluster insertion into Rieske protein and cluster dysfunction leads to full inhibition of respiration. This effect on respiration is attributed to impaired complex II-complex III activity and disruption of III_2/IV_2 supercomplexes (Conte and Zara, 2011). These findings suggest that some members of the Fe S-IBG subsystem-assembly participate in the maturation of III/IV supercomplexes and in an optimal functionality of the ETC. Thus, we investigated the effects of *IBA57* deletion on the expression of Rieske protein in a haploid, monozygotic strain of *S. cerevisiae* to avoid heterozygous complementation. We also evaluated the effects of this deletion on integration of mitochondrial supercomplexes and on mitochondrial ETC function.

2. Materials and methods

2.1. Yeast strains, growth conditions, and survival tests

Mutant strains *grx5*Δ, *iba57*Δ, *rip1*Δ, *sdh2*Δ, and *cox11*Δ correspond to the haploid *S. cerevisiae* BY4741 wild type (Mat a, *his3*Δ, *leu2*Δ0, *met15*Δ0, *ura3*Δ0, *KanMX4*), all strains were obtained from Open Biosystems. Growth tests were carried out using yeast extract peptone dextrose (YPD) culture medium. Culture medium was inoculated with overnight-grown yeast cultures that had reached an optical density of 0.1 at 600 nm (OD_{600}) and incubated at 30 °C with low-speed shaking (50 rpm). Yeast growth (biomass) was spectrophotometrically monitored at OD_{600}.

2.2. Determination of in situ mitochondrial oxygen consumption rate

S. cerevisiae cells (25 mg wet weight) were placed in 2.5 mL of MES-TEA buffer (pH 6.0) in a sealed glass chamber with constant stirring at 25 °C. The oxygen consumption rate (OCR) was measured with a Clark-type oxygen electrode coupled to a biological oxygen monitor (YSI 5300). Basal oxygen consumption (state 4), was induced by adding 20 mM glucose as substrate, and 3 min later, 5 μM of the uncoupling agent carbonyl cyanide *m*-chlorophenyl hydrazone (CCCP) was added to stimulate maximal OCR (uncoupled (U) state). To discriminate the mitochondrial oxygen consumption from unspecific-cytosolic oxygen utilization, the mitochondrial ETC was inhibited with 1 μg antimycin A and a further addition of 0.5 mM KCN (Brand and Nicholls, 2011).

2.3. Mitochondria isolation and determination of the ETC complexes activity

Mitochondria of *S. cerevisiae* were isolated from cultures grown in liquid medium YPD at 30 °C in a shaking incubator by 12 h, using a previously described method (Perez-Gallardo et al., 2013). Detergent permeabilized mitochondria were mixed 250 μL of intact mitochondria (10 mg of protein) plus 750 μL of hypotonic buffer [(KCl 100 mM, $MgCl_2$ 10 mM, Tris-base 10 mM, pH 7.5, and Triton X-100 (0.02%))] with vigorous shaking in a vortex for 15 s. This suspension was centrifuged at 18,600 × *g* for 15 min at 4 °C. Supernatants were discarded and the mitochondrial pellets suspended in buffer composed of 50 mM KH_2PO_4, pH 7.6 and protein was quantified by the Biuret method. Suspensions of permeabilized mitochondria were used to determine the activity of the ETC complexes, as described below.

2.4. Determination of the ETC complexes activity

The activity of complex II was evaluated by measuring the succinate-DCIP oxidoreductase activity of solubilized mitochondria (Perez-Gallardo et al., 2013). For determination of complex II-III activity, the activity of antimycin A-sensitive succinate-cytochrome *c* oxidoreductase was measured using endogenous ubiquinol-6 and succinate as substrates (Perez-Gallardo et al., 2013). While that for determination of complex III activity, it was assayed under the same conditions used for the determination of complex II-III activity, except that decylubiquinol (reduced with $NaBH_4$) was added instead succinate (Cortes-Rojo et al., 2009). Finally, for determination of the complex IV activity, cytochrome *c* oxidase activity was measured as the rate of cyanide-sensitive cytochrome *c* oxidation in presence of antimycin A by adding dithionite-reduced cytochrome *c* (Perez-Gallardo et al., 2013).

2.5. Determination of cis-aconitase activity

Aconitase activity was determined by a modification of the method of Henson and Cleland (Henson and Cleland, 1967) as described elsewhere (Perez-Gallardo et al., 2013).

2.6. Mitochondrial membrane potential

Membrane potential in cells suspensions was determined using the fluorescent, cell-permeable indicator Rhodamine 123 (Rho123; Sigma). Cells suspensions (1×10^7 cells/mL) were loaded with Rho123 (5 μg/mL) and incubated at 30 °C for 30 min in the dark. Suspensions were harvested, washed once and re-suspended in PBS. Membrane potential in suspensions was determined by fluorescence generation and quantified by flow cytometry using a BD Accuri C6 Flow Cytometer (BD Biosciences), monitoring the emission fluorescence in channel FL1 (533/30 nm) (Gomez et al., 2014).

2.7. Raman spectroscopy of mitochondria

Suspensions of intact mitochondria (250 μg) from yeast cultures grown on YPD were subjected to Raman spectroscopy as described previously (Gomez et al., 2014), using a microRaman spectrometer (Dilor model LabRam) equipped with a confocal microscope with 50 × amplification, using He-Ne laser emitting at 632.8 nm and 30 mW at sample point for excitation. Mitochondrial dried-pellets were collocated in a copper plate and laser impacted into a spot of 2 μm with an integration time of 60 s; a 256 × 1024 pixel charge-coupled device (CCD) was used as a photon detector. The spectra obtained correspond to the average of spectra overlapped by 60 s of recording.

2.8. UV spectroscopy of mitochondrial cytochrome

Suspensions of intact mitochondria (2 mg/mL) from yeast cultures grown on YPD were collocated into quartz cell and absorbance spectra were recorded using a spectrophotometer (UV-2550 Shimadzu), monitoring spectrum from 400 to 650 nm. Basal spectrum was obtained using phosphates buffer adding 10 μL KCN (0.4 M) and 10 μL succinate (1 M) incubating 3 min before run the spectrum to determine cytochrome functionality. After, 10 μL antimycin A (0.09 M) was added, incubated by 3 min to total cytochrome *b* reduction. Finally, 0.1 mg dithionite was added in the cuvette and run the spectrum monitoring to determine total cytochrome presence. The spectra obtained correspond to the average of spectra overlapped at least 6 times.

2.9. DNA gene amplification

DNA amplification was carried out by standard PCR method using total or mitochondrial DNA from the *S. cerevisiae* strains, using the Platinum Pfx DNA polymerase (Invitrogen) performed according to manufacturer's instructions. The primers used for gene amplification were designed from the *S. cerevisiae* genome: *IBA57* (fw GGTACCAAA ATGTTCATCAGTAGAAG and rev GCGGCCGCTTTATGAGGCCCGTT ATT), *GRX5* (fw AAGCTTAAAATGTTTCTCCCAAAATTC and rev CTCGAGACGATCTTTGGTTTCTTCTTC), *RIP1* (fw GGATCCAAAATGTT AGGAATAAGATCATCT and rev CTCGAGACCAACAATGACCTTATC ACCATC), *COX2* (fw TCAGGATTCAGCAACACCAA and rev

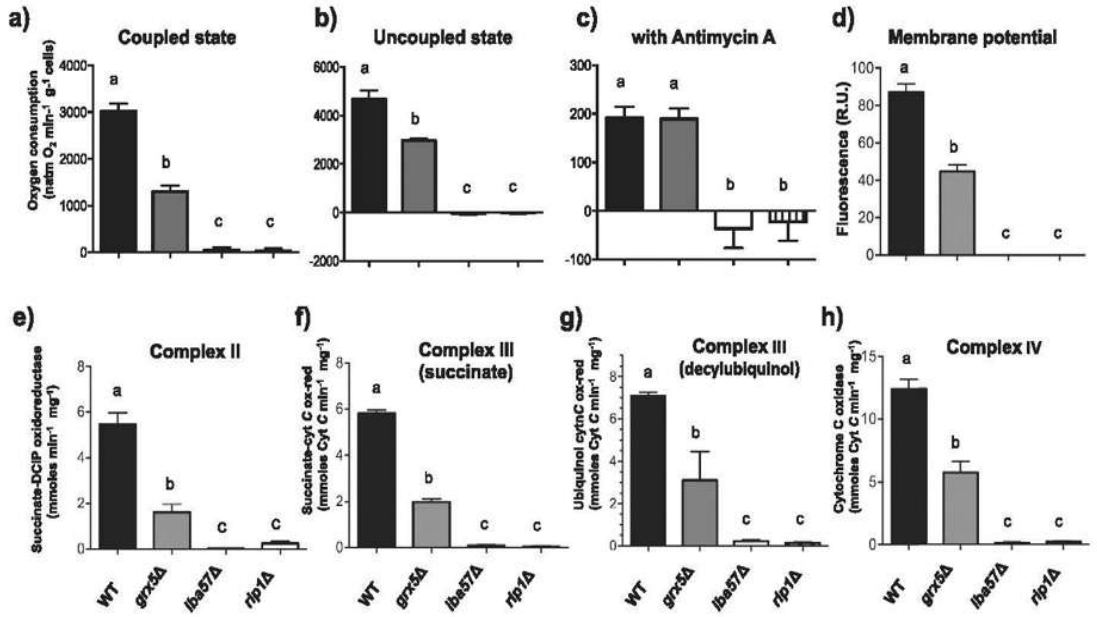

Fig. 1. Evaluation of mitochondrial ETC functionality and [Fe–S]-content in the Iba57p mutant of *Saccharomyces cerevisiae*. a–h) Mitochondria function was evaluated in mitochondria suspensions obtained as described in the Material and Methods, except for (d), in which cells suspensions were used. a–c) Basal oxygen consumption rate (OCR) with glucose as a substrate: a) OCR under coupled state conditions; b) OCR under uncoupled state conditions using CCCP for uncoupling; and c) OCR under complex III-blocking conditions using antimycin A as an inhibitor. d) Membrane potential in cell suspensions. e) Activity of succinate-DCIP oxidoreductase. f) Activity of succinate-cytochrome *c* oxidoreductase using succinate as substrate. g) Activity of ubiquinol-cytochrome *c* oxidoreductase activity using decylubiquinol as substrate. h) Activity of cytochrome *c* oxidase. Values are the mean of three independent experiments. SEs are indicated as bars ($n = 9$), one-way analysis of variance (ANOVA) with Tukey's post hoc test was used to compare yeast strains, and significant differences ($p < 0.05$) were indicated by different lowercase letters.

TCAAATTCAACAGTTTCACCACT), *COX3* (fw TTAGGTGCATGTTGACC ACC and rev CCATCAGAGATAGTGAATGCAGC).

2.10. Native gel electrophoresis and western blot

For native polyacrylamide gel electrophoresis, samples of 100 µg of mitochondrial protein isolated as described above, and solubilized using buffer A containing dodecylmaltoside (1 g/g), triton X-100 (2.4 g/g), or using digitonin (3 g/g) as described (Schagger, 2006), and separated by native polyacrylamide gel electrophoresis on 8% Bis-tris gels (BN-PAGE) (Musatov and Robinson, 2012; Schagger and Pfeiffer, 2000; Stames and O'Toole, 2013). After electrophoresis, the mitochondrial complexes visualized in the gel were excised in both horizontal or vertical manner, and incubated for 30 min in a solution containing 60 mM Tris/HCl (pH 6.8) and 0.2% SDS at room temperature. Each gel slice was placed horizontally and encased in 5% polyacrylamide stacking gel in the gel for the second dimension (SDS-PAGE), already containing the separation gel (12% polyacrylamide and 0.2% SDS). The gels were subjected to electrophoresis and in one side they were silver-stained and on the other side transferred to polyvinylidene difluoride (PVDF) membranes for Western blot procedure. Additionally, SDS-PAGE was also applied for separation in mitochondrial and cell-free extracts. For immunodetection assays, 50 µg of mitochondrial protein or cellular extracts were run in 12% SDS-PAGE gels and transferred to PVDF membranes. Membranes were blocked using dry milk in PBS-T and blotted with the *S. cerevisiae* antibodies (anti-Rip1p, anti-Cox2p or anti-Cox3p) as first antibody in blocking medium at a 1:20000 dilution for 2 h at 4 °C. After washing, the membranes were incubated with the secondary antibody, a monoclonal anti-mouse IgG HRP-conjugate (Promega), in blocking medium at a 1:10,000 dilution for 2 h at 4 °C; the membranes were washed with PBS-T and developed using Supersignal West Pico Luminol (Pierce) and exposing in light-sensitive films or luminescence determined by using a ChemiDoc MP imaging system (BioRad). Assays were conducted by at least three independent assays and representative images are shown. Bands intensities in gels or films were quantified using the Image J software.

2.11. Confocal microscopy of yeast suspensions

S. cerevisiae YPD-grown cultures were harvested and suspended in PBS at 1×10^7 cell/mL and loaded with the fluorescent probe. DNA staining in cells was visualized by fluorescence resonance energy transfer (FRET). Cells were suspended in deionized water and added 1 µL/mL of SYTO9 and propidium iodide stain mix (Live/dead FungaLight yeast viability kit for flow cytometry; Molecular Probes, Invitrogen) incubating 30 min at room temperature; after this, samples were observed by confocal microscopy at 482/502 nm and 535/617 nm, respectively. Images were acquired at 40–60 × magnifications.

3. Results

3.1. Mitochondrial ETC function is affected by IBA57 deletion

Mutants in the Fe–S-IBG subsystem components have been considered as respiratory-deficient strains, but possess normal capability to grow in fermentative conditions, suggesting that their lack of a mitochondrial DNA (mitDNA) causes the failure of respiratory complexes (petite or rho$^-$ phenotypes) (Muhlenhoff et al., 2011). However, GRX5 mutants partially maintain their mitDNA (Rodríguez-Manzaneque et al., 2002). We observed that the *isa1*Δ mutant showed respiratory deficiency and strong/null formation of respiratory supercomplexes, while only partial effects were observed for the *grx5*Δ mutant (Gomez et al., 2014). These results suggest that some Fe–S-IBG subsystem components causing respiratory-deficiency are not a consequence of the

total lack of mtDNA; therefore, the Fe S-IBG subsystem may affect respiratory complex conformation. Proteins other than Grx5p, such as Iba57p, may be involved in this process.

To determine to what extent *IBA57* mutation impairs the overall functionality of the ETC in *S. cerevisiae*, in situ mitochondrial oxygen consumption rates (OCRs) of the mutant were measured. Respiration was fully inhibited in both coupled and uncoupled states in the mitochondria of *iba57*Δ and *rip1*Δ mutants, whereas in the *grx5*Δ mutant, only a partial decrease in OCR was observed compared to in the WT strain (Fig. 1a–b). Notably, antimycin A treatment caused oxygen release rather than oxygen consumption in the assay chamber in the *iba57*Δ and *rip1*Δ mutants compared to the WT and *grx5*Δ mutant (Fig. 1c). Additionally, in accordance with its inability to respire, the *iba57*Δ and *rip1*Δ mutants did not exhibit membrane potential (Δp) (Fig. 1d). The partial reduction in OCR in the uncoupled state observed in *grx5*Δ cells supported the partial dissipation of membrane potential detected in this mutant.

Partial reactions of the ETC were analyzed to determine whether the deletion of Iba57 protein, which is part of the Fe–S-IBG subsystem dedicated to the maturation of [4Fe 4S] clusters, also affects the activity of mitochondrial complexes lacking this type of Fe–S center (i.e., III and IV). As expected, the activity of complex II, a protein complex containing a [4Fe–4S] center, was fully inhibited in *iba57*Δ and *rip1*Δ mutants; in contrast, the *grx5*Δ mutant displayed ~30–40% of activity compared to WT cells (Fig. 1c). A similar trend was observed for complexes III and IV (Fig. 1f–h).

Antimycin A-sensitive succinate cytochrome *c* oxidoreductase activity (i.e. complex II-complex III activity) is dependent on electron transfer between complex II and complex III. Thus, to eliminate the possibility that impaired succinate–cytochrome *c* oxidoreductase activity resulted from impaired complex II activity and not from direct damage to complex III, we tested the activity of complex III by measuring the oxidation of decylubiquinol (Fig. 1g). The activity of complex III was fully abolished in *iba57*Δ and *rip1*Δ mutants, while mitochondria from *grx5*Δ exhibited activity of ~40% compared to that from the WT strain (Fig. 1g). These results indicate that deletion of *IBA57* causes the dysfunction of the ETC, and this deletion is likely associated with the disintegration of ETC supercomplexes.

3.2. [Fe–S] cluster-containing proteins are affected by IBA57 deletion

Determination of the enzymatic activity of *cis*-aconitase has been used to monitor the assembly of [4Fe 4S] centers into target proteins (Gardner, 1997; Muhlenhoff et al., 2011). Accordingly, we determined the aconitase activity in mitochondria of the *iba57*Δ mutant. As expected, aconitase activity was nearly completely abolished in the *iba57*Δ mutant, while decreased activity was observed in the *grx5*Δ mutant (described as no essential protein for aconitase assembly) (Fig. 2a). Additionally, we tested aconitase activity in the *rip1*Δ mutant (used here as a strain lacking complex III activity because of deletion of the Rieske subunit), and found that its activity was decreased to approximately 50% compared to the WT strain. These results indicate that in the *iba57*Δ mutant, the insertion of [4Fe–4S] clusters into aconitase target proteins was prevented, confirming that the Fe–S-IBG subsystem participates in assembly of apoproteins [4Fe 4S]-dependent. This was further confirmed using Raman spectroscopy analysis in mitochondria isolated from the *iba57*Δ mutant, as in the *rip1*Δ mutant. Signal intensities at 460–545 cm^{-1} and 640–660 cm^{-1} in the 632.8 nm Raman spectra corresponding to photonic emission characteristics of the [Fe–S] centers were markedly diminished (Fig. 2b). The Raman signal peaks were clearly observed with high intensity in the mitochondria from the WT and *grx5*Δ mutant. Decreased [Fe–S] content observed in the *iba57*Δ mutant further confirmed that Iba57p is involved in the biosynthesis and assembly of [Fe–S] clusters into mitochondrial target proteins. Thus, *IBA57* deletion may be associated with the dysfunction of ETC supercomplexes, and this deletion likely affects the insertion or maturation process of the [Fe S] center-containing proteins. In addition, the [Fe–S] centers analyzed by Raman spectrometry in the *rip1*Δ mutant indicate that the Rieske protein is related to respiratory supercomplexes maturation/assembly.

3.3. ETC supercomplexes maturation are affected by IBA57 deletion

To determine whether the deletion of Iba57p directly or indirectly disturbs the formation of III/IV supercomplexes by preventing the maturation of [Fe–S] clusters containing-proteins in mitochondrial complexes, we tested the effects of Iba57p on supercomplex maturation and the influence of Rieske protein. We analyzed ETC supercomplex assembly by blue native polyacrylamide gel electrophoresis (BN-PAGE) with two types of mitochondrial protein-solubilizing treatments: digitonin (light condition) and dodecylmaltoside (stronger condition). In addition, we conducted immunodetection with the anti-Rip1 antibody for Rieske-containing supercomplex identification in mitochondrial supercomplexes.

Mitochondrial extracts from WT cells evaluated by BN-PAGE (first dimension) showed five well-defined protein bands, B1–B5 (Fig. 3a–b). When the contents of the WT gel lane were resolved in a second dimension by SDS-PAGE, and immunodetected, the B2 and B3 bands reacted with the anti-Rip1p antibody (Fig. 3c–d). In addition, the BN-PAGE gels immunodetected with anti-Rip1p antibody showed strong signals in the B1, B2, and B3 bands, as well as in the B3, B4, and B5 bands when the anti-Cox3p antibody was used (Fig. 3e–g). These results confirm that bands B2 and B3 corresponded to the III_2IV_2 and III_2IV_1 supercomplexes, respectively (Fig. 3g). Determination of band intensity of the supercomplexes in the BN-PAGE gels showed that in mitochondria from the negative control strain *rip1*Δ, bands B1, B2, and B3 were significantly decreased (Fig. 3a–b). Remarkably, a similar banding pattern was observed for the *iba57*Δ and *grx5*Δ mutants compared to that for WT yeast or for the two control mutant strains, such as the *cox11*Δ and *sdh2*Δ. *cox11*Δ (which lacks cytochrome *c* oxidase subunit 11 of complex IV) and *sdh2*Δ (which lacks succinate dehydrogenase that forms complex II) are mutations that do not affect Rip1p expression.

On 2-D SDS-PAGE gels, the lane corresponding to the *iba57*Δ mutant from the BN-PAGE gel like the B3 band, indicated a decrease in protein content compared to in the WT strain (Fig. 3h and Supplementary Fig. S1a–b).

Immunoblotting of bands B2 and B3 cut horizontally from the BN-PAGE gels showed that Rip1 protein integration into supercomplexes III_2IV_2 and III_2IV_1 was absent in *iba57*Δ and *rip1*Δ mutants, but not in *cox11*Δ, *sdh2*Δ, and the WT strain (Fig. 4a). For the *grx5*Δ mutant, Rip1p was absent in the B2 band, but was observed in the B3 band in a similar proportion as in the WT. Interestingly, in both the *cox11*Δ and *sdh2*Δ mutants, the Rip1p blotting signal was stronger for both, B2 and B3 bands (Fig. 4a). When BN-PAGE gels were run using dodecylmaltoside-treated samples (stronger solubilizing conditions), the B3 band corresponding to the III_2IV_1 supercomplex was clearly absent from the *iba57*Δ and *rip1*Δ mutants, light in *grx5*Δ, but not affected in the *sdh2*Δ mutant (see Supplementary Fig. S1c). These results indicate that Iba57p deletion abolished III_2IV_2 and III_2IV_1 supercomplex formation.

3.4. ETC supercomplex maturation is mediated by Rieske protein integrity

The [Fe–S] centers Raman signals and bands corresponding to the respiratory supercomplexes decreased in the *iba57*Δ and *rip1*Δ mutants, suggesting that Iba57p is involved in Rieske protein maturation and, in turn, Rieske protein is related to respiratory supercomplex formation as previously suggested (Conte et al., 2015; Conte and Zara, 2011). Thus, we determined the levels of Rip1p in mitochondrial extracts of the *iba57*Δ and *rip1*Δ mutants.

As expected, Rip1p expression was not observed in the mitochondria of the *rip1*Δ mutant (Fig. 4b). However, expression of Rip1p in the mitochondria of the *iba57*Δ and *grx5*Δ mutants was decreased

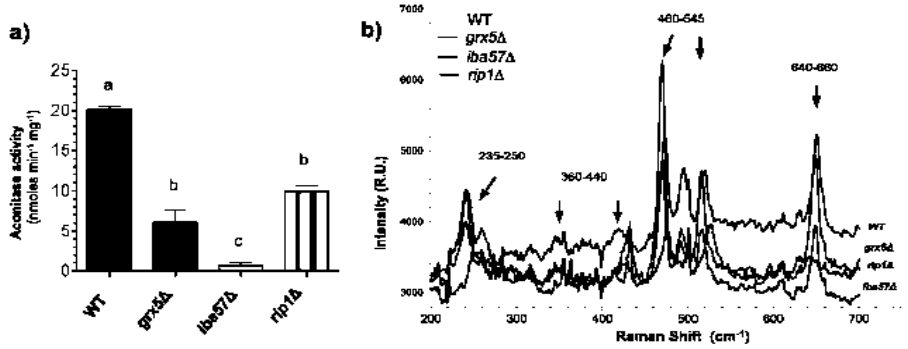

Fig. 2. Evaluation of [Fe-S] containing proteins in *Saccharomyces cerevisiae*. a) Enzymatic activity of its aconitase was determined in mitochondrial suspensions as described in the Materials and Methods. Values are the mean of three independent experiments. SE values are indicated as bars ($n = 3$); one way analysis of variance (ANOVA) with Tukey's post-hoc test was used to compare yeast strains, and significant differences ($p < 0.05$) are indicated by lowercase letters. b) Analysis of mitochondria for S containing proteins in *S. cerevisiae* by Raman spectroscopy. Mitochondrial suspensions were used for Raman spectra determination, recorded at a laser excitation of 632.8 nm at 30 mW. Each spectrum is the average of scans recorded over 60 s, using photon counting at 0.5 cm^{-1} increment spectral resolution. Bands corresponding to the [2Fe-2S], [3Fe-4S], and [4Fe-4S] clusters are indicated with arrows (Chang et al., 2013).

significantly compared to in WT. In the *sdh2*Δ mutant, Rip1p expression was similar to that in the WT strain. The Cox2 and Cox3 proteins (which form the core of cytochrome *c* oxidase complex and are encoded by mitDNA) were blotted on the same membrane. The results showed that Cox2 protein was expressed at low levels in the *iba57*Δ and *rip1*Δ mutants, but Cox3 protein was unaffected (Fig. 4b). Densitometry analysis of protein expression, normalized to Cox3p expression, showed that in the *iba57*Δ and *rip1*Δ mutants, Rip1p and Cox2p expression was decreased significantly (Fig. 4c). These results indicate that Iba57p deletion affected Rip1p maturation into the mitochondrial complexes, affecting the integrity of Rieske protein associated with supercomplex maturation.

Additionally, to evaluate cytochrome integrity in the mitochondrial supercomplexes, cytochrome functionality and presence was monitored in the *iba57*Δ and *rip1*Δ mutants. Cytochrome content monitoring by spectra profiles in the WT strain clearly revealed cytochromes $c + c_1$ (signal at 550 nm), cytochromes *b* (signal at 560 nm), and cytochromes *a* (signal at 610 nm) (Fig. 5a). Interestingly, cytochromes $c + c_1$ and cytochromes *b* were also observed in the *iba57*Δ, *grx5*Δ, *rip1*Δ, and *cox1*Δ mutants, although with lower signals compared to in the WT strain, but did were not observed in the rho$^-$ strain. While that cytochrome functionality determined by their capability of electron transport was observed in the WT strain, although slight signal also as in the *iba57*Δ, *grx5*Δ, and *cox1*Δ mutants, but not in the *rip1*Δ mutant and rho$^-$ strain (Fig. 5b). These results indicated that in the *iba57*Δ mutant, Cox2p, Cox3p, and cytochromes *c* and *b* were expressed and functional, indicating that the *iba57*Δ mutant contains mitDNA, further confirming that the Iba57p affects complex III of the ETC.

The expression data for Cox2 and Cox3 proteins encoded by mitDNA were further confirmed by DNA gene amplification via PCR for mitochondria from the mutants. *COX2* and *COX3* (mitochondrial encoded genes) amplification was observed in WT strain, also as in *iba57*Δ, *rip1*Δ, and *grx5*Δ mutants; as expected, expression in a constructed petite mutant was not detected (Fig. 6). Unexpectedly, however, in the *grx5*Δ mutant, the *COX2* and *COX3* DNA fragments were different sizes. Confocal microscopy analysis also indicated the presence of DNA-containing mitochondrial structures in the *iba57*Δ mutant, but not in the petite yeast (Fig. 7).

4. Discussion

Isa1p is required for the maturation of [4Fe-4S] clusters (Muhlenhoff et al., 2011; Sheftel et al., 2012), which precludes its participation in both, the maturation of the [2Fe-2S] cluster contained in the Rip1 subunit of complex III and in the biogenesis or functioning of the complex IV (because this complex lacks of an [Fe-S] cluster). Thus, our previous findings regarding impaired supercomplex formation and decreased activities of both complexes III and IV in the *isa1*Δ mutant was unexpected, as we predicted that only decreased complex II activity would occur without interfering in supercomplex formation, as this complex does not take part in this process or possess a [4Fe-4S] cluster (Gomez et al., 2014). Thus, we tested the effects of mutation in *IBA57*, whose product forms the Fe-S-IBG subsystem on supercomplex formation, ETC function, emphasizing the probable participation of Rip1p in this process given that its participation in supercomplex integration has been widely recognized (Cruz et al., 2015; Cui et al., 2014; Zara et al., 2009).

Respiratory supercomplexes are now considered the functional units mediating optimal electron transfer from reducing equivalents (i.e. NADH or $FADH_2$) to molecular oxygen by channeling substrates and decreasing ROS generation (Vartak et al., 2013). Therefore, impaired respiration and mitochondrial depolarization in the *iba57*Δ mutant (Fig. 1), and the inability of the mutant to form III/IV supercomplexes (Fig. 3) are in agreement with this hypothesis. Moreover, the role of Rip1p in the integrity of the supercomplexes is reinforced by the observation of full impairment of respiration and membrane potential observed in the *rip1*Δ mutant (Fig. 1). The increased release of oxygen in the *iba57*Δ and *rip1*Δ mutants in response to antimycin A suggest that increased superoxide generation occurred at the level of complex III (see Fig. 1 in Gomez-Gallardo et al., in press). It has been reported that the failure to insert the [2Fe-2S] cluster of Rip1p alters the environment of quinone redox sites of complex III (Gutierrez-Cirlos et al., 2002). These alterations may lead to enhanced ROS generation because of augmented electron leakage at these redox sites. In agreement with this prediction, the *rip1*Δ mutant exhibited a phenotype similar to that of the *iba57*Δ mutant (see Fig. 1 in Gomez-Gallardo et al., in press). This suggests that Rip1p deletion alters electron transfer between the redox sites of the complex III, likely because of the lack of [2Fe-2S] cluster insertion, which occurs in the *rip1*Δ mutant.

The role of the Fe-S-IBG subsystem in the formation of supercomplexes through a mechanism dependent on Rip1p was supported by the negligible expression of Rip1p in cellular extracts of the *iba57*Δ and *grx5*Δ mutants (Fig. 3). These results suggest that the Fe-S-IBG system affects the expression of Rip1p, the catalytic subunit [2Fe-2S] cluster

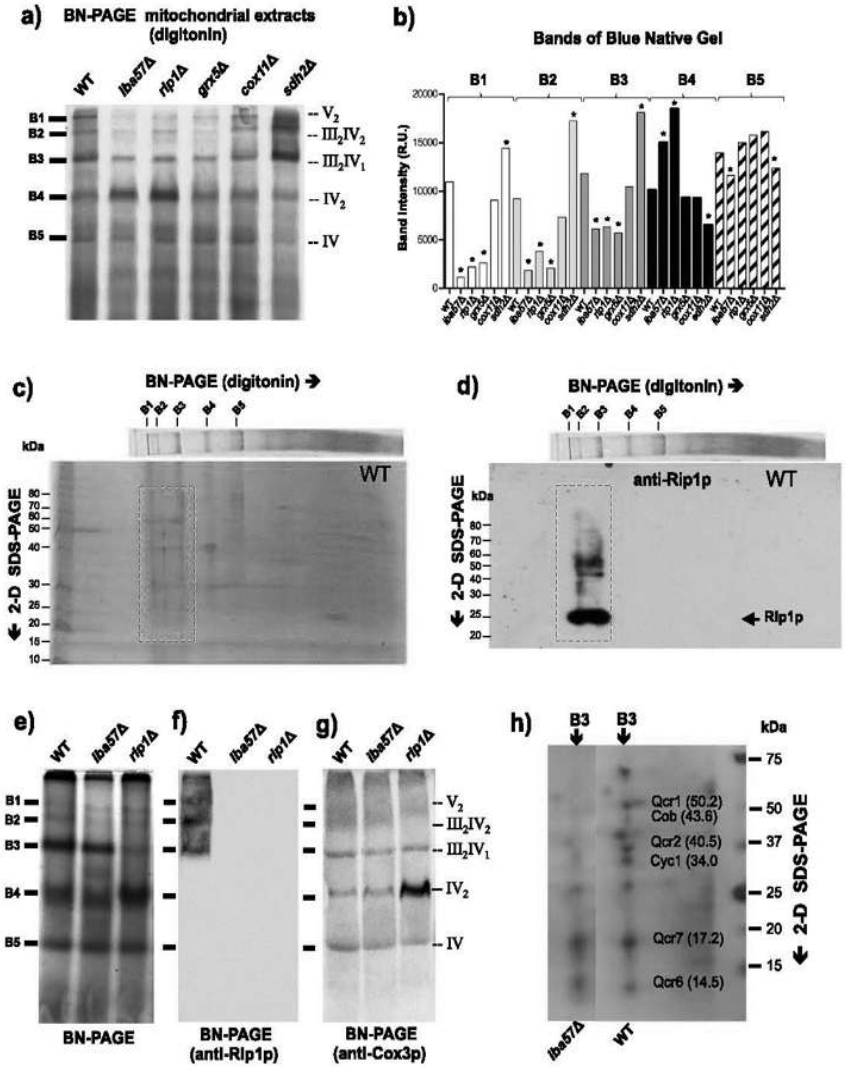

Fig. 3. Evaluation of ETC mitochondrial supercomplexes formation in the Iba57p mutant of *Saccharomyces cerevisiae*. Mitochondrial suspensions were solubilized with digitonin and the proteins were separated using blue native polyacrylamide gel electrophoresis (BN-PAGE), as described in the Materials and Methods. The ETC mitochondrial supercomplexes are indicated to the right of the gels, based on the results shown. a) BN-PAGE of mitochondrial suspensions solubilized with digitonin; B1–B5, major protein bands corresponding to mitochondrial supercomplexes. b) Densitometry analysis plot of the bands corresponding to supercomplex bands observed in panel (a) using Image J software. Values are the mean and SE values are indicated as bars (n = 3), one-way analysis of variance (ANOVA) with Tukey's post hoc test was used to compare yeast strains, and significant differences ($p < 0.05$) are indicated with asterisks. c) Second dimension (SDS-PAGE) of gel slice from BN-PAGE corresponding to the WT strain, silver-stained, SDS-PAGE BenchMark Protein Ladder (Invitrogen) is showed. d) Western blot of 2-D SDS-PAGE gel (c) using anti-Rip1 antibody and monoclonal anti-mouse IgG horseradish peroxidase (HRP) conjugate as the second antibody. e–g) Lines from BN-PAGE gel (e) were transferred to PVDF membranes and detected by western blotting using anti-Rip1 antibody (f) and anti-Cox3p antibody (g). h) 2-D SDS-PAGE gel of the B3 band from BN-PAGE gel. Proteins are indicated. Molecular mass marker in kilodaltons is shown to the right of the gel.

containing of cytochrome *c*, via cluster integration. This could be inferred as it has been demonstrated that failure in the insertion of the [2Fe–2S] cluster into Rip1p leads to augmented susceptibility to proteolysis (Gutierrez-Cirlos et al., 2002). Another line of evidence further supporting a role for the Fe–S-IBG subsystem in the formation of supercomplexes and likely in the maturation of the [2Fe–2S] cluster of Rip1p was the decreased levels of supercomplexes III_2IV_2 and III_2IV_1, observed in the *iba57*Δ mutant of the Fe–S-IBG subsystem, whose banding pattern was very similar to that observed for the *rip1*Δ mutant. Moreover, the role the Fe–S-IBG subsystem became more evident when supercomplex bands were run in a second dimension, which revealed the absence of Rip1p in the remaining supercomplex bands of *iba57*Δ and when supercomplex analysis was conducted under conditions more severe mitochondrial proteins solubilization (see Supplementary Fig. S1c). These results further suggest that Rip1p integrity plays important roles in supercomplex conformation and that its maturation depends on Iba57p from the Fe–S-IBG subsystem. In agreement with this idea, Rip1p expression was unaffected in the *sdh2*Δ mutant (which lacks succinate dehydrogenase to form complex II) and *cox11*Δ mutant (which lacks cytochrome *c* oxidase subunit 11 of complex IV) (Fig. 3).

The activity of the complex II-complex III segment of the ETC was fully inhibited in the *iba57*Δ mutant and *rip1*Δ control strain (Fig. 1).

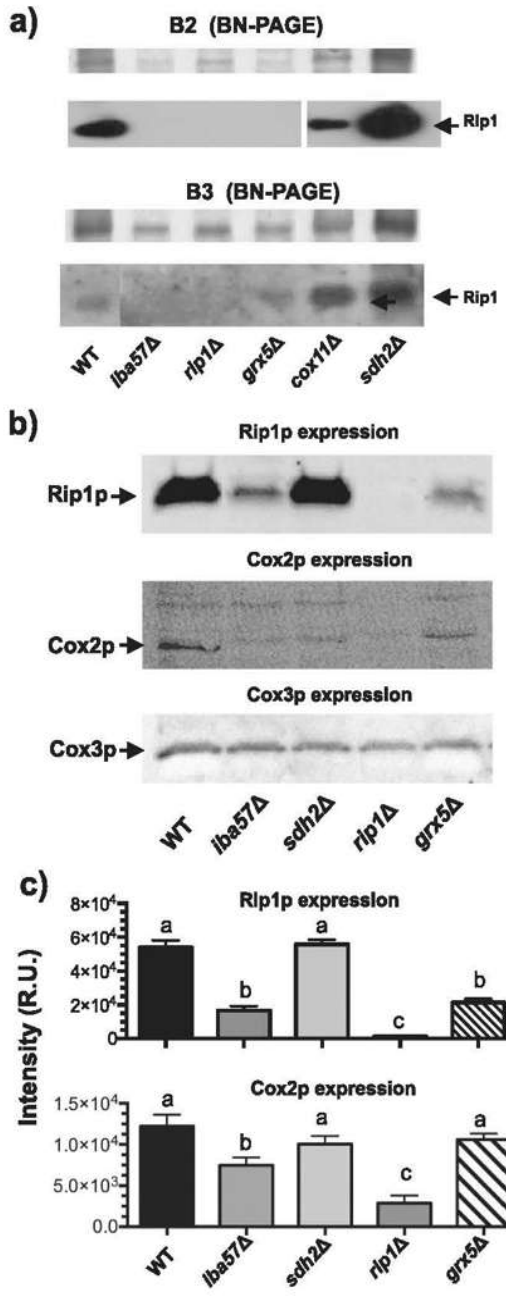

Fig. 4. Immunodetection of Rieske protein in the Iba57p mutant of *Saccharomyces cerevisiae*. a) Immunoblotting of lines B2 and B3 cut from mitochondrial extracts separated by BN-PAGE gels. b) Mitochondrial extracts separated by SDS-PAGE gels, after western blot using anti-Rip1p, anti-Cox2p, and anti-Cox3p antibodies as the primary antibody and monoclonal anti-mouse IgG horseradish peroxidase (HRP) conjugate as the secondary antibody. c) Densitometry analysis of (b) normalizing with Cox3p expression, data correspond to three independent assays determining the band intensity by densitometry analysis using Image J software. Values are the mean and SE values are indicated as bars ($n = 3$), one-way analysis of variance (ANOVA) with Tukey's post hoc test was used to compare yeast strains, and significant differences ($p < 0.05$) are indicated by lowercase

Although this observation may be the result of impaired complex II activity (i.e., a complex containing [4Fe–4S] clusters) arising from the use of succinate as a substrate, we observed the same result using decylubiquinol, a direct substrate for complex III. Therefore, dysfunction of complex III in the *iba57*Δ mutant may be associated with impaired Rieske subunit assembly as shown in Fig. 3. Impaired complex III activity may have resulted from oxidative damage due to uncontrolled ROS production as observed in these mutants (see Figs. 1–2 in Gomez-Gallardo et al., in press). However, based on the results of aconitase activity, this is not the main reason, as aconitase, a protein whose activity is a marker of oxidative stress (Gardner, 1997; Muhlenhoff et al., 2011), was moderately impaired in the *rip1*Δ mutant, which exhibited neither Rip1p expression nor complex III activity. This indicates that enhanced oxidative stress is not sufficient for inducing complete impairment of complex III activity.

Complex IV activity was also fully inhibited in the *iba57*Δ mutant and decreased in the *grx5*Δ mutant, which lack an [Fe–S] cluster. This may be explained by their inability or instability to form ETC supercomplexes; when complex III has an incorrect conformation, it is susceptible to protein degradation, which may strongly affect the activity of complex IV. This suggestion agrees with the observation that when complex III has an incorrect conformation, which may be associated with the absence of Rip1p, the activity of complex IV is strongly affected (Schilke et al., 2006). Therefore, the assembly of ETC supercomplexes formed by complexes III and IV is favored by integration of Rip1p into complex III (Conte et al., 2015; Conte and Zara, 2011; Cui et al., 2012; Diaz et al., 2012). In the absence of the [2Fe–2S] cluster, Rip1p is susceptible to protease degradation, although apo-Rip1 (without a Fe–S cluster) has been detected to be inserted into complex III, resulting in a nonfunctional complex (Smith et al., 2012).

Mutants in the ISC assembly system, as in the Fe–S-IBG subsystem, are unable to conduct mitochondrial respiration and are considered as $rho^{0/-}$ mutants. This suggests that the effects on supercomplexes in the *iba57*Δ mutant occurred because of the absence or down-regulation of expression of mitDNA. However, we identified in mitochondrion extracts of the *iba57*Δ mutant, the expression of Cox2 and Cox3 proteins (proteins that form the core of cytochrome *c* oxidase complex) and in isolated mitochondria the presence of cytochrome *c* and *b*, although slight signals observed, both in its functional status and presence were found (Fig. 5). Additionally, DNA staining in the mitochondria and DNA amplification of *COX2* and *COX3* in the *iba57*Δ mutant (Figs. 6–7) indicated that the *iba57*Δ mutant possesses mitDNA; thus, its inability to respire and decrease supercomplex maturation or cytochrome content is not completely attributed to its rho^- phenotype, although the less defined mitochondrial structures suggest decreased mitDNA content. ETC dysfunction has been associated to events of regulation of expression, large deletions, or less mitDNA content (rho^-). In this sense, mitDNA integrity depends on ATP synthase assembly, whose dysfunction due to either nuclear or mitochondrial mutations lead to rapid mitDNA loss, generating rho^- phenotypes; additionally, mitDNA rearrangements associated to introns may occur (Lipinski et al., 2010) or dysfunction in respiration depending on complex III of the ETC increases the levels of ROS, contributing to mitDNA loss (Gomes et al., 2013).

The Isa1/Isa2 and Iba57 proteins have been extensively described to participate in the assembly of [4Fe–4S]-type centers from specific apoproteins (Brancaccio et al., 2014; Muhlenhoff et al., 2011; Sheftel et al., 2012). The present study revealed that Iba57p may also be involved in the maturation of the Rieske subunit of ETC complex III and is probably associated with transference or recycling of its [2Fe–2S] cluster (see Fig. 3 in Gomez-Gallardo et al., in press). Although our results may appear to be in conflict with the idea of a central role for Isa1/Isa2 and Iba57 in the assembly of [4Fe–4S] clusters, this system may have a dual function in directly transferring [2Fe–2S] centers to Rip1 apoprotein or participate in the maturation of [4Fe–4S] by a fusion of two [2Fe–2S] centers, as proposed previously (Banci et al., 2014). In their working

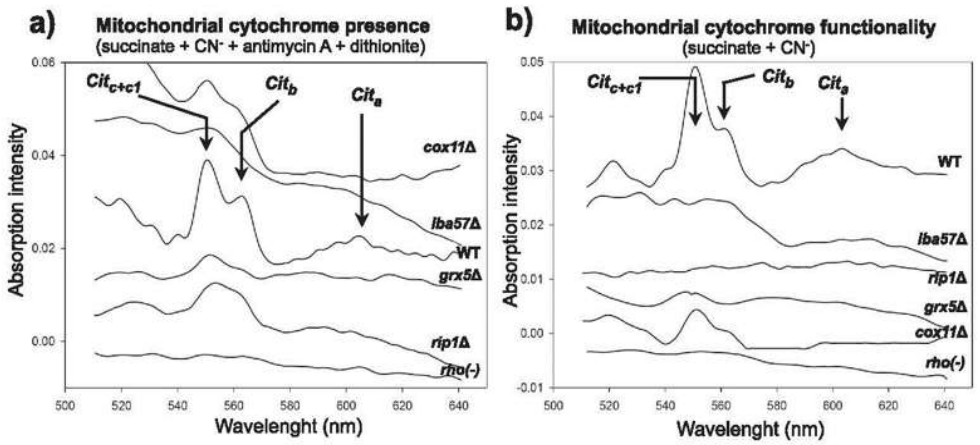

Fig. 5. Analysis of mitochondrial cytochromes in *S. cerevisiae* by UV spectroscopy. Mitochondrial suspensions were used for UV spectra determination, recording spectrum from 400 to 650 nm. a) Basal spectrum of mitochondrial suspensions using succinate as substrate, cyanide and antimycin A as inhibitors, and dithionite as cytochrome-reducing agent (to determine cytochrome presence). b) Using succinate as substrate and cyanide as inhibitor (to determine cytochrome functionality). The spectra obtained correspond to the average of spectra overlapped at least 6 times. Bands corresponding to the cytochromes are indicated with arrows.

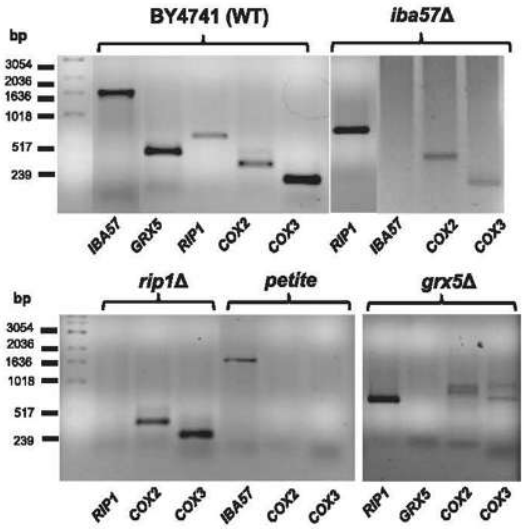

Fig. 6. Gene amplification of nuclear and mitochondrial genes in *Saccharomyces cerevisiae* strains. PCR products obtained from total DNA amplification using oligonucleotides specific for each gene as described in the Materials and Methods section. Representative agarose gels stained with ethidium bromide are presented. Petite rho^0 strain was obtained from BY4741 wild-type yeast by ethidium bromide reagent treatment. Expected sizes of DNA fragments were as follows: *IBA57* (1508 bp), RIP1(654 bp), *GRX5* (460 bp), *COX2* (357 bp), and (*COX3* (239 bp).

model, they found that the ISCA1/ISCA2 heterodimer in humans (Isa1/2p homologs of yeast) can bind either [2Fe–2S] or [4Fe–4S] clusters, with the human GRX5 (Grx5p homolog) also binding $[2Fe–2S]^{2+}$ clusters (Ajit Bolar et al., 2013; Al-Hassnan et al., 2015; Beilschmidt et al., 2017). In this mechanism, two GRX5-$[2Fe–2S]^{2+}$ complexes may generate a $[4Fe–4S]^{2+}$ cluster that can be donated to a heterodimeric ISCA1/ISCA2 complex, suggesting that the protein formed acts as an "assembler" of [4Fe–4S] clusters and is the functional unit in mitochondria that receives [2Fe–2S] clusters from human GRX5 and assembles [4Fe–4S] clusters before their transfer to the final target apoproteins. Recently, the existence of heterocomplexes [2Fe–2S]-BOLA1-GRX5 and [2Fe–2S]-BOLA3-GRX5 was also confirmed (Nasta et al., 2017). In addition, examination of the levels of several Fe/S proteins by RNAi in human HeLa cells showed that for mitochondrial aconitase, succinate dehydrogenase, several proteins of complex I, and Rieske protein, but not ferrochelatese (a [2Fe–2S]-dependent protein) and heme content, their expression decreased under deficiency of ISCA1, ISCA2, and IBA57; additionally, alterations in the mitochondrial morphology and loss of cristae membranes were observed (Sheftel et al., 2012). The authors suggested that these effects were a consequence of pleiotropic effects on other members of the ETC. However, our results support a role for Iba57p in inserting [2Fe–2S] in the Rieske subunit, likely via the Isa1/Isa2 proteins, which agrees with the ability of ISCA1/2 to bind this type of Fe–S cluster, as suggested previously (Banci et al., 2014; Beilschmidt et al., 2017; Braymer and Lill, 2017; Nasta et al., 2017).

Other approaches supporting this hypothesis are related to the bacterial fumarate and nitrate reduction regulator, which functions as a switch between aerobic and anaerobic metabolism, where its Fe–S cluster transforms from the active $[4Fe–4S]^{2+}$ form in oxygen-limiting conditions to a $[2Fe–2S]^{2+}$ form during oxygen or superoxide exposure, with $[3Fe–4S]^{1+}$ as an intermediary form, suggesting that the Fe–S cluster is involved in the molecular mechanism of O_2 sensing by fumarate and nitrate reduction regulator (Crack et al., 2007; Jervis et al., 2009; Zhang et al., 2012). Similarly, some $[2Fe–2S]^{2+}$ clusters are remodeled during O_2-induced degradation of the $[4Fe–4S]^{2+}$ clusters in biotin synthase. This suggests the occurrence of $[4Fe–4S]^{2+} \leftrightarrow [2Fe–2S]^{2+}$ cluster interconversion and raises the possibility that this process is used in vivo to regulate enzyme activity in response to oxidative stress (Zhang et al., 2012). Thus, the Isa1/Isa2/Iba57/Grx5 subsystem may participate in the sorting of both [4Fe–4S] and [2Fe–2S] clusters, where oxygen tension and/or excessive ROS generation may be the factors or "switch" controlling which type of [Fe–S] cluster is inserted into the apoproteins. This may be physiologically important for yeast because of their anaerobic metabolism, although a hypothetical signal that allows this system to "switch" between the delivery of [2Fe–2S] or [4Fe–4S] centers requires further investigation. In agreement with the versatility of the Fe–S-IBG subsystem in the metabolism of a variety of [Fe–S] species, we observed large decreases in the levels of [Fe–S] clusters and cytochromes analyzed by Raman and UV spectrometry in isolated mitochondria from the

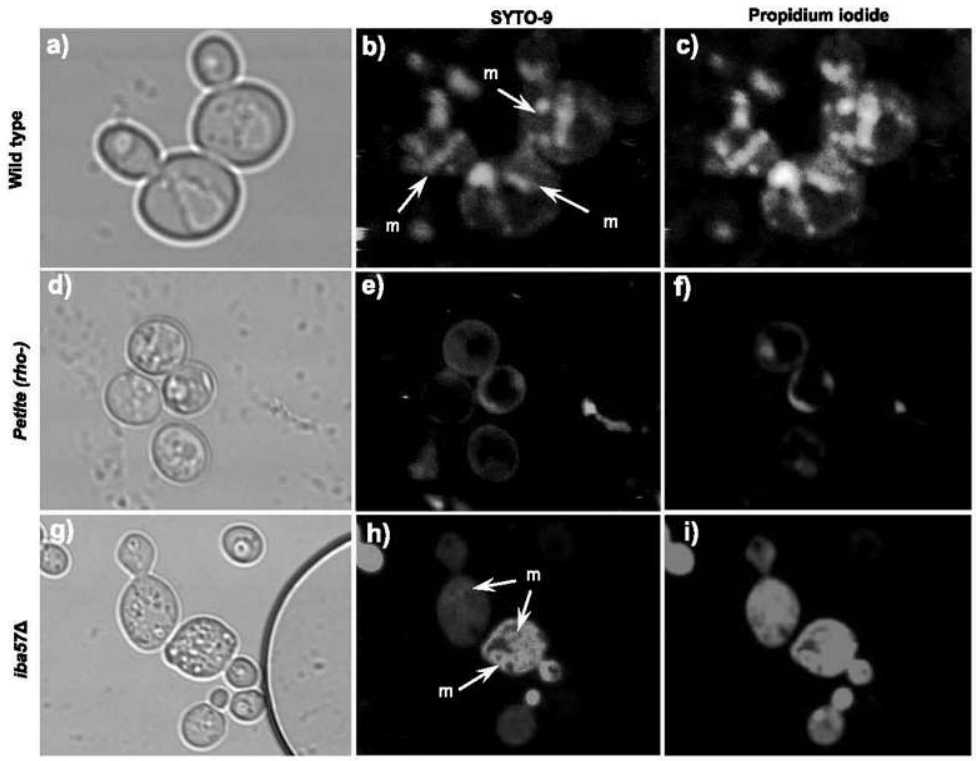

Fig. 7. Microscopy images of *Saccharomyces cerevisiae* cells and mitochondrial structures. YPD-grown yeast cultures were visualized by fluorescence resonance energy transfer (FRET) using SYTO9 and propidium iodide stain mix (Live/dead FungaLight yeast viability kit); samples were observed at 482/502 and 535/617 nm, respectively, using a confocal microscope (Olympus FV1000). a–c) Wild type BY4741 (WT) yeast; d–f) petite (rho $^-$) BY4741 strain; g–i) *iba57*Δ mutant. Cells are shown in which mitochondria is indicated by (m). Images of the cells were taken at 40–60 × magnification.

*iba57*Δ mutant, as well as in the positive control strain *rip1*Δ.

In *S. cerevisiae*, supercomplex III_2/IV_2 was significantly affected in mitochondria isolated from *iba57*Δ and *rip1*Δ mutants; interestingly, the activity of complexes II and III in the *grx5*Δ mutant, although reduced, was not completely inhibited as in other mutants. These results confirm that the Iba57 protein plays an important role in the maturation or insertion of the Rieske subunit on the supercomplex III/IV of the ETC in a process influenced by the integrity of the Rieske protein. Thus, the mitochondrial energy metabolism of yeast is strongly dependent on the correct assembly of Rieske protein in complex III and, in turn, on the possibility that the Fe–S-IBG assembly subsystem is involved directly or indirectly in the maturation of the [2Fe–2S] cluster into the Rieske subunit of complex III.

Supplementary data to this article can be found online at https://doi.org/10.1016/j.mito.2018.01.003.

Acknowledgments

This research was funded by CONACYT (106567), FOMIX-C01-117130, and C.I.C. 2.14/UMSNH grants and Fundación Marcos Moshisky-2014. LAS and MG received a scholarship by CONACYT. We thanks to Drs. G. Del Río and S. Funes from Instituto de Fisiología Celular/UNAM by yeast strains donation. To González-Halphen D. by anti-Cox2p and anti-Cox3p antibodies supply and to Conte L. and Zara V. by anti-Rip1 antibody donation.

References

Ajit Bolar, N., Vanlander, A.V., Wilbrecht, C., Van der Aa, N., Smet, J., De Paepe, B., Vandeweyer, G., Kooy, F., Eyskens, F., De Latter, E., Delanghe, G., Govaert, P., Leroy, J.G., Loeys, B., Lill, R., Van Laer, L., Van Coster, R., 2013. Mutation of the iron-sulfur cluster assembly gene *IBA57* causes severe myopathy and encephalopathy. Hum. Mol. Genet. 22, 2590–2602.

Al-Hassnan, Z.N., Al-Dosary, M., Alfadhel, M., Faqeih, E.A., Alsagob, M., Kenana, R., Almass, R., Al-Harazi, O.S., Al-Hindi, H., Malibari, O.I., Almutari, F.B., Tulbah, S., Alhadeq, F., Al-Sheddi, T., Alamro, R., AlAsmari, A., Almuntashri, M., Alshaalan, H., Al-Mohanna, F.A., Colak, D., Kaya, N., 2015. *ISCA2* mutation causes infantile neurodegenerative mitochondrial disorder. J. Med. Genet. 52, 186–194.

Banci, L., Brancaccio, D., Ciofi-Baffoni, S., Del Conte, R., Gadepalli, R., Mikolajczyk, M., Neri, S., Piccioli, M., Winkelmann, J., 2014. [2Fe-2S] cluster transfer in iron-sulfur protein biogenesis. Proc. Natl. Acad. Sci. U. S. A. 111, 6203–6208.

Beilschmidt, L.K., Ollagnier de Choudens, S., Fournier, M., Sanakis, I., Hograindleur, M.-A., Clémancey, M., Blondin, G., Schmucker, S., Eisenmann, A., Weiss, A., Koebel, P., Messaddeq, N., Puccio, H., Martelli, A., 2017. *ISCA1* is essential for mitochondrial Fe4S4 biogenesis in vivo. Nat. Commun. 8, 15124.

Brancaccio, D., Gallo, A., Mikolajczyk, M., Zovo, K., Palumaa, P., Novellino, E., Piccioli, M., Ciofi-Baffoni, S., Banci, L., 2014. Formation of [4Fe-4S] clusters in the mitochondrial iron-sulfur cluster assembly machinery. J. Am. Chem. Soc. 136, 16240–16250.

Brand, M.D., Nicholls, D.G., 2011. Assessing mitochondrial dysfunction in cells. The Biochem. J. 435, 297–312.

Braymer, J.J., Lill, R., 2017. Iron-sulfur cluster biogenesis and trafficking in mitochondria. J. Biol. Chem. 292, 12754–12763.

Cortes-Rojo, C., Calderon-Cortes, E., Clemente-Guerrero, M., Estrada-Villagomez, M., Manzo-Avalos, S., Mejia-Zepeda, R., Boldogh, I., Saavedra-Molina, A., 2009. Elucidation of the effects of lipoperoxidation on the mitochondrial electron transport chain using yeast mitochondria with manipulated fatty acid content. J. Bioenerg. Biomembr. 41, 15–28.

Conte, L., Zara, V., 2011. The Rieske iron-sulfur protein: import and assembly into the cytochrome bc(1) complex of yeast mitochondria. Bioinorg. Chem. Appl. 2011, 363941.

Conte, A., Papa, B., Ferramosca, A., Zara, V., 2015. The dimerization of the yeast cytochrome bc1 complex is an early event and is independent of Rip1. Biochim. Biophys. Acta 1853, 987–995.
Crack, J.C., Green, J., Cheesman, M.R., Le Brun, N.E., Thomson, A.J., 2007. Superoxide-mediated amplification of the oxygen-induced switch from [4Fe-4S] to [2Fe-2S] clusters in the transcriptional regulator FNR. Proc. Natl. Acad. Sci. U. S. A. 104, 2092–2097.
Cui, T.Z., Smith, P.M., Fox, J.L., Khalimonchuk, O., Winge, D.R., 2012. Late-stage maturation of the Rieske Fe/S protein: Mzm1 stabilizes Rip1 but does not facilitate its translocation by the AAA ATPase Bcs1. Mol. Cell. Biol. 32, 4400–4409.
Cui, T.Z., Conte, A., Fox, J.L., Zara, V., Winge, D.R., 2014. Modulation of the respiratory supercomplexes in yeast: enhanced formation of cytochrome oxidase increases the stability and abundance of respiratory supercomplexes. J. Biol. Chem. 289, 6133–6141.
Diaz, F., Enriquez, J.A., Moraes, C.T., 2012. Cells lacking Rieske iron-sulfur protein have a reactive oxygen species-associated decrease in respiratory complexes I and IV. Mol. Cell. Biol. 32, 415–429.
Gardner, P.R., 1997. Superoxide-driven aconitase FE-S center cycling. Biosci. Rep. 17, 33–42.
Gomes, F., Tahara, E.B., Busso, C., Kowaltowski, A.J., Barros, M.H., 2013. nde1 deletion improves mitochondrial DNA maintenance in *Saccharomyces cerevisiae* coenzyme Q mutants. The Biochem. J. 449, 595–603.
Gomez, M., Perez-Gallardo, R.V., Sanchez, L.A., Diaz-Perez, A.L., Cortes-Rojo, C., Meza Carmen, V., Saavedra-Molina, A., Lara-Romero, J., Jimenez-Sandoval, S., Rodriguez, F., Rodriguez-Zavala, J.S., Campos-Garcia, J., 2014. Malfunctioning of the iron-sulfur cluster assembly machinery in *Saccharomyces cerevisiae* produces oxidative stress via an iron-dependent mechanism, causing dysfunction in respiratory complexes. PLoS One 9, e111585.
Gutierrez-Cirlos, E.B., Merbitz-Zahradnik, T., Trumpower, B.L., 2002. Failure to insert the iron-sulfur cluster into the Rieske iron-sulfur protein impairs both center N and center P of the cytochrome bc1 complex. J. Biol. Chem. 277, 50703–50709.
Henson, C.P., Cleland, W.W., 1967. Purification and kinetic studies of beef liver cytoplasmic aconitase. J. Biol. Chem. 242, 3833–3838.
Jervis, A.J., Crack, J.C., White, G., Artymiuk, P.J., Cheesman, M.R., Thomson, A.J., Le Brun, N.E., Green, J., 2009. The O2 sensitivity of the transcription factor FNR is controlled by Ser24 modulating the kinetics of [4Fe-4S] to [2Fe-2S] conversion. Proc. Natl. Acad. Sci. U. S. A. 106, 4659–4664.
Lill, R., 2009. Function and biogenesis of iron-sulphur proteins. Nature 460, 831–838.
Lill, R., Muhlenhoff, U., 2006. Iron-sulfur protein biogenesis in eukaryotes: components and mechanisms. Annu. Rev. Cell Dev. Biol. 22, 457–486.
Lill, R., Hoffmann, B., Molik, S., Pierik, A.J., Rietzschel, N., Stehling, O., Uzarska, M.A., Webert, H., Wilbrecht, C., Muhlenhoff, U., 2012. The role of mitochondria in cellular iron-sulfur protein biogenesis and iron metabolism. Biochim. Biophys. Acta 1823, 1491–1508.
Lipinski, K.A., Kaniak-Golik, A., Golik, P., 2010. Maintenance and expression of the *S. cerevisiae* mitochondrial genome—from genetics to evolution and systems biology. Biochimica et Biophysica Acta (BBA) - Bioenergetics 1797, 1086–1098.
Muhlenhoff, U., Richter, N., Pines, O., Pierik, A.J., Lill, R., 2011. Specialized function of yeast Isa1 and Isa2 proteins in the maturation of mitochondrial [4Fe-4S] proteins. J. Biol. Chem. 286, 41205–41216.
Musatov, A., Robinson, N.C., 2012. Susceptibility of mitochondrial electron-transport complexes to oxidative damage. Focus on cytochrome c oxidase. Free Radic. Res. 46, 1313–1326.
Nasta, V., Giachetti, A., Ciofi-Baffoni, S., Banci, L., 2017. Structural insights into the molecular function of human [2Fe-2S] BOLA1-GRX5 and [2Fe-2S] BOLA3-GRX5 complexes. Biochim. Biophys. Acta Gen. Subj. 1861, 2119–2131.
Perez-Gallardo, R.V., Briones, L.S., Diaz-Perez, A.L., Gutierrez, S., Rodriguez-Zavala, J.S., Campos-Garcia, J., 2013. Reactive oxygen species production induced by ethanol in *Saccharomyces cerevisiae* increases because of a dysfunctional mitochondrial iron-sulfur cluster assembly system. FEMS Yeast Res. 13, 804–819.
Rodriguez-Manzaneque, M.T., Tamarit, J., Belli, G., Ros, J., Herrero, E., 2002. Grx5 is a mitochondrial glutaredoxin required for the activity of iron/sulfur enzymes. Mol. Biol. Cell 13, 1109–1121.
Schagger, H., 2006. Tricine-SDS-PAGE. Nat. Protoc. 1, 16–22.
Schagger, H., Pfeiffer, K., 2000. Supercomplexes in the respiratory chains of yeast and mammalian mitochondria. EMBO J. 19, 1777–1783.
Schilke, B., Williams, B., Kniesz ner, H., Pukszta, S., D'Silva, P., Craig, E.A., Marszalek, J., 2006. Evolution of mitochondrial chaperones utilized in Fe-S cluster biogenesis. Current Biol. 16, 1660–1665.
Sheftel, A.D., Wilbrecht, C., Stehling, O., Niggemeyer, B., Elsasser, H.P., Muhlenhoff, U., Lill, R., 2012. The human mitochondrial *ISCA1*, *ISCA2*, and *IBA57* proteins are required for [4Fe-4S] protein maturation. Mol. Biol. Cell 23, 1157–1166.
Smith, P.M., Fox, J.L., Winge, D.R., 2012. Biogenesis of the cytochrome bc(1) complex and role of assembly factors. Biochim. Biophys. Acta 1817, 276–286.
Stames, E.M., OToole, J.F., 2013. Mitochondrial aminopeptidase deletion increases chronological lifespan and oxidative stress resistance while decreasing respiratory metabolism in *S. cerevisiae*. PLoS One 8, e77234.
Vartak, R., Porras, C.A., Bai, Y., 2013. Respiratory supercomplexes: structure, function and assembly. Protein and Cell 4, 582–590.
Zara, V., Conte, L., Trumpower, B.L., 2009. Evidence that the assembly of the yeast cytochrome bc1 complex involves the formation of a large core structure in the inner mitochondrial membrane. FEBS J. 276, 1900–1914.
Zhang, B., Crack, J.C., Subramanian, S., Green, J., Thomson, A.J., Le Brun, N.E., Johnson, M.K., 2012. Reversible cycling between cysteine persulfide-ligated [2Fe-2S] and cysteine-ligated [4Fe-4S] clusters in the FNR regulatory protein. Proc. Natl. Acad. Sci. U. S. A. 109, 15734–15739.

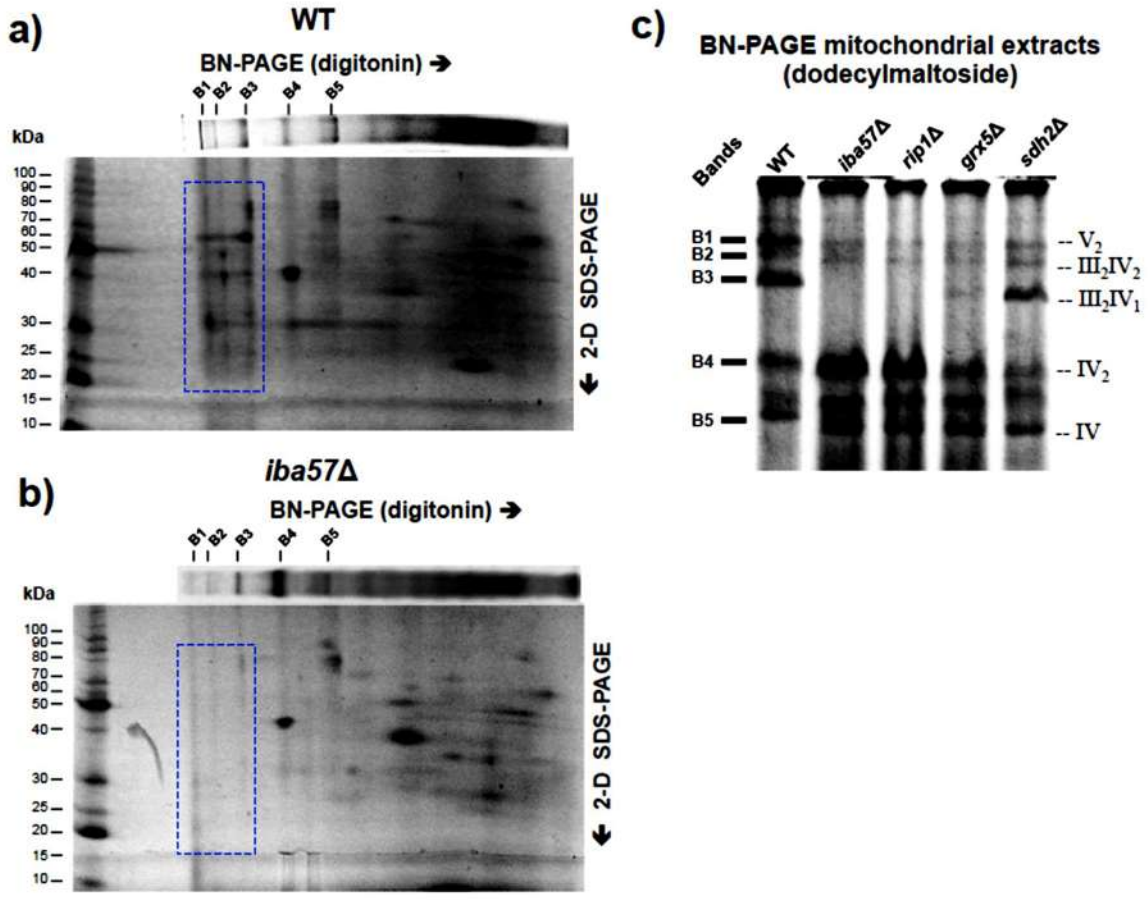

Figure S1. Evaluation of ETC mitochondrial supercomplexes formation in the Iba57p mutant of *Saccharomyces cerevisiae*.

Mitochondrial suspensions were solubilized with digitonin and the proteins were separated using blue native polyacrylamide gel electrophoresis (BN-PAGE), after gel lanes were resolved in a second dimension by SDS-PAGE as described in the Material and Methods. BN-PAGE line resolved in SDS-PAGE gel corresponding to the WT strain (**a**) and to the *iba57*Δ mutant (**b**). B1–B5, major protein bands corresponding to mitochondrial supercomplexes are shown. BenchMark Protein Ladder (Invitrogen) is showed in silver-stained, SDS-PAGE gels. **c**) BN-PAGE gel of mitochondrial extract solubilized using dodecylmaltoside (1 g/g) and triton X-100 (2.4 g/g) as described in Materials and Methods section. Bands corresponding to mitochondrial supercomplexes are shown.

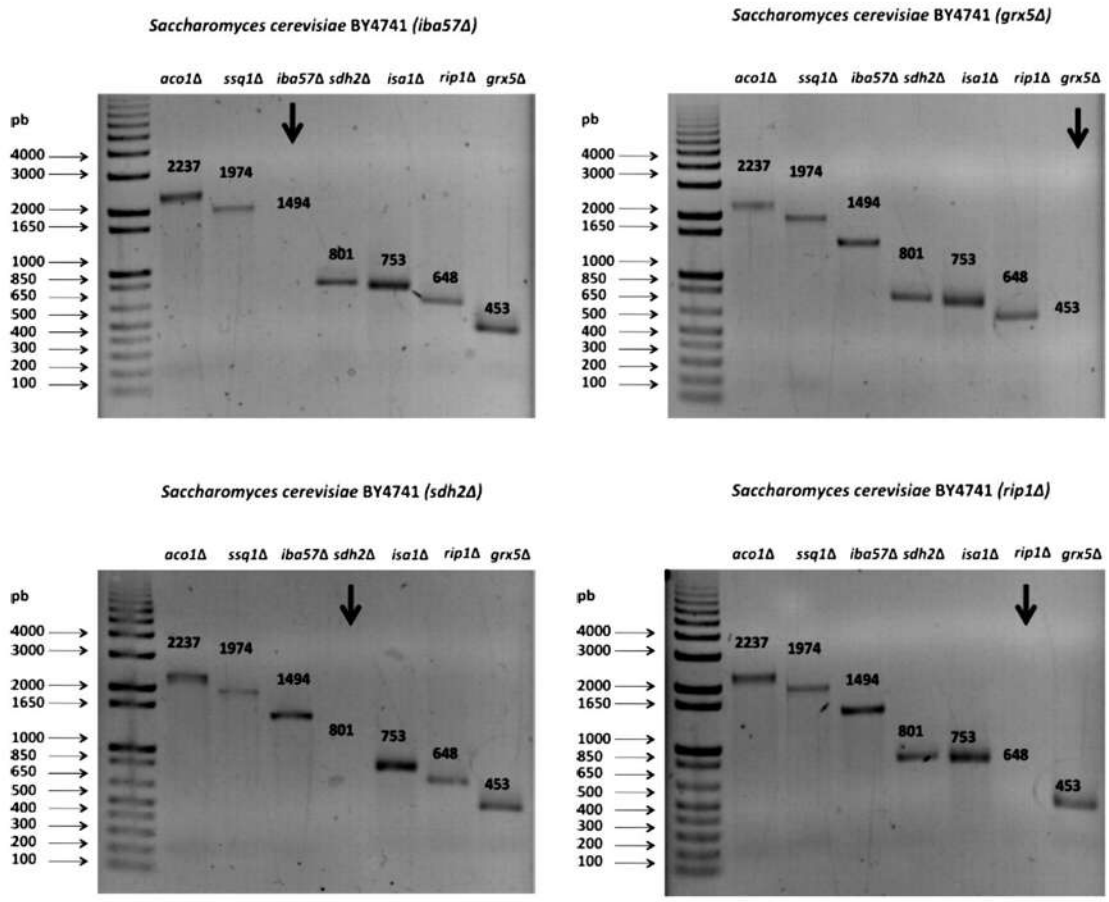

Figure S2. Characterization by PCR of the *Saccharomyces cerevisiae* BY4741 mutants used in this study.

Total DNA of each strain was used for PCR amplification using specific oligonucleotides. Arrows in the gels show the lack of DNA fragment amplification, indicating the deletion in the corresponding gene.

5.2 Capítulo 2

Data in Brief 18 (2018) 198–202

Contents lists available at ScienceDirect

Data in Brief

journal homepage: www.elsevier.com/locate/dib

Data Article

Data on the role of iba57p in free Fe^{2+} release and $O_2^{\bullet-}$ generation in *Saccharomyces cerevisiae*

Mauricio Gomez-Gallardo [a,1], Luis A. Sánchez [a,1], Alma L. Díaz-Pérez [a], Christian Cortés-Rojo [b], Jesús Campos-García [a,*]

[a] *Lab. de Biotecnología Microbiana, Instituto de Investigaciones Químico Biológicas, Universidad Michoacana de San Nicolás de Hidalgo, Morelia, Mich., Mexico*
[b] *Lab. de Bioquímica, Instituto de Investigaciones Químico Biológicas, Universidad Michoacana de San Nicolás de Hidalgo, Morelia, Mich., Mexico*

ARTICLE INFO

Article history:
Received 12 January 2018
Received in revised form
3 March 2018
Accepted 5 March 2018
Available online 11 March 2018

ABSTRACT

The related study has confirmed that in *Saccharomyces cerevisiae*, iba57 protein participates in maturation of the [2Fe–2S] cluster into the Rieske protein, which plays important roles in the conformation and functionality of mitochondrial supercomplexes III/IV in the electron transport chain (Sánchez et al., 2018) [1]. We determined in *S. cerevisiae* the effects of mutation in the *IBA57* gene on reactive oxygen species (ROS) and iron homeostasis. Flow cytometry and confocal microscopy analyses showed an increased generation of ROS, correlated with free Fe^{2+} release in the *IBA57* mutant yeast. Data obtained support that a dysfunction in the Rieske protein has close relationship between ROS generation and free Fe^{2+} content, and which is possible that free Fe^{2+} release mainly proceeds from [Fe–S] cluster-containing proteins.

DOI of original article: https://doi.org/10.1016/j.mito.2018.01.003
* Correspondence to: Lab. de Biotecnología Microbiana, Instituto de Investigaciones Químico Biológicas, Universidad Michoacana de San Nicolás de Hidalgo, Edif. B-3, Ciudad Universitaria, 58030 Morelia, Michoacán, Mexico.
E-mail address: jcgarcia@umich.mx (J. Campos-García).
[1] Both authors contributed equally to this work and share first authorship.

https://doi.org/10.1016/j.dib.2018.03.023

Participación de las proteínas Grx5p, Isa2p e Iba57p en el ensamble del centro [2Fe-2S] en la subunidad Rip1p y su impacto en la formación de los supercomplejos respiratorios en *Saccharomyces cerevisiae*

Specifications Table

Subject area	*Biology*
More specific subject area	*Cell biology*
Type of data	*Graphs, figures*
How data was acquired	*ROS and Fe^{2+} determination by flow cytometry using a BD Accuri C6 Flow Cytometer (BD Biosciences) and observation by using a confocal microscope (Olympus FV1000).*
Data format	*Analyzed and images*
Experimental factors	*ROS and Fe^{2+} determination in S. cerevisiae cells using fluorescent probes.*
Experimental features	*Real-time quantification of ROS and Fe^{2+} in S. cerevisiae cells suspensions were determined by flow cytometry and cellular structures were co-localized by confocal microscopy.*
Data source location	*Instituto de Investigaciones Químico Biológicas, Universidad Michoacana de San Nicolás de Hidalgo, Morelia, Michoacán, México.*
Data accessibility	*Data are provided with this article.*

Value of the data

- There is an established relation between *IBA57* mutation and the Rieske protein maturation in *S. cerevisiae*, which affects the electron transport chain functionality.
- *IBA57* mutation in *S. cerevisiae* is correlated with ROS generation and loss of iron homeostasis.
- This dataset provides new insights into the mechanism of ROS generation in *S. cerevisiae*, dependent of the ETC functionality.

1. Data

Treatments with 80 μM menadione in the *Saccharomyces cerevisiae iba57Δ* mutant caused significant impairment in its growth rate (Fig. 1a–b). The levels of free Fe^{2+} even without oxidant were significantly incremented in a time-dependent fashion in cell suspensions of the *iba57Δ* mutant yeast (Fig. 1c). The *iba57Δ* mutant displayed a significant increment of superoxide radical ($O_2^{\bullet-}$) generation with a dose-dependent of Fe^{2-}, determined by flow cytometry (Fig. 1d).

The western blot assays showed that the Rieske protein (Rip1p) was absent in the *rip1Δ* mutant, and decreased expression level was found in the *iba57Δ* mutant (Fig. 1e). When extracts from cultures grown on YPD plus high Fe^{2+} concentration (20 μM) or menadione as ROS-inducer were used, the Rip1p expression increased significantly in the WT, but not in the *iba57Δ* mutant.

Microscopy analysis shows an increment in ROS generation, associated with release of free Fe^{2+} in the *iba57Δ* mutant (Fig. 2). Interestingly, the high-intensity fluorescence observed in the *iba57Δ* mutant, which exhibited a full dissipation of mitochondrial membrane potential was associated with loss of iron homeostasis in the yeast cells.

2. Materials and methods

2.1. Yeast strains and growth conditions

Mutant strains *iba57Δ*, *rip1Δ*, and *grx5Δ* correspond to the haploid *S. cerevisiae* BY4741 (Mat a, *his3Δ*, *leu2Δ0*, *met15Δ0*, *ura3Δ0*) and its *KanMX4* interruption gene (Open Biosystems). Growth tests were carried out as described [1].

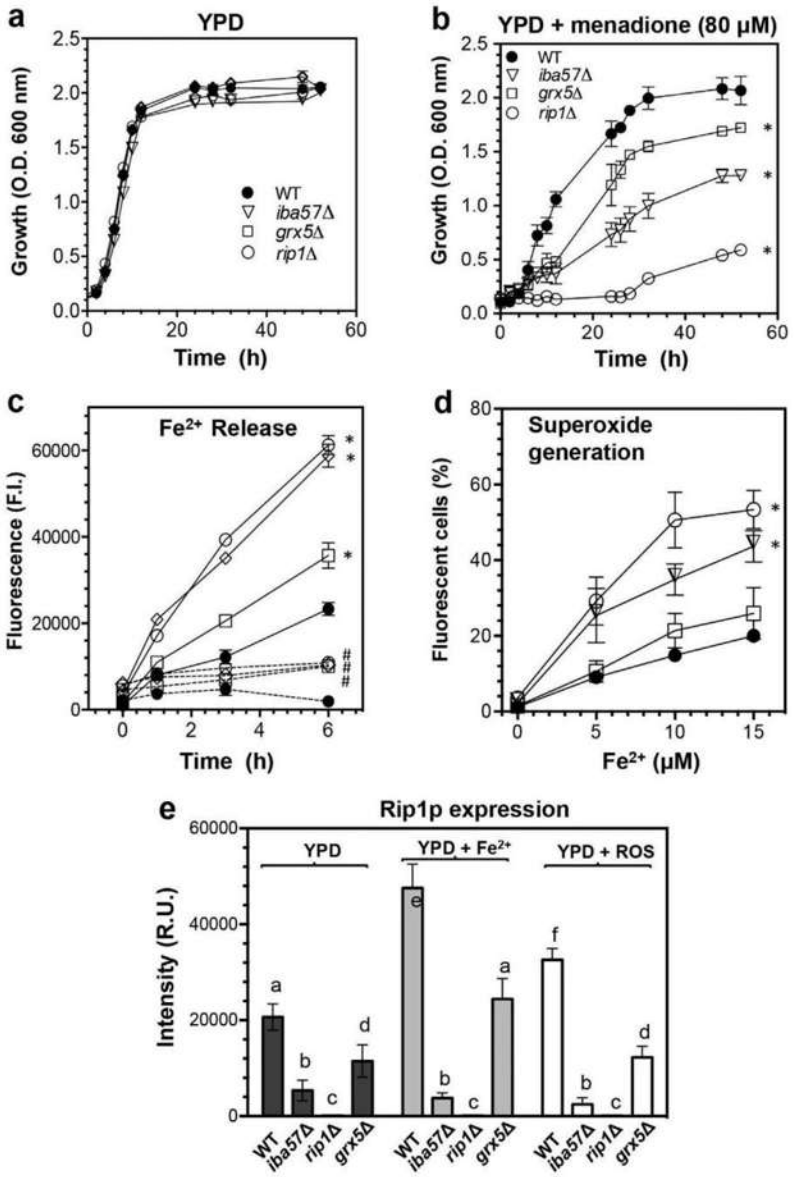

Fig. 1. Effect of the *IBA57* deletion over the growth of *Saccharomyces cerevisiae*, iron release, superoxide generation and Rip1 protein expression. a–b) Growth kinetics of *S. cerevisiae* strains grown without and in the presence of menadione 80 μM as ROS-inducer. **c**) Kinetics of Fe^{2+} release. Treatments without menadione (dashed lines) and with 80 μM menadione (continuous lines). d) $O_2^{\bullet-}$ generation in yeast suspensions treated with different concentrations of Fe^{2+} [$FeSO_4(NH_4)$]. a–d) Values are the mean of three independent experiments. **e**) Densitometry analysis of cellular extracts free-cells immunoblotted for Rip1p expression; yeast extract of cultures grown on: YPD (glucose), YPD with Fe^{2+} [$FeSO_4(NH_4)$] 20 μM, and YPD with menadione 80 μM. Means and SE are indicated as bars ($n = 3$). ANOVA was used to compare treatments. Significant differences ($p < 0.05$) are indicated as symbols (*, #) or with different lowercase letters.

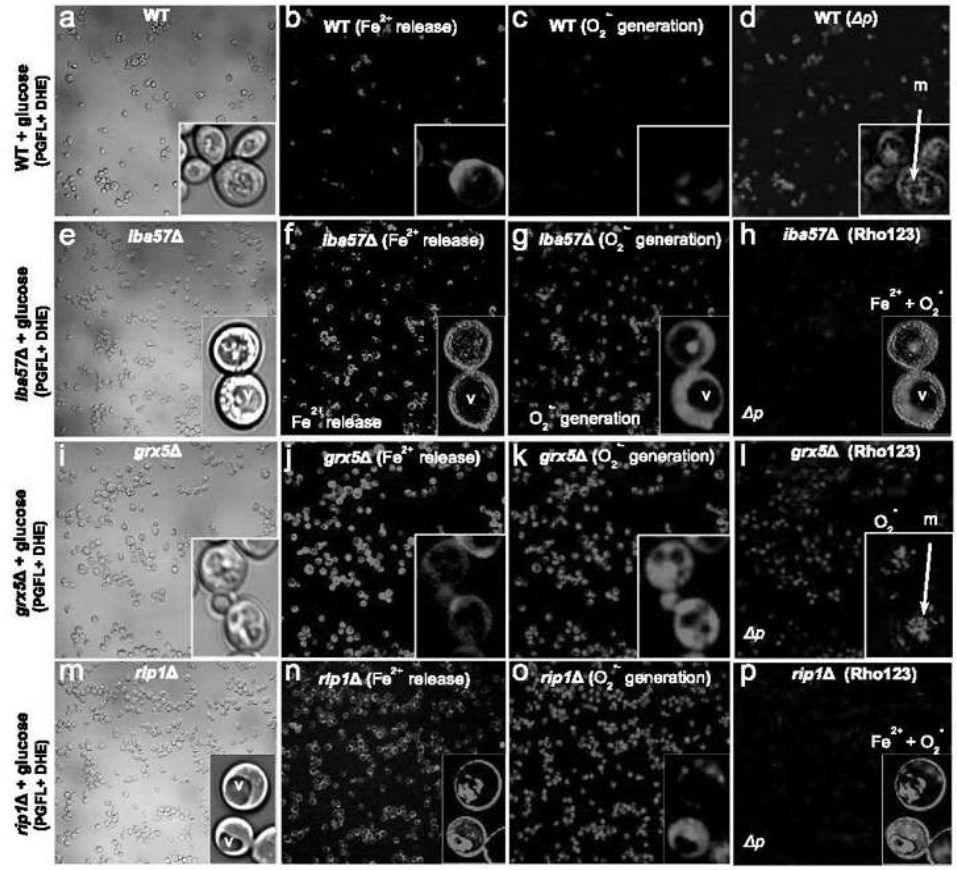

Fig. 2. Microscopy images of *Saccharomyces cerevisiae* cells for co-localization of free Fe^{2+} and superoxide in intracellular compartments. YPD-grown yeast cultures were loaded with the fluorescent probes PGFL and DHE for determination of free Fe^{2+} and $O_2^{\bullet}$, respectively; incubated for 30 min at 30 °C and co-loaded with Rhodamine 123 for membrane potential (Δp) detection as a mitochondrial co-localization marker, and observed using a confocal microscope. a–d) Wild type (WT) yeast; e-h) *iba57*Δ mutant; i-l) *grx5*Δ mutant; and m-p) *rip1*Δ mutant. Cells are shown in which mitochondria and vacuoles are indicated by (m) and (v), respectively. Free Fe^{2+} accumulation is shown as green cells and green granules within the cells, $O_2^{\bullet}$ generation areas are shown as red granules within the cells, and mitochondrial structures (Δp) are shown as cyan granules within the cells, using the Rho123 probe. Images of the cells were taken at 10× to 60× magnifications using a confocal microscope (Olympus FV1000).

2.2. *Real-time quantification of ROS and Fe^{2+} content in S. cerevisiae cultures*

Intracellular ROS and Fe^{2+} in cell suspensions were determined using cell-permeant fluorescent probes quantified by flow cytometry [1–3]. For superoxide ($O_2^{\bullet-}$) determination, yeast were incubated with 5 μg/mL dihydroethidium (DHE, Molecular Probes, Invitrogen); while as for free Fe^{2+} was used the indicator for heavy metals Phen green FL 5 μg/mL (PGFL; Molecular Probes, Invitrogen) in presence of 1 mM of the chelator 1,10-Phenanthroline (Sigma). DHE- and PGFL-fluorescence was quantified by flow cytometry monitoring the emission fluorescence at 587/40 nm and 533/30 nm, respectively; using a BD AccuriC6 Flow Cytometer (BD Biosciences).

2.3. Determination of Rip1p expression by Western blot in S. cerevisiae

Mitochondrial protein extracts 50 μg were separated by electrophoresis on SDS-PAGE gels, membranes for Western blot procedure were treated as described [1–3]. Bands intensity in films were quantified using the Image J software and data graphed as Rip1p expression intensity.

2.4. Confocal microscopy of yeast suspensions

S. cerevisiae YPD-grown cultures were loaded with the fluorescent probes DHE or PGFL and Rhodamine 123 as detailed [1–3], treated with menadione (80 μM) and mitochondrial co-localization was analyzed using a confocal microscope (Olympus FV1000). The emission signal of fluorescence was monitored at 560–580 nm for DHE, 405–505 nm for PGFL, and 533–563 nm for Rhodamine 123.

Acknowledgements

This research was funded by CONACYT (106567) and C.I.C.2.14/UMSNH grants. MG and LAS received a scholarship by CONACYT.

Transparency document. Supplementary material

Transparency document associated with this article can be found in the online version at https://doi.org/10.1016/j.dib.2018.03.023.

References

[1] L.A. Sanchez, M. Gomez-Gallardo, A.L. Diaz-Perez, C. Cortes-Rojo, J. Campos-Garcia, Iba57p participates in maturation of a [2Fe–2S]-cluster Rieske protein and in formation of supercomplexes III/IV of *Saccharomyces cerevisiae* electron transport chain, Mitochondrion (17) (2018) 30136–30138. http://dx.doi.org/10.1016/j.mito.2018.01.003.

[2] M. Gomez, R.V. Perez-Gallardo, L.A. Sanchez, A.L. Diaz-Perez, C. Cortes-Rojo, V. Meza Carmen, A. Saavedra-Molina, J. Lara-Romero, S. Jimenez-Sandoval, F. Rodriguez, J.S. Rodriguez-Zavala, J. Campos-Garcia, Malfunctioning of the iron-sulfur cluster assembly machinery in *Saccharomyces cerevisiae* produces oxidative stress via an iron-dependent mechanism, causing dysfunction in respiratory complexes, PLoS One 9 (2014) e111585.

[3] R.V. Perez-Gallardo, L.S. Briones, A.L. Diaz-Perez, S. Gutierrez, J.S. Rodriguez-Zavala, J. Campos-Garcia, Reactive oxygen species production induced by ethanol in *Saccharomyces cerevisiae* increases because of a dysfunctional mitochondrial iron-sulfur cluster assembly system, FEMS Yeast Res. 13 (2013) 804–819.

5.3 Capítulo 3

In *Saccharomyces cerevisiae* the Isa2p is essential for the [2Fe-2S] cluster assembly into Rieske subunit of the cytochrome *bc1* complex and mitochondrial function

Luis A. Sánchez[1], Mauricio Gomez-Gallardo[1], Christian Cortes-Rojo[2], Elizabeth Sánchez-Duarte[3] and Jesús Campos-García[1]*.

[1]Lab. de Biotecnología Microbiana, [2]Lab. de Bioquímica; Instituto de Investigaciones Químico Biológicas, Universidad Michoacana de San Nicolás de Hidalgo, Morelia, Mich., México. [3] Departamento de Ciencias Aplicadas al Deporte, Universidad de Guanajuato, León Gto.

Running title: Rieske protein maturation is Isa2p-dependent

*To whom correspondence should be addressed:

Jesús Campos-García, Lab. de Biotecnología Microbiana, Instituto de Investigaciones Químico Biológicas, Universidad Michoacana de San Nicolás de Hidalgo, Edif. U-3, Ciudad Universitaria, 58030, Morelia, Michoacán, México. Phone/Fax: (52) 443 3265788. E-mail: jcgarcia@umich.mx

Abstract

In *Saccharomyces cerevisiae*, the [Fe–S] late-acting subsystem comprised of Isa1p/Isa2p, Grx5p, and Iba57p proteins (Fe–S-IBG subsystem) has been involved in [4Fe–4S]-cluster protein assembly and in mitochondrial respiratory complex integration and functionality. Although the Isa2p be part of the Fe–S-IBG subsystem, it has been considered as a specific protein required for [4Fe-4S] proteins biogenesis also as Isa1p, but others studies have described dual roles of these in [4Fe-4S] and [2Fe–2S] proteins biogenesis. In this work, the effect of *ISA2* deletion in a haploid strain of *S. cerevisiae* was evaluated. The *isa2*Δ mutant showed decreased tolerance to ethanol as stressor, increased ROS content, and disbalance in glutathione content; which phenotypes were restored by the *ISA2* complementation. Increased levels of ROS were correlated with iron release in the yeast cells. Additionally, the *ISA2* deletion caused decrease of the Rieske protein on mitochondrion, causing dysfunction in the electron transport chain by affecting the structure of supercomplexes III_2IV_2 and III_2IV_1 and their integration into the mitochondria. The results confirm that Isa2p participates in maturation of both proteins the *cis*-aconitase ([4Fe–4S]-containing cluster), and the Rieske subunit [2Fe–2S]-protein, suggesting a dual function of the Fe-S-IBG

subsystem in the [4Fe-4S]/[2Fe–2S] clusters assembly . This work present by first time, that the Isa2p interact directly with the respiratory supercomplexes to assembly the Rieske subunit. Additionally, the findings showed the importance that plays the Rieske protein in the conformation and functionality of mitochondrial supercomplex III/IV in the electron transport chain.

Keywords: *Saccharomyces cerevisiae*, mitochondria, iron–sulfur cluster, Rieske protein, supercomplexes, iron homeostasis, reactive oxygen species.

Introduction

The Iron–Sulfur clusters [Fe–S] biogenesis in eukaryotes is a process compartmentalized, in mitochondria is conducted by the *ISC* (Iron Sulphur Cluster) machinery and in cytosol by the *CIA* (Cytosolic Iron–sulphur cluster Assembly) machinery (Lill 2009). In the last 20 years, these processes have been described with detail; however, questions remain unresolved. There are a diversity of [Fe–S] clusters types; however, of the most studied are the rhombic form [2Fe–2S] and the cubic [4Fe–4S]. The mitochondrial biogenesis of [Fe–S] clusters is divided in two main phases; first, the formation the [Fe–S] of *novo* by the Isu1/2 scaffold proteins, which is mediated by the frataxin (Yfh1p) and the cysteine desulfurase complex (Nfs1p-Isd11p) (donors of Fe^{+2} and S^{0}, respectively), and the ferredoxin Yah1p–Arh1p (electrons donor) (Lill, Hoffmann et al. 2012). Second, the cofactors trafficking to their target proteins mediated by the subsystem conformed by the chaperone/co-chaperone (Hsp70/Hsp20), the glutarredoxin (Grx5p), and the heterocomplex Isa1p/Isa2p/Iba57p called as Fe–S-IBG (Lill 2009, Muhlenhoff, Richter et al. 2011, Lill, Hoffmann et al. 2012, Banci, Brancaccio et al. 2014). Iba57p together with the Isa1p and Isa2p have been established as a protein complex that regulates the transference and synthesis of [4Fe–4S] clusters in yeast (Gelling, Dawes et al. 2008, Muhlenhoff, Richter et al. 2011). Mutation of any of these proteins cause similar phenotypes in *S. cerevisiae*; null activity of aconitase and lipoic acid synthase are some of the enzymes affected by the lack of cubic type [4Fe–4S] clusters (Gelling, Dawes et al. 2008). Among the most controversial aspects to elucidate involves the insertion of the [Fe–S] clusters on their respective target apo-proteins. In this context, the complete maturation of Rip1p (Rieske protein) is a process that has not yet been fully elucidated, Rip1p is the only catalytic subunit of the cytochrome *bc1* complex with a cluster [2Fe–2S], responsible for oxidizing quinol by the Q cycle (Snyder, Gutierrez-Cirlos et al. 2000 and Atkinson, Kapralov Aa Fau - Yanamala et al. 2011)),. Rip1p is a protein encoded in the nucleus with a consensus sequence in the amino-terminal that let to be translocated to the mitochondrial matrix by the Tim/Tom transporters (Kulawiak, Höpker et al. 2013). Subsequently, Rip1p acquires its [2Fe–2S] cluster by the *ISC* machinery and then is translocated to the *bc1* complex by the Bcs1p(Stephan and Ott). In addition, Rip1p has an important role in the stabilization of the *bc1* complex in its dimeric form (Zara, Conte et

al. 2009, Conte and Zara 2011, Conte, Papa et al. 2015). Thus, the correct function and formation of respiratory supercomplexes for the functionality of the ETC (Genova and Lenaz 2014).

Previous studies have been described that the dysfunction of the Isa1p and Isa2p in *S. cerevisiae* cause respiratory deficiency, iron homeostasis and decreased activity of enzymes that contains [4Fe–4S] clusters,considering these proteins do not have redundant roles in the [Fe–S] clusters biogenesis (Isu1p/Isu2p) (Jensen and Culotta 2000). The Isa1p but not Isa2p can be functionally replaces by bacterial homologues, being these proteins capable to form heterocomplexes required for maturation of mitochondrial [4Fe–4S] proteins; however, these were described to be dispensable for generation of mitochondrial [2Fe–2S] proteins, neither needed as donor for *de novo* assembly of the [2Fe–2S] cluster on the scaffold proteins Isu1p/Isu2p (Muhlenhoff, Richter et al. 2011). In this sense, the human homologues proteins ISCA1 and ISCA2 are required for [4Fe–4S] protein maturation in HeLa cells, its mutation affecting the activities of enzymes such as aconitase, respiratory complex I, and lipoic acid synthase, but not the [2Fe–2S] of the ferrochelatase (Sheftel, Wilbrecht et al. 2012). In contrast, recent studies in mammals *in vitro* and *in vivo* showed that the ISCA1, ISCA2, and IBA57 to those homologous proteins described in yeast, Isa1p/Isa2p/Iba57p show dual behaviors; structural studies have indicated that the ISCA1/ISCA2 heterocomplex is the functional unit in mitochondria to receive [2Fe–2S] centers from GRX5 and assembly [4Fe–4S] centers before their transfer to target apo-proteins(Brancaccio, Gallo et al. 2014); Additionally, it was proposed that ISCA1 and ISCA2 may have different roles depending on the redox status of the cell, only ISCA2 is capable of forming an association with IBA57 mediated by a cluster [2Fe–2S], this complex is resistant to oxidative stress and is capable of reactivating apo -aconitase (Gourdoupis, Nasta et al. 2018). Experiments in mouse skeletal muscle and neurons cultures suggest that ISCA1, but not ISCA2, is required for mitochondrial [4Fe–4S] proteins biogenesis (Beilschmidt, Ollagnier de Choudens et al. 2017); however, the ISCA2 also was capable to incorporate the [2Fe-2S] cluster into the apo-ferredoxin, suggesting that ISCA2 can to transfer both the [2Fe-2S] and [4Fe–4S] clusters in a redox-depend condition (Beilschmidt, Ollagnier de Choudens et al. 2017). In this sense, previous results in our group indicate that the mutation of the *IBA57* gene in *S. cerevisiae* affects the expression levels of Rip1p in the complex III of the ETC, suggesting that the Iba57p is involved in the maturation of the [2Fe–2S]-containing Rip1 protein (Sánchez, Gómez-Gallardo et al. 2019). In consequence, electrons transference in the ETC is impaired by affecting the stability of the respiratory supercomplexes, which are mediated by the Rieske protein of the *bc1* complex (Conte, Papa et al. 2015). These findings can suggest that in *S. cerevisiae* the Fe–S-IBG subsystem of late stage in the biogenesis of [Fe–S] clusters, participates also in the assembly of proteins that contains [2Fe–2S] clusters (Gomez, Perez-Gallardo et al. 2014, Sánchez, Gómez-Gallardo et al. 2019). Thus, with the objective to deep in the participation of the Isa1p and Isa2p in the [Fe–S] cluster maturation and assembly, in this work we focusing in the function of the Isa2p over the mitochondrial function dependent of the Rip1 protein contained in the *bc1* complex using as model the haploid yeast strain of *S. cerevisiae* BY4741.

Materials and Methods

Strains, vectors, and growth

We used the bacterial strain *Escherichia coli* JM101 for plasmids manipulations (pGEM®-T-Easy, Promega and pYES2/CT, Invitrogen). Bacteria were grown at 37 °C in Luria Bertani medium (LB; 10 g peptone, 5 g yeast extract, and 5 g NaCl) supplemented with 100 µg/mL ampicillin. The haploid *S. cerevisiae* BY4741 (Mat a, *his3*Δ, *leu2*Δ0, *met15*Δ0, *ura3*Δ0) and its *KanMX4* interruption gene mutants, *grx5*Δ, *isa2*Δ, and *rip1*Δ were obtained from Open Biosystems. The strains were grown in yeast extract peptone dextrose (YPD; 10 g peptone, 5 g yeast extract) culture medium added with the respective antibiotic selection. The minimal SC medium (6.7 g YNB without amino acids; 2 g Drop out mix without uracil both of Sigma-Aldrich; 2 g of Dextrose or Galactose, and 15 g of agar for solid medium) was used to growth transformed yeast strains.

Oligonucleotides, PCR conditions and cloning

We used the serial cloner 2.6.1 software to design the following oligonucleotides, from the sequence available in the online Yeast Genome; for *ISA2* gene, the forward primer 5'- A AAG CTT ATG CAG GCT AAA TTA TTG TTT ACC- 3'and the reverse primer 5'- T CTC GAG ATT TTC AAT ATC AAA ACT ACT TCC – 3', inserting the Xho1 and Hind III restriction sites. For *GRX5* gene, the forward primer 5'- A AAG CTT ATG TTT CTC CCA AAA TTC AAT CCC – 3' and the reverse primer 5' - T CTC GAG ACG ATC TTT GGT TTC TTC TTC TTC – 3', inserting the Xho1 and Hind III restriction sites. We used the Platinum® PCR Supermix (Invitrogen) for polymerase chain reaction (PCR) with the following conditions: one cycle at 94 °C, 5 min; after denaturation 94 °C, 1 min, annealing 56 °C, 40 sec, elongation, at 70 °C, 2 min by 35 cycles; final elongation 68 °C, 5 min, hold at 4 °C. The genes amplified by PCR were cloned in the vector pGEM®-T-Easy (Promega) following the manufacturer instructions. *E. coli* JM101 was transformed for electroporation (2.4 mV for 5 mS), plated in LB with ampicillin plates, after incubation at 37 °C by 24 h, bacterial colonies were screened to isolation resulting plasmids. The *ISA2* and *GRX5* genes cloned into the vector were sequenced in the research institute LANGEBIO-CINVESTAV, Irapuato, Guanajuato, Mexico. The DNA sequence analysis showed that the genes did not show mutations, and these plasmids were used for subcloning.

Yeast transformation and protein induction

The pYES2/CT vector that contains the yeast strains, this contains the yeast GAL1 promoter for induction of protein expression in yeast, the 2µ origin for episomal maintenance and high copy replication, the auxotrophic marker for selection of yeast transformants the URA3 gene, the ampicillin resistance gene for selection in *E.coli*, and a polyhistidine (6-His) tag for detection and purification of the recombinant fusioned protein. The *ISA2* and *GRX5* genes cloned into the pGEM®-T-Easy vector were release by endonucleases digestion and sub-

cloned into the pYES2/CT vector, rendering the pYES2:*ISA*2 and pYES2:*GRX5* plasmids, which were introduced on yeast strains by using the Frozen EZ Yeast Transformation II kit from Zimo Reseach following the instructions of manufacturer with light modifications. Briefly, the mutant yeast cells were grown in 5 mL of YPD medium at O.D. 0.8-1.0 at 600 nm), 1 mL of culture was centrifugated at 5,000 × g for 4 min and pellet was suspended in 1 mL of EZ1 solution to wash the pellet, after 100 µL of EZ2 solution was added to obtain competent cells. 50 µL of competent cells were mixing with 0.2 µg of plasmid DNA for transformation, EZ3 buffer was added (300 µL) and incubated for 60 min at 30 °C. The cells were plated in minimal medium SC without uracil for 48-72 h. The prototroph yeasts were corroborated with the transformation of the *E.coli* JM101 electrocompetent cells using the pDNA isolated from the yeast transformed, plasmid isolation of transformed clones was carried out and confirmed by enzymatic restriction analysis.

To induce the recombinant proteins expression, the transformed yeast clones were grown in 5 mL of SC medium without uracil with 2% glucose by overnight at 30 °C with shaking, after these cultures were used to seed 40 ml of SC-DG or YPDG (1% dextrose, and 1% galactose) induction medium, samples were taken every 4 h during the first 12 h of inoculation and every 24 h for subsequent expression screening by SDS-PAGE and Western blot assays.

Ethanol tolerance grown test

The yeast strains were challenged growth in increasing concentrations of ethanol, dilutions of cultures grown overnight in YPDG sequential dilutions were prepared (1:10, 1:100, 1:1,000, 1:10,000); dilutions of cultures were spreaded in petri dishes with YPDG solid medium, allowed to grow at 30 °C for 72 h. Additionally, 50 mL of SC-U 1% dextrose, 1% galactose medium were inoculated with 3 mL of inoculum grown overnight at 30°C, the growth kinetics were performed at 30 °C for 72 h, monitoring spectrophotometrically at 600 nm.

Mitochondrial isolation

Mitochondria of *S. cerevisiae* were isolated from cultures grown in liquid medium YPD at 30°C in a shaking incubator by 12 h, using a previously described method (Perez-Gallardo, Briones et al. 2013). Detergent permeabilized mitochondria were mixed 250 µL of intact mitochondria (10 mg of protein) plus 750 µL of hypotonic buffer [(KCl 100 mM, $MgCl_2$ 10 mM, Tris-base 10 mM, pH 7.5, and Triton X-100 (0.02%)] with vigorous shaking in a vortex for 15 sec. This suspension was centrifuged at 18,600 × *g* for 15 min at 4°C. Supernatants were discarded and the mitochondrial pellets suspended in buffer composed of 50 mM KH_2PO_4, pH 7.6 and protein was quantified by using the Bradford reagent (Bio Rad). Suspensions of permeabilized mitochondria were used to determine the activity of the ETC complexes, as described below.

Determination of *in situ* mitochondrial oxygen consumption rate

S. cerevisiae cells (25 mg wet weight) were placed in 2.5 mL of MES-TEA buffer (pH 6.0) in a sealed glass chamber with constant stirring at 25°C. The oxygen consumption rate (OCR) was measured with a Clark-type oxygen electrode coupled to a biological oxygen monitor (YSI 5300). Basal oxygen consumption (state 4), was induced by adding 20 mM glucose as substrate, and 3 min later, 5 µM of the uncoupling agent carbonyl cyanide m-chlorophenyl hydrazone (CCCP) was added to stimulate maximal OCR (uncoupled (U) state). To rest the mitochondrial oxygen consumption from unspecific-cytosolic oxygen utilization, the mitochondrial ETC was inhibited with 1 µg antimycin A and a further addition of 0.5 mM KCN (Brand and Nicholls 2011).

Real-time quantification of ROS in *S. cerevisiae* cultures

Yeast cultures were grown for 72 h in 3 mL of YPD medium, the cells were harvested and suspended in 1 mL of PBS buffer; quantification of intracellular ROS in cell suspensions were determined using the oxidant-sensitive, cell-permeant fluorescent probe H_2DCFDA (Molecular Probes, Invitrogen) used at 10 µg/µL in 100 µL of cell suspensions as described (Perez-Gallardo, Briones et al. 2013, Gomez, Perez-Gallardo et al. 2014). The fluorescence intensity in the yeast cells was quantified by flow cytometry in the FL1 channel (533/30 nm) using a BD Accuri C6 Flow Cytometer (BD Biosciences). For mitochondrial ROS quantification, 100 µL of yeast cell suspensions were incubated with 5 µg/µL of dihydrorhodamine 123 (DHR123; Sigma-Aldrich) and fluorescence intensity were quantified by flow cytometry in the FL1 channel (533/30 nm). For mitochondrial superoxide we used 5 µg/µL of dihydroethidium (Molecular Probes, Invitrogen) on 100 µL of yeast cell suspensions and the fluorescence intensity was quantified by flow cytometry in the FL2 channel (587/40 nm). A minimum of 40,000 cellular events were analyzed for each determination point, and the fluorescence intensity (FI) as well as the percentage of fluorescent cells (PFC) were determined in the monoparametric histograms of fluorescence emission obtained from the dot plots and labeled as percentage of cells and as relative units of fluorescence.

Confocal microscopy of yeast cells

Saccharomyces cerevisiae YPD-grown cultures were harvested and suspended in PBS at 1 □ 10^7 cell/mL and loaded with the fluorescent probe Phen green FL (PGFL; Molecular Probes, Invitrogen) (5 µg/mL) at 30°C for 30 min in darkness to determinate free Fe^{2+} adding 1 mM of the chelator 1,10-Phenanthroline. Afterwards, the cell suspensions were incubated with 5 µg/mL dihydroethidium (DHE, Molecular Probes, Invitrogen) for superoxide ($O_2^{\bullet-}$) determination during 30 min for cell co-localization and analyzed using a confocal microscope (Olympus FV1000). The signal evaluating fluorescence emission was observed between 560-580 nm for DHE and between 405-505 nm for PGFL. Images were acquired at 65× magnification of yeast cells.

Determination of glutathione levels (GSH/GSSG) in yeast spheroblasts and mitochondria

Spheroblasts or mitochondria were obtained as described above, the GSH/GSSG levels was determinate as Perez-Gallardo et al (2013) with light modifications (Perez-Gallardo, Briones et al. 2013). 0.1 mg of protein were suspended in lysis buffer (K_2HPO_4 0.5M, KH_2PO_4 0.5M, sulpho-salicylic acid 0.6%, triton 0.01%, pH 7.0). Spheroblasts or mitochondria suspensions were sonicated one-three times at 20 amplitude power for 3 sec, then were frozen in liquid nitrogen. The samples were centrifuged at 10,000 × g for 5 min at 4°C, supernatants obtained were used for GSH/GSSG determinations. The reduced GSH and oxidized GSSG species were quantified using the glutathione assay kit (Sigma-Aldrich). The total GSH/GSSG were quantified based on the enzymatic reaction using a reaction buffer (K_2HPO_4 0.5M, KH_2PO_4 0.5M, DTNB 3 mM, glutathione reductase 0.1 U/mL and NADPH 2 mM, pH 7.0) to produce yellow colored compound 5-thio-2-nitrobenzoic acid (TNB) (Shaik and Mehvar 2006). The kinetics of conversion of DTNB into TNB were followed spectrophotometrically at 412 nm. For quantitation of oxidized glutathione (GSSG), samples were pre-treated with 5% (vol/vol) 2-vinylpyridine for 1 h at room temperature before analysis.

Determination of the ETC complexes activity and *cis*-aconitase activity

The activity of complex II was evaluated by measuring the succinate-DCIP oxidoreductase activity of solubilized mitochondria (Perez-Gallardo, Briones et al. 2013). For determination of complex II-III activity, the activity of antimycin A-sensitive succinate-cytochrome *c* oxidoreductase was measured using endogenous ubiquinol-6 and succinate as substrates (Cortes-Rojo, Calderon-Cortes et al. 2009, Perez-Gallardo, Briones et al. 2013). While that for determination of complex III activity, it was assayed under the same conditions used for the determination of complex II-III activity, except that decylubiquinol (reduced with NaBH4) was added instead succinate (Cortes-Rojo, Calderon-Cortes et al. 2009, Perez-Gallardo, Briones et al. 2013). Finally, for determination of the complex IV activity, cytochrome *c* oxidase activity was measured as the rate of cyanide-sensitive cytochrome *c* oxidation in presence of antimycin A by adding dithionite-reduced cytochrome *c* (Perez-Gallardo, Briones et al. 2013, Gomez, Perez-Gallardo et al. 2014).

Aconitase activity was determined by a modification of the method of Henson and Cleland (Henson and Cleland 1967) as described elsewhere (Perez-Gallardo, Briones et al. 2013).

Blue native polyacrylamide gel electrophoresis and western blot

Blue native polyacrylamide gel at 8% (BN-PAGE) were utilized for analysis of the supercomplexes formation. 100 µg of mitochondrial protein was solubilized with digitonin (3 g/g) as described Shagger (2006) (Schagger 2006), mitochondrial supercomplex were identified after electrophoresis as describe elsewhere (Schagger and Pfeiffer 2000, Schagger 2006, Musatov and Robinson 2012, Sánchez, Gómez-Gallardo et al. 2019). We

performed the immunodetection by Western blot for the recombinant proteins by BN-PAGE and SDS-PAGE; and second dimension from lanes cut from BN-PAGE (2D-BN-PAGE/SDS-PAGE) (Schagger 2006, Jha, Wang et al. 2016, Sánchez, Gómez-Gallardo et al. 2019). Gels were transferred to PVDF membranes for immunoblotting assays. Briefly, PVDF membranes were incubated with TBS-T (Tris-HCL 10 mM pH 7.8, 0.9% NaCl, 0.1% tween-20, 0.5% dry milk). PVDF membranes were incubated with the indicated antibodies at the concentration suggested by the manufacturer, the antibodies used included anti-His/tag at 1:50,000 dilution (Santa Cruz Biotechnology) or anti-Rip1 (Conte and Zara 2011) at 1:20,000 dilution. Following 12 h of incubation (4°C) for the primary antibody, membranes were washed and incubated with secondary antibody anti-mouse IgG-HRP (Santa Cruz Biotechnology) at 1:5,000 dilution in blocking medium for 4 h at 4°C; the membranes were washed twice with TBS-T buffer and developed using hydrogen peroxide and Supersignal West Pico Luminol (Pierce, Thermo Fisher Scientific). Images were then captured using a ChemiDoc™ MP System (Bio-Rad). Assays were conducted at least three times, representative images were obtained and band intensities in gels images were quantified using the Image J software (NIH Image).

Results and discussion

Ethanol toxicity in *S. cerevisiae* yeast is increased by the *ISA2* deletion

In nature, many events are related to ROS generation, whose of these have addressed to disturbances in mitochondrial free iron from [Fe–S]clusters as molecular mechanism. Earlier reports have identified a link between ROS overproduction and iron overload in the toxic effects caused by ethanol (Perez-Gallardo, Briones et al. 2013). These ROS overproduction observed in yeast cells during ethanol stress was exacerbated by mutations in *ISC* genes, which participate in the various steps in [Fe–S]biogenesis.

The Fe–S-IBG subsystem (comprised of Isa1p, Isa2p, Iba57p, and Grx5p proteins) has been widely described as essential for the maturation of [4Fe–4S] clusters (Schilke, Williams et al. 2006, Muhlenhoff, Richter et al. 2011); however, its participation has been involved also in the maturation of the [2Fe-2S] cluster contained in some apo-proteins such as the Rip1psubunit of complex III (Banci, Brancaccio et al. 2014, Gourdoupis, Nasta et al. 2018, Sánchez, Gómez-Gallardo et al. 2019). In agree, our previous findings regarding impaired supercomplex formation and decreased activities of both complexes III and IV in the *isa1*Δ and *iba57*Δ mutants, whose supercomplexes not contain [4Fe-4S] clusters (Gomez, Perez-Gallardo et al. 2014). Thus, we tested the essentiality of the *ISA2* on ETC mitochondrial function, supercomplexes formation, and emphasizing the monitoring of the Rip1p participation of in these processes.

As biological material we used gene deletion in the haploid *S. cerevisiae* BY4741 (*isa2*Δ) and plasmid complementation as described in Materials and Methods. We constructed two plasmids, the pYES2:*ISA2* and pYES2:*GRX5* that were analyzed using restriction analysis, observing a DNA band of ~6,000 pb for linearized vector and ~570 bp for *ISA2* insert and

of ~465 bp for *GRX5* insert (Figure S1a; supplementary material). In the figure S1b is showed the amplification of the nuclear genes *ISA2, GRX5*, and the control genes used in this works, *RIP1* (nuclear located), and the mitochondrial genes *COX2* and *COX3*. PCR findings indicate that in the *isa2*Δ and *grx5*Δ mutants, their respective genes are deleted, while that in the plasmid-transformed strains, the *ISA2* and *GRX5* genes were amplified. In addition, the presence of the *COX2* and *COX3* mitochondrial genes in all yeast strains indicates that mitochondrial DNA is present. Once confirmed the genotype of the yeast strains utilized in this work, the *S. cerevisiae* BY4741 *isa2*Δ and *grx5*Δ mutants and their complemented strains were utilized in subsequent studies.

To study the involvement of the *ISA2* gene product on mitochondria functionality, the haploid yeast *S. cerevisiae* mutants were utilized to determinate generation/accumulation of ROS and the capability to ROS scavenge. In this sense, ethanol addition to yeast cultures was used as stressor. Plates with solid YPDG medium were incubated with ethanol in the range of 0–12% (v/v) determining ethanol tolerance in *S. cerevisiae* yeast strains (Figure 1a). The yeast mutants *isa2*Δ and *grx5*Δ showed impaired growth in YPDG containing ethanol, comparing with the wild type (WT) yeast, while the their complemented clones with plasmids containing the wild type genes [*isa2*Δ (pYES2:*ISA2*) and *grx*5Δ (pYES2:*GRX5*)], showed a recovery of ethanol tolerance with similar behavior to the WT yeast (Fig. 1a). Additionally, tolerance assays were conducted to explore the growth rate in the presence of toxic ethanol concentrations using minimal SC-U liquid medium. The growth kinetic results indicated that in the *isa2*Δ and *grx5*Δ mutants, their growth was impaired at 8% ethanol and totally inhibited at 12% ethanol (Fig. 1b). However, when the mutant strains were complemented with the plasmids containing the wild type genes, the ethanol tolerance was recovered significantly in the *isa2*Δ (pYES2:*ISA2*) strain but not in the *grx*5Δ (pYES2:*GRX5*). These data indicate that the *ISA2* gene deletion caused an impaired ethanol tolerance in *S. cerevisiae*.

Both the Isa2p and Grx5p recombinants proteins were efficiently expressed in protein extract of cultures; but interestingly, protein expression was abolished in cultures treated with ethanol in a doses-dependent manner (Fig. 2), indicating that the mechanism of toxicity of ethanol involves the inhibition of Isa2p and Grx5p expression or by a protein inactivation mechanism as described below.

ROS generation in *S. cerevisiae* is exacerbated by the *ISA2* deletion

The toxic effects caused by ethanol in *S. cerevisiae* have been associated with an increase in oxidative stress, inactivation of related enzymes, and dysfunctional mitochondrial metabolism (Perez-Gallardo, Briones et al. 2013). We hypothesized that the protein components involved in [Fe–S]assembly such as Isa2p, which had not been described to be essential as the Isa1p, is also related to the generation of ROS induced by stressors such as ethanol.

ROS generation induced by ethanol in *S. cerevisiae* was determined under real-time quantification by flow cytometry using fluorescent ROS indicators. H_2DCFDA for general

intracellular ROS and the DHR123 probe for mitochondrial ROS. As described above, all yeast strains were able to tolerate 8% (v/v) ethanol (Fig. 1a-b). Therefore, real-time ROS quantification was carried out at 8% ethanol during the period of 8 h (Figure 3).

First, we determined ROS generation in the yeast population (percentage of fluorescent cells, PFC) and the median fluorescence intensity (FI) in cultures treated with 8% ethanol. Using the H_2DCFDA, the PFC values in yeast suspensions with ethanol treatment were <5% at 8 h treatment and basal fluorescence intensity in the WT yeast, while that in the *isa2*Δ and *grx5*Δ mutants PFC increased significantly to ~40% of population which increased logarithmic units of the fluorescence intensity (Fig. 3a). Interestingly, the *isa2*Δ mutant complemented with the pYES2:*ISA2* plasmid, decreased the PFC and FI in the yeast population, but not for the *grx*5Δ (pYES2:*GRX5*). Similar results were obtained with the DHRhodamine 123 probe, with exception in the WT, which showed an increased PFC at 6–8 h of ethanol treatment, but with low fluorescence intensity, indicating basal mitochondrial activity (Fig. 3a-b).

In addition, confocal microscopic analysis showed that the *ISA2* mutation caused an increment in superoxide ($O_2^{\bullet-}$) co-localized with release of labile Fe^{2+}, which was partially reverted with the *ISA2*-contained plasmid complementation (Fig. 4). As is observed, in the WT cells, $O_2^{\bullet-}$ and free Fe^{2+} basal levels are showed in lesser levels than in the hyper ROS generation *rip1*Δ mutant and in minor degree in the *grx5*Δ mutant as described previously (Sánchez, Gómez-Gallardo et al. 2019). Further, co-localization images showed that in the *isa2*Δ mutant, free Fe^{2+} fluorescence was observed in all cells, but with greatest intensity in inside of the cytoplasmic membrane, which it was restored in the complemented mutant (Fig. 4). These results confirm that *ISA2* mutation cause an increase in ROS content which was associated with labile iron release, but diminished by the *ISA2* gene complementation. This indicates a close relationship between levels of free iron and ROS generation, where the [Fe–S] assembly system plays a relevant role in iron homeostasis and its dysfunction may partially contribute to excessive iron availability out of cellular compartments on the cell.

GSH/GSSG content and balance is affected by the *ISA2* deletion

Since it has been reported that the mitochondria is a glutathione reservoir that contributes to cell ROS scavenging, we determined the GSSG and GSH contents in yeast spheroplasts and mitochondria isolated from yeast strains. To determine whether the increased ROS generation caused by ethanol treatment in the *isa2*Δ and *grx5*Δ mutants, the cellular GSH/GSSG ratio as marker of antioxidant defense was measured (Fig. 5). Results indicated that in yeast spheroplasts of the *isa2*Δ or *grx5*Δ mutations not caused significant modifications in the content and in the redox state of GSSG and GSH (Fig. 5a). While that when the total glutathione content was determined in mitochondrion isolated from each yeast strain a significant decrease was observed in the *isa2*Δ or *grx5*Δ mutants, which content was recovery by their respective gene complementation (Fig. 5b). This behavior was consistent with the increase of the oxidized specie (GSSG) and decreased content of reduced specie (GSH), which consistently correlated with the GSH/GSSG ratio. These

results clearly indicated that these mutants had a glutathione imbalance which correlated with ROS generation/content, and that probably it is mainly associated with mitochondrion activity; as expected, the control mutant *rip1*Δ showed impaired GSH/GSSG ratios compared to WT.

Mitochondrial ETC functionality is affected by the *ISA2* deletion

Biogenesis of Fe–S centers in *S. cerevisiae* occurs mainly in mitochondria, in a dependent manner on the functionality of *ISC* gene products. Iron is an essential component of this process, and its cellular content is dependent on transport systems, chelating proteins and storage. It is well known that iron can be released from [Fe–S]proteins by ROS, which in turn can lead to the generation of the strongly oxidant $OH^{\bullet}$ radical via Fenton's chemistry (Lill, Hoffmann et al. 2012).

The Fe–S-IBG subsystem dedicated to the maturation of [4Fe–4S] clusters, also has been described to be involved in the activity of mitochondrial complexes which contains different type of [Fe–S]center such as [2Fe–2S] (i.e., III) (Beilschmidt, Ollagnier de Choudens et al. 2017, Gourdoupis, Nasta et al. 2018, Sánchez, Gómez-Gallardo et al. 2019). In other context, mutants in the Fe–S-IBG subsystem components have been considered as respiratory-deficient strains, but possess normal capability to grow in fermentative conditions, suggesting that their lack of mitochondrial DNA (mitDNA) causes the failure of respiratory complexes (petite or *rho*- phenotypes) (Muhlenhoff, Richter et al. 2011). However, *GRX5* mutants maintain their mitDNA (Rodríguez-Manzaneque and Tamarit 2002), also as *ISA1* and *IBA57* mutants (Sánchez, Gómez-Gallardo et al. 2019). Authors describe that the *isa1*Δ and *iba57*Δ mutants showed respiratory deficiency and strong/null formation of respiratory supercomplexes, suggesting that the Fe–S-IBG subsystem components may cause respiratory-deficiency by affecting the respiratory complex conformation (Sánchez, Gómez-Gallardo et al. 2019). With these antecedents, we evaluated the *in situ* mitochondrial oxygen consumption rates (OCR) to determinate the mitochondrial functionality in the *isa2*Δ mutant. In this case, *grx5*Δ and *rip1*Δ mutants were included as controls. Respiration was completely abolished in both the coupled and uncoupled states in the *isa2*Δ mutant similar to unable to respire *rip1*Δ mutant, contrary to the *grx5*Δ mutant (diminished in respiration rate); however, the OCR in the complemented *isa2*Δ mutant was partially recovered (Fig. 6a-b).

In *S. cerevisiae* mitochondria, complex III is the mayor site of ROS generation in the ETC, since it lacks a rotenone-sensitive complex I, the other site of ROS production in the ETC of superior eukaryotes. We exposed the cells to antimycin A, an inhibitor of complex III, to further explore the possible role of complex III in ROS generation. Remarkably, when the antimycin A plus KCN was added an oxygen release in the assay chamber (i.e. negative values for OCR, Fig. 6c) instead of oxygen consumption in *isa2*Δ mutant was showed. This is suggestive of ROS production, since superoxide dismutase catalyzes the conversion of $O_2^{\bullet-}$ to O_2 and H_2O_2, while catalase converts the latter species into H_2O and O_2. In contrast

to the behavior of *rip1*Δ mutant, which shows affected iron homeostasis, displayed an OCR abolished in comparison to that of the WT strain.

To determine which segment of the ETC was responsible for the effects described above, partial ETC reactions were analyzed. Succinate-DCIP oxidoreductase activity (representative of complex II activity) was observed to be abolished in *isa2*Δ mutant, and to be severely affected but not abolished in control mutants *grx5*Δ and *rip1*Δ, which displayed behavior around 30–40% of the WT activity (Fig. 7a). The same trend was observed in both antimycin A-sensitive succinate-cytochrome *c* oxidoreductase (representative of the activity of complexes II+III, using the endogenous ubiquinol-6 pool as a substrate and cytochrome *c* oxidase (representative of complex IV) activities; also testing the activity of complex III by measuring the oxidation of decylubiquinol. Results showed that their activities in complexes III and IV were entirely abolished in *isa21*Δ and *rip1*Δ mutants, whereas in *grx5*Δ strain, a remain activity of ~20–40% with respect to WT mitochondria was detected (Fig. 7b-d). This is concordant with the fact that Isa1p has been described as participating in the assembly of [2Fe–2S] centers, which is the type of ISC present in the Rieske subunit of complex III, also associated with loss or diminution of mitochondrial proteins containing heme groups (Gomez, Perez-Gallardo et al. 2014, Sánchez, Gómez-Gallardo et al. 2019). The last observation is in accordance with the ETC functionality that depend on Fe–S proteins, as seen in the mitochondrial from *isa2*Δ mutant, suggesting that this protein could also be essential for [Fe–S] assembly in mitochondrial respiratory complexes and electron transport activity. Our results indicate that deletion of *ISA2* causes the dysfunction of the ETC, which deletion is likely associated with the instability of ETC surpercomplexes as described to occur in the complex-conformed Isa1p and Iba57p mutants (Sánchez, Gómez-Gallardo et al. 2019).

Determination of the enzymatic activity of *cis*-aconitase has been used to monitor the assembly of [4Fe–4S] centers into target proteins (Muhlenhoff, Richter et al. 2011). Accordingly, we determined the aconitase activity in mitochondria of the *isa2*Δ mutant. Aconitase activity was among totally abrogated at similar levels as previously reported to occurred in the *isa1*Δ and *iba57*Δ mutants, while partially decreased in the *grx5*Δ and *rip1*Δ mutants (Fig. 8). The results showed that in the *isa2*Δ mutant, the insertion of [4Fe–4S] clusters into aconitase target proteins was prevented, confirming that components of the Fe–S-IBG subsystem participate in assembly of apoproteins [4Fe–4S]-dependent. Thus, *ISA2* deletion is also associated with the dysfunction of ETC supercomplexes, likely affects the insertion or maturation process of the [Fe–S] center-containing proteins such as occurred with another Fe–S-IBG subsystem participants.

ETC supercomplexes maturation is affected by *ISA2* deletion

To determine whether the *ISA2* deletion, directly or indirectly disturbs the formation of III/IV supercomplexes by preventing the maturation of [Fe–S] clusters containing-proteins in mitochondrial complexes, we tested its effect on supercomplex maturation by blue native polyacrylamide gel electrophoresis (BN-PAGE). Mitochondrial extracts from WT cells

evaluated by BN-PAGE (first dimension) showed well-defined protein bands (B1–B5) in the mitochondrial extracts as in the *isa2*Δ mutant and its complemented strain (Fig. 9a). When the BN-PAGE gels were immunoblotted with anti-Rip1p antibody (anti Rieske protein), the *isa2*Δ mutant not showed blot signaling, but defined bands were observed in the WT and the complemented *isa2*Δ mutant (Fig. 9b). As expected, only immunoblot signaling was observed in the *isa2*Δ complemented mutant when the anti-His-tag antibody was used (Fig. 9c). Interestingly, when BN-PAGE gels were immunoblotted using the anti-Cox3 antibody, well defined band signals were observed in the WT mitochondrial extracts, but not in the corresponding band to supercomplexes $CIII_2$ + CIV in the *isa2*Δ mutant, which were partially recovery in the complemented *isa2*Δ mutant (Fig. 9d). When lanes of BN-PAGE gels were resolved in a second dimension by SDS-PAGE and immunodetected, with the anti-Rip1p antibody, clearly was identified the Rip1p protein spot (Fig. 10a).

Importantly, the anti-rip1 signal was over expressed in the *isa2*Δ mutant plasmid-complemented [*isa2*Δ (pYES2:*ISA2*)], while that the rip1p signal was clearly observed in both supercomplex bands ($CIII_2$ + CIV_2 and $CIII_2$ + CIV) (Fig. 10c), which was no observed in the *grx5*Δ mutant (Fig. 10b). This fact was confirmed when mitochondrion extracts from the complemented [*isa2*Δ (pYES2:*ISA2*)] strain immunoblotted with anti-His-tag antibody (Fig. 10d), showing similar behavior to anti-rip1p immunodetection. These results confirm that bands corresponded to respiratory supercomplexes were affected by the *ISA2* deletion, and immunoblotting of lines cut from the BN-PAGE gels and run in SDS-PAGE showed that Rip1 protein integration into supercomplexes III_2IV_2 and III_2IV_1 absent in the *isa2*Δ were recovered in the complemented yeast (Fig. 10d). Thus, the assembly of ETC supercomplexes formed by complexes III and IV is favored by integration of Rip1p into complex III (Conte, Papa et al. 2015) , but in the absence of the [2Fe–2S] cluster, Rip1p is susceptible to protease degradation, although apo-Rip1p (without a Fe–S cluster) has been detected to be inserted into complex III, resulting in a nonfunctional complex (Smith, Fox et al. 2012, Sánchez, Gómez-Gallardo et al. 2019). These results indicate that *ISA2* deletion abolished III_2IV_2 and III_2IV_1 supercomplex formation. The fact to be found similar spot signals when membranes were developed with both antibodies (anti-rip1p and anti-His-tag) show evidences which suggest that Isa2p directly interacts with Rip1p into the supercomplexes assembly, supposition that was elucidated below.

Isa2p is required for Rieske protein integration in mitochondrion

The dysfunction in the ETC in the *isa2*Δ mutant suggests that this is required for the respiratory supercomplexes formation such as occurs for the Isa1p, Iba57p, and Grx5p; where these are involved in Rieske protein maturation and, in turn, the Rieske protein assembly for the respiratory supercomplex formation as described (Conte et al., 2015; Conte and Zara, 2011). Thus, we determined the levels of Rip1p content in mitochondrial extracts of the *isa2*Δ mutant.

As expected, Rip1p expression was almost totally lacked in the mitochondria of the *rip1*Δ, *iba57*Δ, and *isa1*Δ mutants when were grown on YPD medium compared with the WT yeast,

showing the *isa2*Δ and *grx5*Δ mutants, lower levels of Rip1p expression than the WT (Fig. 11a). However, expression of Rip1p in the mitochondria of yeast of the complemented *isa2*Δ (pYES2:*ISA2*) strain, an hyper-expression of Rip1p was observed. In addition, yeast cultured in YPD plus ethanol (4 %) as ROS-generator, the Rip1p was not showed in the *rip1*Δ, *iba57*Δ, *isa1*Δ, also as in the *isa2*Δ mutant, but not in the *grx5*Δ mutant and WT yeast (Fig. 11b). These result showed that the Isa2p also is essential for the Rip1p assembly and mitochondrial function also as others proteinic components of the Fe–S-IBG subsystem, confirming that a direct interaction between Isa2p (Fe–S-IBG subsystem) occurred in the Rieske subunit integration on the respiratory supercomplexes.

Respiratory supercomplexes are now considered the functional units mediating optimal electron transfer from reducing equivalents to molecular oxygen by channeling substrates and decreasing ROS generation (Vartak, Porras et al. 2013). Therefore, impaired respiration and mitochondrial dysfunction in the *isa2*Δ mutant, and the inability of the mutant to form III/IV supercomplexes are in agreement with this hypothesis. Moreover, the role of Rip1p in the integrity of the supercomplexes is reinforced by the observation of full impairment of respiration observed in the *isa2*Δ mutant. The increased release of oxygen in the *isa2*Δ mutant in response to antimycin A suggest that increased superoxide generation occurred at the level of complex III (Gomez, Perez-Gallardo et al. 2014). It has been reported that the failure to insert the [2Fe–2S] cluster of Rip1p alters the environment of quinone redox sites of complex III (Gutierrez-Cirlos, Merbitz-Zahradnik et al. 2002). These alterations may lead to enhanced ROS generation because of augmented electron leakage at these redox sites, because similar phenotypes exhibited the *isa2*Δ mutant to that of the *rip1*Δ mutant. This suggests that Rip1p deletion alters electron transfer between the redox sites of the complex III, likely because of the lack of [2Fe–2S] cluster insertion, as occurs in the *rip1*Δ mutant.

The role of the Fe–S-IBG subsystem in the formation of supercomplexes through a mechanism on Rip1p plays an important role was supported by the negligible expression on mitochondrial extracts (Figs. 10-11). These results indicate that the Fe–S-IBG system affects the expression of Rip1p, the catalytic subunit [2Fe–2S] cluster containing of cytochrome *c*, via cluster integration; failure in the insertion of the [2Fe–2S] cluster into Rip1p leads to augmented susceptibility to proteolysis (Gutierrez-Cirlos, Merbitz-Zahradnik et al. 2002). Another could be supported by the Fe–S-IBG subsystem role in the formation/maturation of supercomplexes, since the Rip1p showed decreased levels on supercomplexes III_2IV_2 and III_2IV_1, observed in the *isa2*Δ mutant. These findings were further confirmed when supercomplex bands were run in a second dimension, which revealed the absence of Rip1p in the remaining supercomplex bands of *isa2*Δ and decreased levels observed in total protein extracts (Figs. 10-11). These results further suggest that Rip1p integrity plays important roles in supercomplex conformation and that its maturation depends also on Isa2p from the Fe–S-IBG subsystem.

The activity of the complex II-complex III segment of the ETC was fully inhibited in the *isa2*Δ mutant and *rip1*Δ control strain (Fig. 5). Although this observation may be the result of

impaired complex II activity (i.e., a complex containing [4Fe–4S] clusters) arising from the use of succinate as a substrate, we observed the same result using decylubiquinol, a direct substrate for complex III. Therefore, dysfunction of complex III in the *isa2*Δ mutant may be associated with impaired Rieske subunit assembly as shown in figure 11. Impaired complex III activity may have resulted from oxidative damage due to uncontrolled ROS production as observed in the *ISC* mutants (Gomez, Perez-Gallardo et al. 2014). However, based on the results of aconitase activity, this is not the main reason, as aconitase, a protein whose activity is a marker of oxidative stress (Gardner 1997, Muhlenhoff, Richter et al. 2011), it was impaired in the *isa2*Δ mutant, which exhibited complex III activity and diminished Rip1p expression. This indicates that enhanced oxidative stress is sufficient for inducing impairment of complex III activity.

Complex IV activity was also fully inhibited in the *isa2*Δ mutant and decreased in the *grx5*Δ mutant, which lack an [Fe–S] cluster. This may be explained by their inability to form ETC supercomplexes; when complex III has an incorrect conformation, it is susceptible to protein degradation, which may strongly affect the activity of complex IV. This suggestion agrees with the observation that when complex III has an incorrect conformation, which may be associated with the absence of Rip1p, the activity of complex IV is strongly affected (Schilke, Williams et al. 2006, Sánchez, Gómez-Gallardo et al. 2019). Therefore, the assembly of ETC supercomplexes formed by complexes III and IV is favored by integration of Rip1p into complex III (Conte and Zara 2011, Diaz, Enriquez et al. 2012, Conte, Papa et al. 2015, Sánchez, Gómez-Gallardo et al. 2019).

Mutants in the ISC assembly system, as in the Fe–S-IBG subsystem, are unable to conduct mitochondrial respiration and are considered as $rho^{0/-}$ mutants. However, we identified in mitochondrion extracts of the *isa2*Δ mutant, the presence of *COX2* and *COX3* (genes that encodes proteins that form the core of cytochrome *c* oxidase complex; thus, *isa2*Δ inability to respire and affected supercomplex maturation is not attributed to its rho^{-} phenotype.

The Isa1p/Isa2p and Iba57p proteins have been extensively described to participate in the assembly of [4Fe–4S]-type centers from specific apo-proteins (Muhlenhoff, Richter et al. 2011, Sheftel, Wilbrecht et al. 2012, Brancaccio, Gallo et al. 2014). In addition, the present study revealed that Isa2p also was involved in the maturation of the Rieske subunit of ETC complex III and associated with transference or recycling of its [2Fe–2S] cluster such as occurred for the Isa1p and Iba57p (Gomez, Perez-Gallardo et al. 2014, Sánchez, Gómez-Gallardo et al. 2019). Thus, our results strength the idea of a central role for Isa1p/Isa2p and Iba57p in the assembly of [4Fe–4S] clusters, this system may have a dual function in directly transferring [2Fe–2S] centers to Rip1 apoprotein or participate in the maturation of [4Fe–4S] by a fusion of two [2Fe–2S] centers as proposed (Banci, Brancaccio et al. 2014, Sánchez, Gómez-Gallardo et al. 2019), in that found that the ISCA1/ISCA2 heterodimer in humans (Isa1p/Isa2p homologs of yeast) can bind either [2Fe–2S] or [4Fe–4S] clusters, with the human GRX5 (Grx5p homolog) also binding $[2Fe–2S]^{2+}$ clusters (Ajit Bolar, Vanlander et al. 2013, Al-Hassnan, Al-Dosary et al. 2015, Beilschmidt, Ollagnier de Choudens et al. 2017). In this mechanism, two GRX5-$[2Fe–2S]^{2+}$ complexes may donated the $[2Fe–2S]^{2+}$ to a heterodimeric ISCA1/ISCA2 complex, suggesting that the protein formed acts as an

"assembler" of [4Fe–4S] clusters and is the functional unit in mitochondria that receives [2Fe–2S] clusters from human GRX5 and assembles [4Fe–4S] clusters before their transfer to the final target apoproteins. The heterocomplexes existence has been described such as the [2Fe–2S]-BOLA1-GRX5 and [2Fe–2S]-BOLA3-GRX5 (Nasta, Giachetti et al. 2017). Other studies that can to help to understand the roles of the Fe–S-IBG subsystem on the dual function of assembly as [4Fe–4S] as [2Fe–2S] clusters involves oxido-reduction of the $[4Fe–4S]^{2+}$ clusters to generate $[2Fe–2S]^{2+}$ clusters during O_2-induced by biotin synthase, suggesting the occurrence of $[4Fe–4S]^{2+} \leftrightarrow [2Fe–2S]^{2+}$ cluster interconversion to regulate enzyme activity in response to oxidative stress (Zhang, Crack et al. 2012). Thus, the Isa1p/Isa2p/Iba57p/Grx5p subsystem may participate in the sorting of both [4Fe–4S] and [2Fe–2S] clusters, where oxygen tension and/or excessive ROS generation may be the factors or "switch" controlling which type of [Fe–S] cluster is inserted into the apoproteins. This may be physiologically important for yeast because of their anaerobic metabolism, although a hypothetical signal that allows this system to "switch" between the delivery of [2Fe–2S] or [4Fe–4S] centers requires further investigation.

In *S. cerevisiae*, supercomplex III_2/IV_2 was significantly affected in mitochondria isolated from *isa2*Δ mutant in comparison to the activity of complexes II and III in the *grx5*Δ mutant, although reduced, was not completely inhibited. These results confirm that the Isa2p plays an important role in the maturation or insertion of the Rieske subunit on the supercomplex III/IV of the ETC in a process influenced by the integrity of the Rieske protein. Thus, the mitochondrial energy metabolism of yeast is strongly dependent on the correct assembly of Rieske protein in complex III and, in turn, strengthens that the Fe–S-IBG assembly subsystem is involved directly in the maturation and insertion of the [2Fe–2S] cluster into the Rieske subunit of complex III.

Figure legends

Figure 1. Studies of growth in plates and growth kinetics of *S. cerevisiae ISA2* mutant. (a) Dilutions of yeast suspensions were cultured on YPD agar plates with ethanol at the indicated concentrations, 30 °C for 48 h. (b) Yeast growth kinetics, yeast cultures were grown on YPD liquid medium with ethanol at the indicated concentrations. Cultures were incubated at 30ºC with light shaking and growth (biomass) was determined by measuring O.D. at 600 nm. Values representing the means and standard errors of the means (SEM) are indicated as bars (n = 3).

Figure 2. Immunodetection of recombinant proteins in the complemented *S. cerevisiae* mutants. Protein extracts obtained of yeast cultures grown on YPD medium induced with galactose were separated by SDS-PAGE gels, after western blot using anti-His-tag antibody was carried out as described in Material and Methods. **a**) Galactose

induction of recombinant proteins in extracts obtained from yeast cultured in YPD medium. **b**) Effect of ethanol on the expression of the recombinant proteins obtained from yeast cultured in YPD + galactose medium plus ethanol as stressor. Representative images are shown of at least three repetitions.

Figure 3. **Kinetics of ROS generation in suspensions of *S. cerevisiae ISA2* mutant.** Yeast cultures were grown in liquid YPD medium with 10% ethanol as ROS stressor and harvested in late exponential growth phase. Yeast YPD-grown cultures were incubated for 30 min with the respective ROS probe. Samples (100 □L) were taken and suspended in PBS buffer for determination of intracellular ROS levels by real-time analysis in a flow cytometer. a) Results represent the percentage of cells that showed positive fluorescence. The ROS fluorescent probes H_2DCFDA (total ROS) and DHR123 (mitochondrial ROS in general) were used. Values are the means of three independent experiments with 40,000 cells counted by flow cytometry per each point. SEM values are indicated as bars (n = 3). b) Representative flow cytometry dot plots show the percentage of fluorescent cells in the Q1 quadrant using the indicated ROS probe.

Figure 4. Confocal microscopy images of *S. cerevisiae* cultures to detect localization of ROS and free Fe^{2+}. Yeast YPD-grown cultures were loaded with the fluorescent probe PGFL and treated with ethanol (10%) as stressor, incubated for 30 min at 30°C and co-loaded with DHE as a ROS probe and observed using a confocal microscope (Olympus FV1000). (a) Yeast cells observed in clear field. (b) Yeast cells stained with DHE probe for superoxide determination. (c) Yeast cells stained with PGFL probe for free Fe^{2+} determination. (d) Merged images of $O_2^{\bullet-}$ and free Fe^{2+} co-localization in yeast cells staining with DHE and PGFL probes. Images of the yeast cells were taken using 65× magnification.

Figure 5. Glutathione content in the *S. cerevisiae ISA2* mutant. Yeast cultures were grown in liquid YPD medium and harvested in the late exponential growth phase. The GSH/GSSG content was determined in whole cells spheroplasts (a) or mitochondrion (b). Oxidized glutathione (GSSG), reduced glutathione (GSH), and GSH/GSSG ratio were determined as described in Materials and Methods. Means and SEM values are indicated as bars (n = 3), one-way ANOVA with Bonferroni post hoc test was used for comparison, significant differences ($P < 0.05$) with respect to WT are indicated with asterisks (*).

Figure 6. Respiration test of mitochondrion suspensions of the *S. cerevisiae ISA2* mutant. Mitochondrial functionality was evaluated in mitochondrion suspensions obtained from cultures grown in liquid YPD medium. Mitochondrion were used for oxygen consumption rate (OCR) measurements with a Clark-type oxygen electrode coupled to a biological oxygen monitor as described in the Materials and Methods. a–c) Basal OCR with glucose as substrate, a) OCR under coupled state conditions. b) OCR under uncoupled state conditions using CCCP for uncoupling. c) OCR under complex III blocking conditions

using antimycin A plus cyanide as inhibitors. Values are the means of three independent experiments. SE values are indicated as bars (n = 3), one-way ANOVA with Tukey's post-hoc test was used to compare yeast strains, significant differences ($P < 0.05$) are indicated with different lowercase letters.

Figure 7. Analyses of the functionality of mitochondrial respiratory chain complexes in the *S. cerevisiae ISA2* mutant. Mitochondrial functionality was evaluated in mitochondrial suspensions obtained from cultures grown in liquid YPD medium, and mitochondrial activities were measured as described in the Materials and Methods. a) Activity of succinate-DCIP oxidoreductase. b) Activity of succinate-cytochrome *c* oxidoreductase. c) Activity of cytochrome *c* oxidoreductase. d) Activity of cytochrome *c* oxidase. Values are the means of three independent experiments. SE values are indicated as bars (n = 3), one-way ANOVA with Tukey's post-hoc test was used to compare yeast strains, significant differences ($P < 0.05$) are indicated with different lowercase letters.

Figure 8. Determination of *cis*-Aconitase activity in the *S. cerevisiae ISA2* mutant. Mitochondrial functionality was evaluated in mitochondrial suspensions obtained from cultures grown in liquid YPD medium, and mitochondrial activities were measured as described in the Materials and Methods. Values are the means of three independent experiments. SE values are indicated as bars (n = 3), one-way ANOVA with Tukey's post-hoc test was used to compare yeast strains, significant differences ($P < 0.05$) are indicated with different lowercase letters.

Figure 9. **Evaluation of ETC mitochondrial supercomplexes formation by BN-PAGE in the *S. cerevisiae ISA2* mutant**. Mitochondrial suspensions were solubilized with digitonin and the proteins were separated using blue native polyacrylamide gel electrophoresis (BN-PAGE) as described in the Material and Methods. The ETC mitochondrial supercomplexes are indicated to the left of the gels. **a**) BN-PAGE of mitochondrial suspensions solubilized with digitonin; B1–B5, major protein bands corresponding to mitochondrial supercomplexes. **b**) Western blot of BN-PAGE gel (**a**) using anti-Rip1 antibody. **c**) Western blot of BN-PAGE gel (**a**) using anti-His-tag antibody. **d**) Western blot of BN-PAGE gel (**a**) using anti-Cox3p antibody. Representative images are shown of at least three repetitions.

Figure 10. **Evaluation of ETC mitochondrial supercomplexes formation by 2-D SDS-PAGE in the *S. cerevisiae ISA2* mutant**. Mitochondrial suspensions were solubilized with digitonin and the proteins were separated using blue native polyacrylamide gel electrophoresis (BN-PAGE). After, second dimension (SDS-PAGE) of gel slice from BN-PAGE corresponding to the yeast strains were run, as described in the Material and Methods. Western blot of 2-D SDS-PAGE gel was carried out and reveled using anti-Rip1 antibody or anti-His-tag antibody. Rip1p protein is indicated in the amplified section between 10-30 kDa molecular mass region. Molecular mass marker in kilodaltons is shown to the left of the images. Representative images are shown of at least three repetitions.

Figure 11. Immunodetection of Rieske protein in the *Saccharomyces cerevisiae* ISA2 mutant. Mitochondrial extracts separated by SDS-PAGE gels were immunoblotted using anti-Rip1p antibody as described in Material and Methods. **a**) Mitochondrial extracts obtained from yeast cultured in YPD medium. **b**) Mitochondrial extracts obtained from yeast cultured in YPD medium plus ethanol 4% as stressor. Representative images are shown of at least three repetitions.

Figure S1. Gene amplification of nuclear and mitochondrial genes in *Saccharomyces cerevisiae* strains. (a) Total yeast DNA was isolated and the strain *E. coli* JM101 was transformed as mentioned in Materials and Methods; restriction of isolated plasmids by electrophoresis agarose gels are shown. M, indicate molecular size marker is shown, the plasmid pYES2/CT was digested with the Xho1 endonuclease, while that the plasmids pYES2:*GRX5* and pYES2:*ISA2* were digested with the Xho1 and HindIII endonucleases, respectively. (b) PCR products obtained from total DNA amplification using oligonucleotides specific for each gene as described in the Materials and Methods section. Representative agarose gels stained with ethidium bromide are showed. Expected sizes of DNA fragments were as follows: *ISA2* (~570 bp), *GRX5* (465 bp), *RIP1* (648 bp), *COX2* (357 bp), and (*COX3* (239 bp).

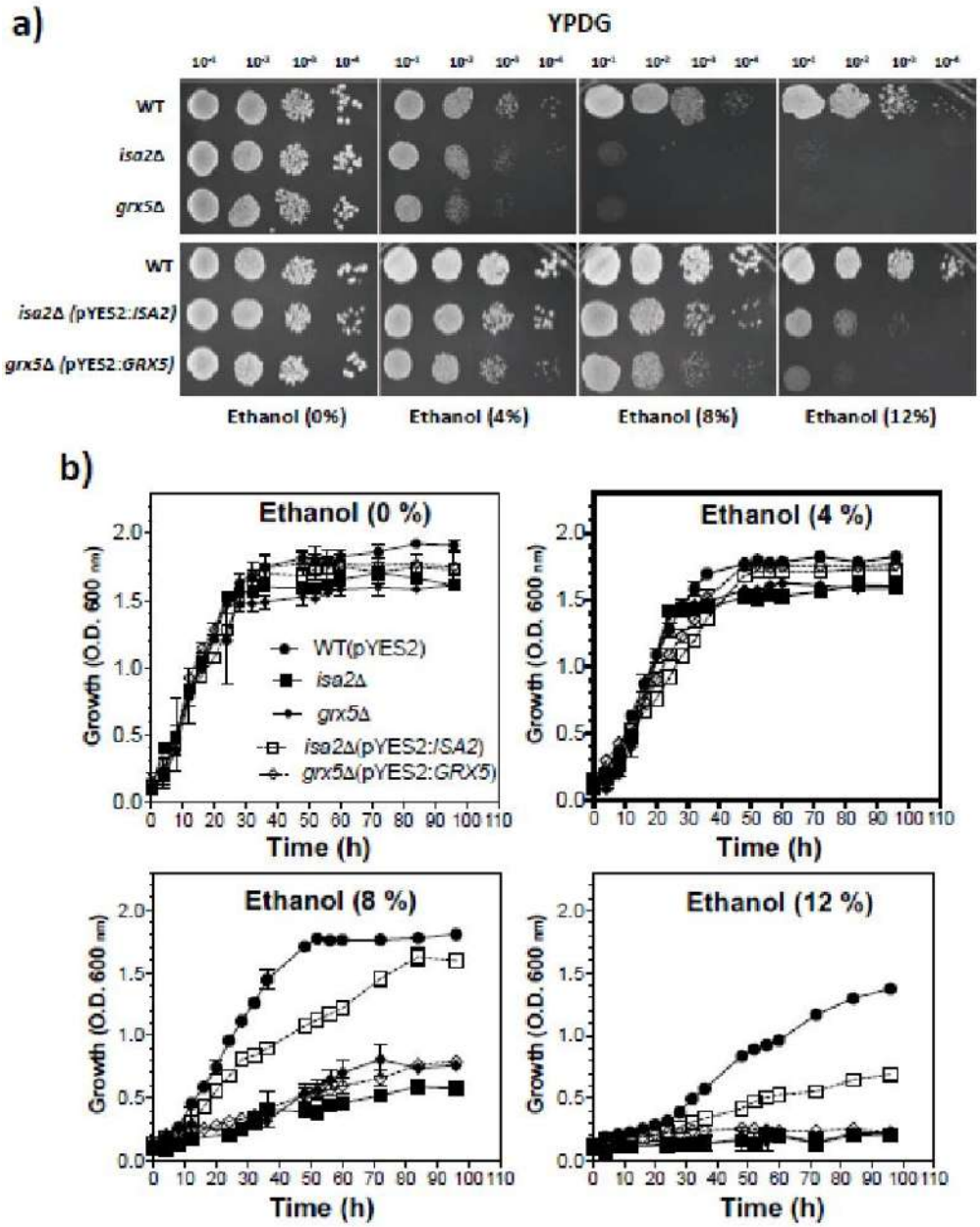
a)
YPDG
WT
isa2Δ
grx5Δ
WT
isa2Δ (pYES2:ISA2)
grx5Δ (pYES2:GRX5)
Ethanol (0%)
Ethanol (4%)
Ethanol (8%)
Ethanol (12%)
b)
Ethanol (0 %)
Ethanol (4 %)
Ethanol (8 %)
Ethanol (12 %)
Growth (O.D. 600 nm)
Time (h)
WT(pYES2)
isa2Δ
grx5Δ
isa2Δ(pYES2:ISA2)
grx5Δ(pYES2:GRX5)

Figure 1

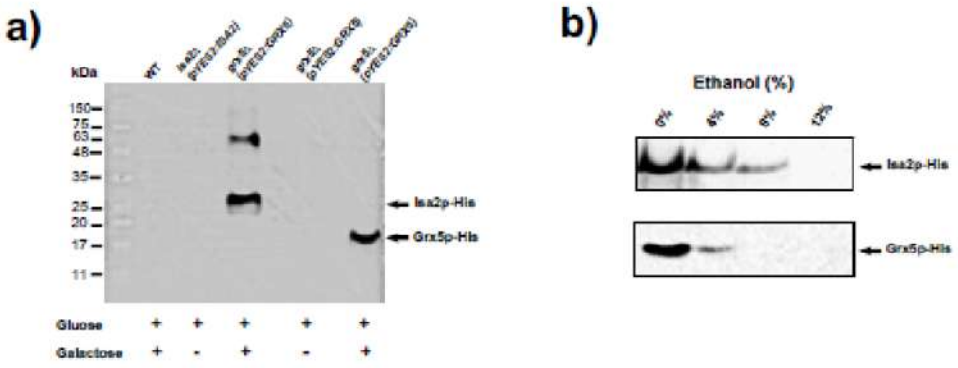
a)
kDa
150
75
63
48
35
25
20
17
11
Isa2p-His
Grx5p-His
Glucose
Galactose
b)
Ethanol (%)
Isa2p-His
Grx5p-His

Figure 2

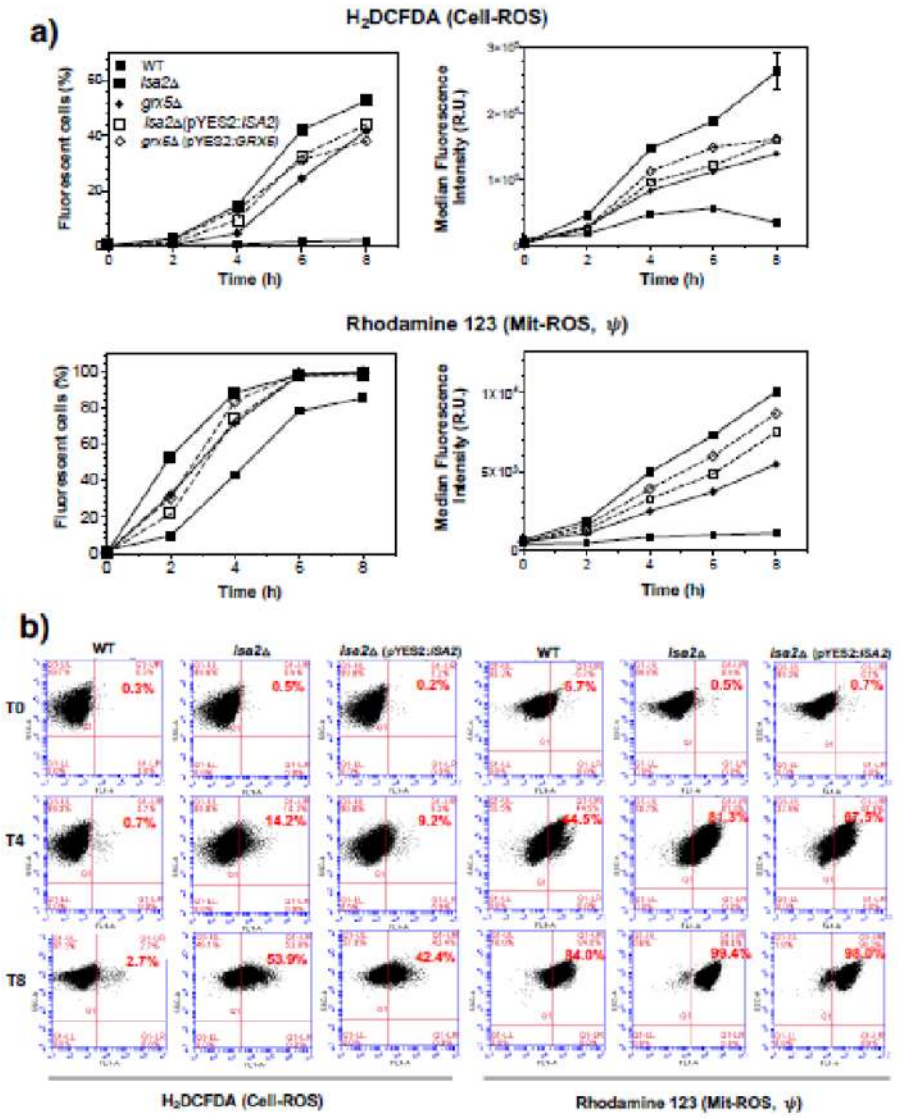
a)
H2DCFDA (Cell-ROS)
WT
Isa2Δ
Grx5Δ
Isa2Δ(pYES2:ISA2)
Grx5Δ (pYES2:GRX5)
Fluorescent cells (%)
Median Fluorescence Intensity (R.U.)
Time (h)
Rhodamine 123 (Mit-ROS, ψ)
b)
WT
Isa2Δ
Isa2Δ (pYES2:ISA2)
T0
T4
T8
0.3%
0.5%
0.2%
6.7%
0.5%
0.7%
0.7%
14.2%
9.2%
44.5%
61.3%
67.5%
2.7%
53.9%
42.4%
84.0%
99.4%
98.0%
H2DCFDA (Cell-ROS)
Rhodamine 123 (Mit-ROS, ψ)

Figure 3

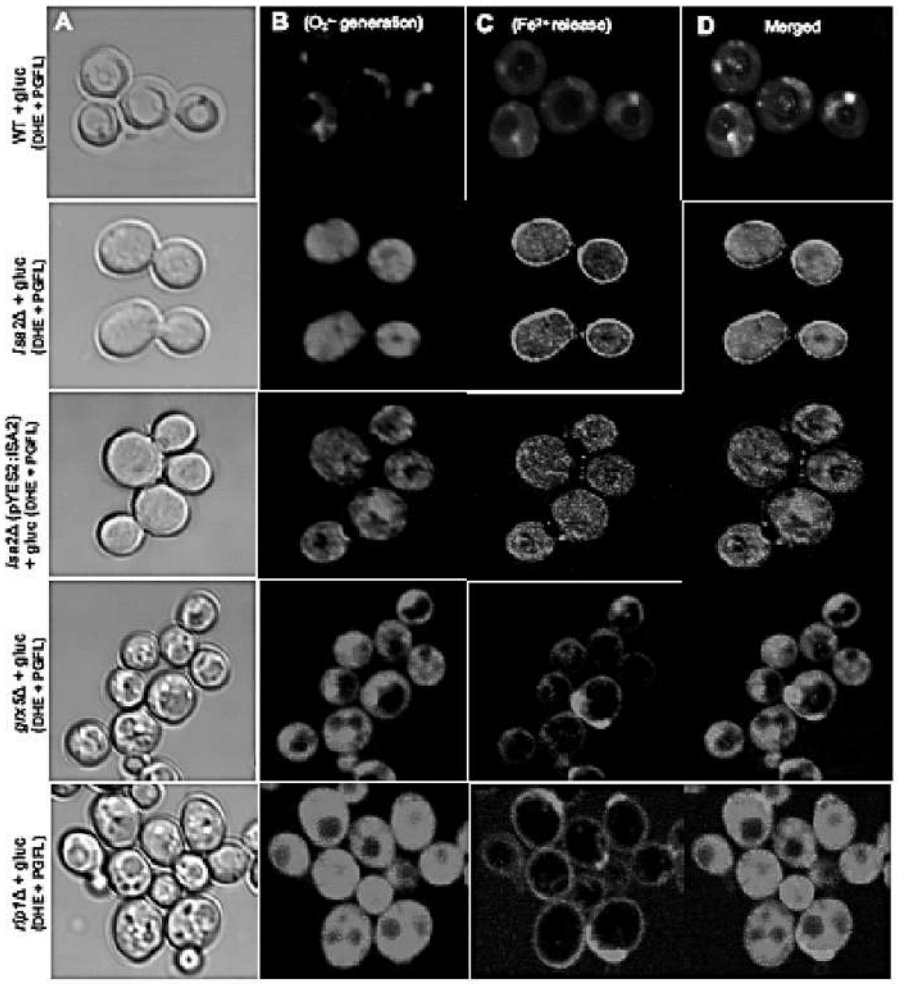
A
B (O_2^- generation)
C (Fe^{2+} release)
D Merged
WT + gluc (DHE + PGFL)
Isa2Δ + gluc (DHE + PGFL)
Isa2Δ (pYES2::ISA2) + gluc (DHE + PGFL)
grx5Δ + gluc (DHE + PGFL)
rip1Δ + gluc (DHE + PGFL)

Figure 4

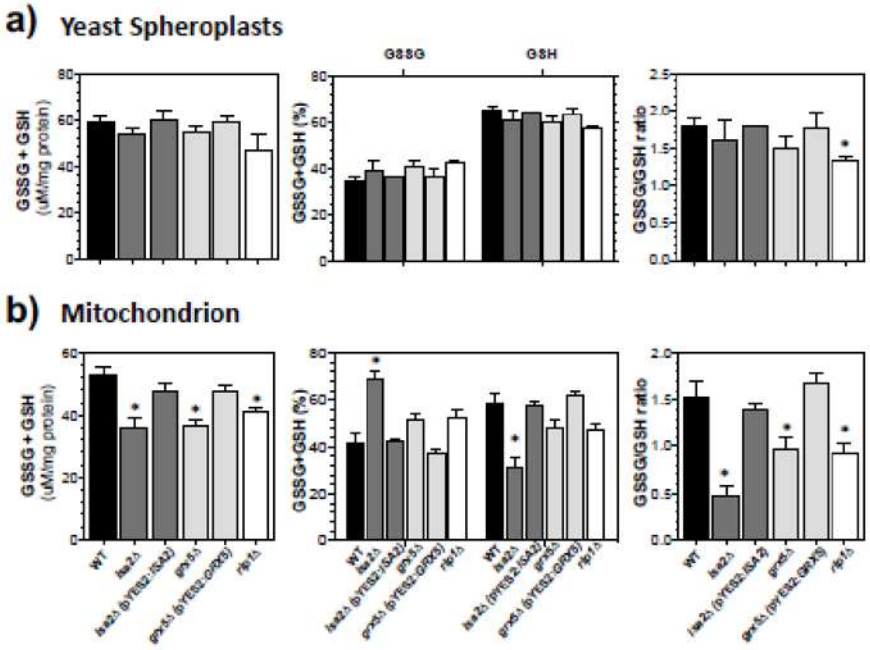
a)
Yeast Spheroplasts
GSSG
GSH
GSSG + GSH (uM/mg protein)
GSSG+GSH (%)
GSSG/GSH ratio
b)
Mitochondrion
GSSG + GSH (uM/mg protein)
GSSG+GSH (%)
GSSG/GSH ratio
WT
isa2Δ
isa2Δ (pYES2.1/ISA2)
grx5Δ
grx5Δ (pYES2.1/GRX5)
rip1Δ

Figure 5

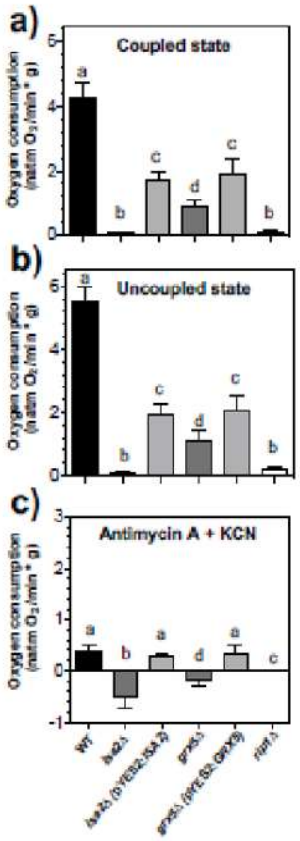

Figure 6

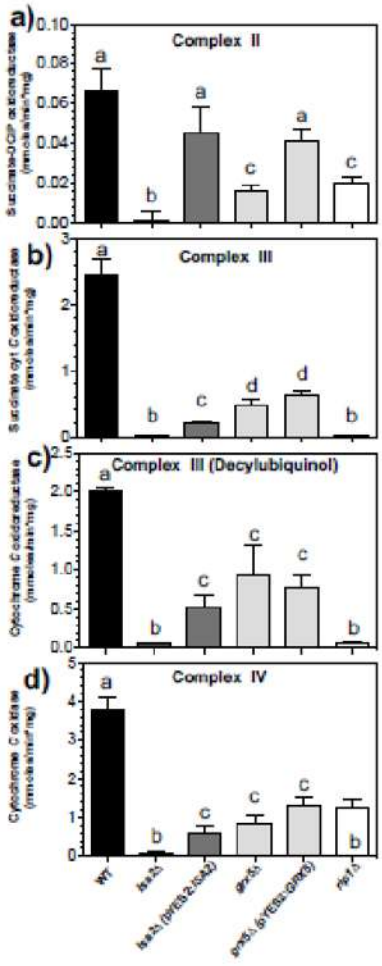
a)
Complex II
b)
Complex III
c)
Complex III (Decylubiquinol)
d)
Complex IV
WT
Isa2Δ
Isa2Δ (pYES2-ISA2)
grx5Δ
grx5Δ (pYES2-GRX5)
rip1Δ

Figure 7

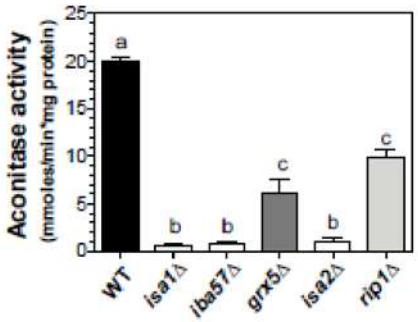
Aconitase activity
(mmoles/min*mg protein)
25
20
15
10
5
0
a
b
b
c
b
c
WT
isa1Δ
iba57Δ
grx5Δ
isa2Δ
rip1Δ

Figure 8

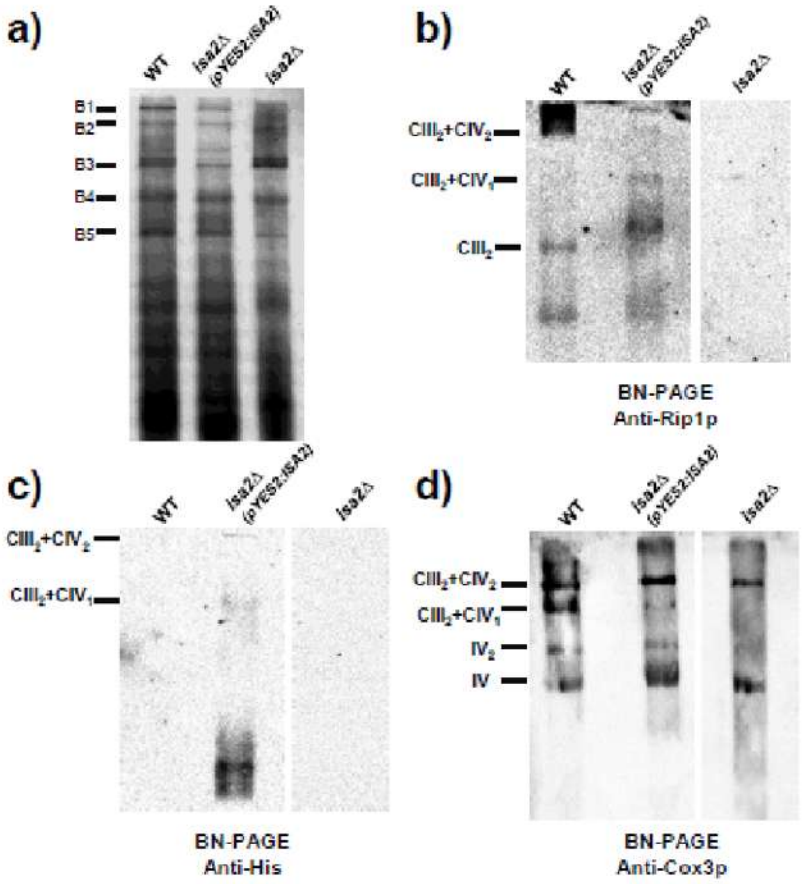
a)
WT
Isa2Δ (pYES2-ISA2)
Isa2Δ
B1
B2
B3
B4
B5
b)
WT
Isa2Δ (pYES2-ISA2)
Isa2Δ
CIII2+CIV2
CIII2+CIV1
CIII2
BN-PAGE
Anti-Rip1p
c)
WT
Isa2Δ (pYES2-ISA2)
Isa2Δ
CIII2+CIV2
CIII2+CIV1
BN-PAGE
Anti-His
d)
WT
Isa2Δ (pYES2-ISA2)
Isa2Δ
CIII2+CIV2
CIII2+CIV1
IV2
IV
BN-PAGE
Anti-Cox3p

Figure 9

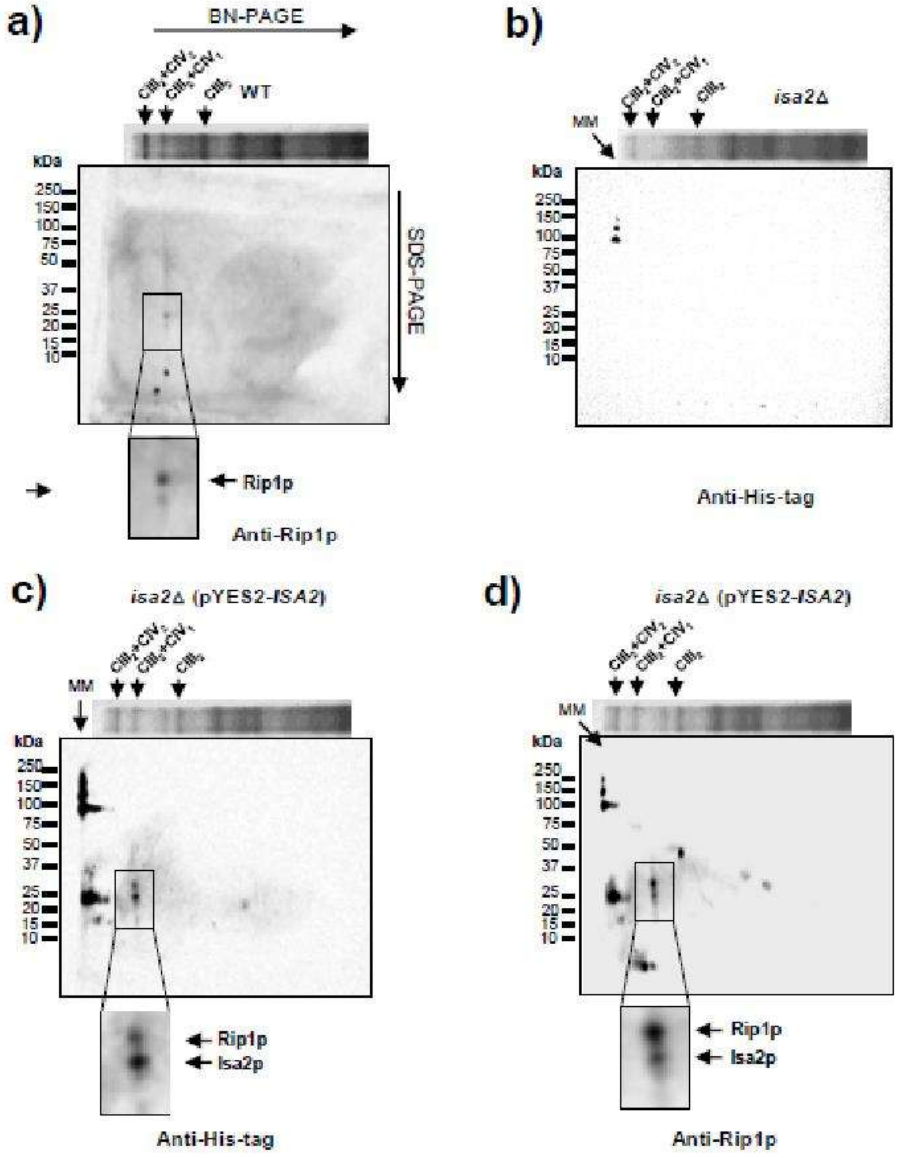
a)
BN-PAGE
WT
kDa
SDS-PAGE
Rip1p
Anti-Rip1p
b)
isa2Δ
MM
Anti-His-tag
c)
isa2Δ (pYES2-ISA2)
MM
Rip1p
Isa2p
Anti-His-tag
d)
isa2Δ (pYES2-ISA2)
MM
Rip1p
Isa2p
Anti-Rip1p

Figure 10

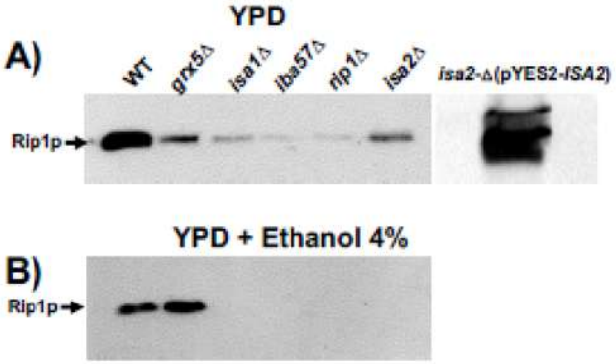
YPD
A)
WT
grx5Δ
isa1Δ
iba57Δ
rip1Δ
isa2Δ
isa2-Δ(pYES2-ISA2)
Rip1p
YPD + Ethanol 4%
B)
Rip1p

Figure 11

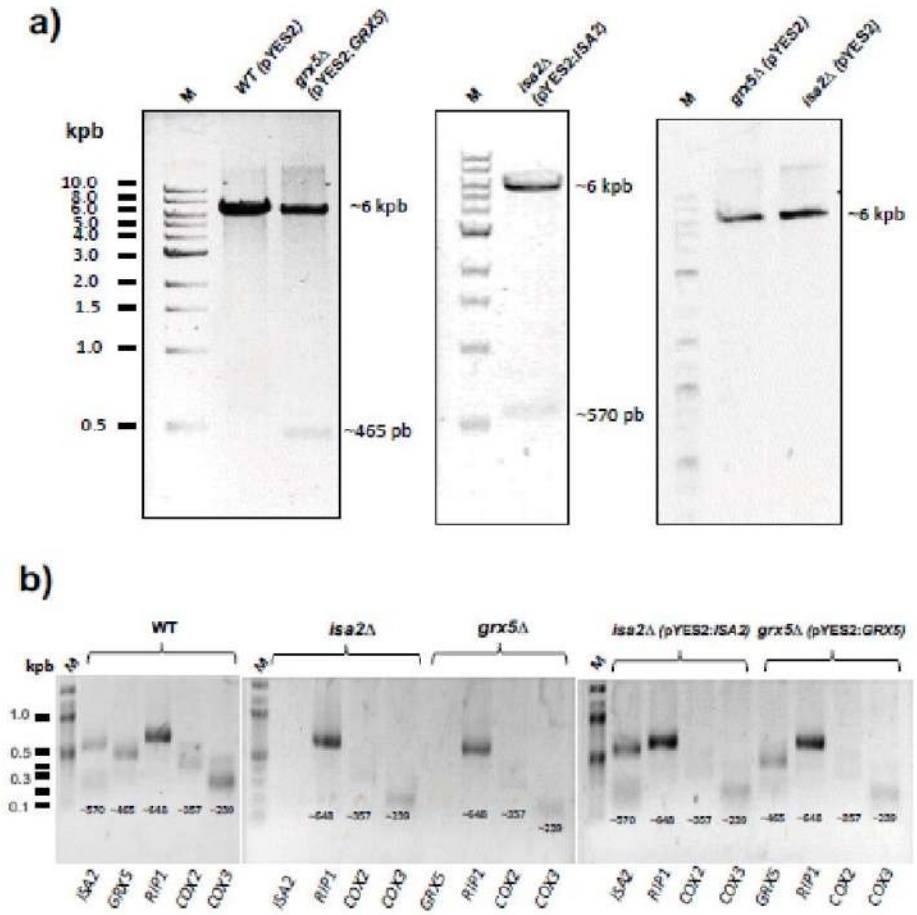
a)
M
WT (pYES2)
grx5Δ (pYES2:GRX5)
isa2Δ (pYES2:ISA2)
grx5Δ (pYES2)
isa2Δ (pYES2)
kpb
10.0
6.0
5.0
4.0
3.0
2.0
1.5
1.0
0.5
~6 kpb
~465 pb
~570 pb
b)
WT
isa2Δ
grx5Δ
isa2Δ (pYES2:ISA2)
grx5Δ (pYES2:GRX5)
kpb
1.0
0.5
0.3
0.1
ISA2
GRX5
RIP1
COX2
COX3

Figure S1

References

Ajit Bolar, N., A. V. Vanlander, C. Wilbrecht, N. Van der Aa, J. Smet, B. De Paepe, G. Vandeweyer, F. Kooy, F. Eyskens, E. De Latter, G. Delanghe, P. Govaert, J. G. Leroy, B. Loeys, R. Lill, L. Van Laer and R. Van Coster (2013). "Mutation of the iron-sulfur cluster assembly gene IBA57 causes severe myopathy and encephalopathy." Hum Mol Genet **22**(13): 2590-2602.

Al-Hassnan, Z. N., M. Al-Dosary, M. Alfadhel, E. A. Faqeih, M. Alsagob, R. Kenana, R. Almass, O. S. Al-Harazi, H. Al-Hindi, O. I. Malibari, F. B. Almutari, S. Tulbah, F. Alhadeq, T. Al-Sheddi, R. Alamro, A. AlAsmari, M. Almuntashri, H. Alshaalan, F. A. Al-Mohanna, D. Colak and N. Kaya (2015). "ISCA2 mutation causes infantile neurodegenerative mitochondrial disorder." J Med Genet **52**(3): 186-194.

Atkinson, J., N. Kapralov Aa Fau - Yanamala, Y. Y. Yanamala N Fau - Tyurina, A. A. Tyurina Yy Fau - Amoscato, L. Amoscato Aa Fau - Pearce, J. Pearce L Fau - Peterson, Z. Peterson J Fau - Huang, J. Huang Z Fau - Jiang, A. K. Jiang J Fau - Samhan-Arias, A. Samhan-Arias Ak Fau - Maeda, W. Maeda A Fau - Feng, K. Feng W Fau - Wasserloos, N. A. Wasserloos K Fau - Belikova, V. A. Belikova Na Fau - Tyurin, H. Tyurin Va Fau - Wang, J. Wang H Fau - Fletcher, Y. Fletcher J Fau - Wang, I. I. Wang Y Fau - Vlasova, J. Vlasova Ii Fau - Klein-Seetharaman, D. A. Klein-Seetharaman J Fau - Stoyanovsky, H. Stoyanovsky Da Fau - Bayîr, B. R. Bayîr H Fau - Pitt, M. W. Pitt Br Fau - Epperly, J. S. Epperly Mw Fau - Greenberger, V. E. Greenberger Js Fau - Kagan and V. E. Kagan (2011). "A mitochondria-targeted inhibitor of cytochrome c peroxidase mitigates radiation-induced death." (2041-1723 (Electronic)).

Banci, L., D. Brancaccio, S. Ciofi-Baffoni, R. Del Conte, R. Gadepalli, M. Mikolajczyk, S. Neri, M. Piccioli and J. Winkelmann (2014). "[2Fe-2S] cluster transfer in iron-sulfur protein biogenesis." Proc Natl Acad Sci U S A **111**(17): 6203-6208.

Beilschmidt, L. K., S. Ollagnier de Choudens, M. Fournier, I. Sanakis, M.-A. Hograindleur, M. Clémancey, G. Blondin, S. Schmucker, A. Eisenmann, A. Weiss, P. Koebel, N. Messaddeq, H. Puccio and A. Martelli (2017). "ISCA1 is essential for mitochondrial Fe4S4 biogenesis in vivo." Nature Communications **8**(1): 15124.

Beilschmidt, L. K., S. Ollagnier de Choudens, M. Fournier, I. Sanakis, M.-A. Hograindleur, M. Clémancey, G. Blondin, S. Schmucker, A. Eisenmann, A. Weiss, P. Koebel, N. Messaddeq, H. Puccio and A. Martelli (2017). "ISCA1 is essential for mitochondrial Fe4S4 biogenesis in vivo." **8**: 15124.

Brancaccio, D., A. Gallo, M. Mikolajczyk, K. Zovo, P. Palumaa, E. Novellino, M. Piccioli, S. Ciofi-Baffoni and L. Banci (2014). "Formation of [4Fe-4S] clusters in the mitochondrial iron-sulfur cluster assembly machinery." J Am Chem Soc **136**(46): 16240-16250.

Brand, M. D. and D. G. Nicholls (2011). "Assessing mitochondrial dysfunction in cells." Biochem J **435**(2): 297-312.

Conte, A., B. Papa, A. Ferramosca and V. Zara (2015). "The dimerization of the yeast cytochrome bc1 complex is an early event and is independent of Rip1." Biochim Biophys Acta **1853**(5): 987-995.

Conte, L. and V. Zara (2011). "The Rieske Iron-Sulfur Protein: Import and Assembly into the Cytochrome bc(1) Complex of Yeast Mitochondria." Bioinorg Chem Appl **2011**: 363941.

Cortes-Rojo, C., E. Calderon-Cortes, M. Clemente-Guerrero, M. Estrada-Villagomez, S. Manzo-Avalos, R. Mejia-Zepeda, I. Boldogh and A. Saavedra-Molina (2009). "Elucidation of the effects of lipoperoxidation on the mitochondrial electron transport chain using yeast mitochondria with manipulated fatty acid content." J Bioenerg Biomembr **41**(1): 15-28.

Diaz, F., J. A. Enriquez and C. T. Moraes (2012). "Cells lacking Rieske iron-sulfur protein have a reactive oxygen species-associated decrease in respiratory complexes I and IV." Mol Cell Biol **32**(2): 415-429.

Gardner, P. R. (1997). "Superoxide-driven aconitase FE-S center cycling." Biosci Rep **17**(1): 33-42.

Gelling, C., I. W. Dawes, N. Richhardt, R. Lill and U. Muhlenhoff (2008). "Mitochondrial Iba57p is required for Fe/S cluster formation on aconitase and activation of radical SAM enzymes." Mol Cell Biol **28**(5): 1851-1861.

Genova, M. L. and G. Lenaz (2014). "Functional role of mitochondrial respiratory supercomplexes." Biochimica et Biophysica Acta (BBA) - Bioenergetics **1837**(0006-3002 (Print)): 427-443.

Gomez, M., R. V. Perez-Gallardo, L. A. Sanchez, A. L. Diaz-Perez, C. Cortes-Rojo, V. Meza Carmen, A. Saavedra-Molina, J. Lara-Romero, S. Jimenez-Sandoval, F. Rodriguez, J. S. Rodriguez-Zavala and J. Campos-Garcia (2014). "Malfunctioning of the iron-sulfur cluster assembly machinery in Saccharomyces cerevisiae produces oxidative stress via an iron-dependent mechanism, causing dysfunction in respiratory complexes." PLoS One **9**(10): e111585.

Gourdoupis, S., V. Nasta, V. Calderone, S. Ciofi-Baffoni and L. Banci (2018). "IBA57 Recruits ISCA2 to Form a [2Fe-2S] Cluster-Mediated Complex." Journal of the American Chemical Society **140**(43): 14401-14412.

Gutierrez-Cirlos, E. B., T. Merbitz-Zahradnik and B. L. Trumpower (2002). "Failure to insert the iron-sulfur cluster into the Rieske iron-sulfur protein impairs both center N and center P of the cytochrome bc1 complex." J Biol Chem **277**(52): 50703-50709.

Henson, C. P. and W. W. Cleland (1967). "Purification and kinetic studies of beef liver cytoplasmic aconitase." J Biol Chem **242**(0021-9258 (Print)): 3833-3838.

Jensen, L. T. and V. C. Culotta (2000). "Role of Saccharomyces cerevisiae ISA1 and ISA2 in iron homeostasis." Molecular and cellular biology **20**(11): 3918-3927.

Jha, P., X. Wang and J. Auwerx (2016). "Analysis of Mitochondrial Respiratory Chain Supercomplexes Using Blue Native Polyacrylamide Gel Electrophoresis (BN-PAGE)." Curr Protoc Mouse Biol **6**(2161-2617 (Electronic)): 1-14.

Kulawiak, B., J. Höpker, M. Gebert, B. Guiard, N. Wiedemann and N. Gebert (2013). "The mitochondrial protein import machinery has multiple connections to the respiratory chain." Biochimica et Biophysica Acta (BBA) - Bioenergetics **1827**(5): 612-626.

Lill, R. (2009). "Function and biogenesis of iron-sulphur proteins." Nature **460**(7257): 831-838.

Lill, R., B. Hoffmann, S. Molik, A. J. Pierik, N. Rietzschel, O. Stehling, M. A. Uzarska, H. Webert, C. Wilbrecht and U. Muhlenhoff (2012). "The role of mitochondria in cellular iron-sulfur protein biogenesis and iron metabolism." Biochim Biophys Acta **1823**(9): 1491-1508.

Muhlenhoff, U., N. Richter, O. Pines, A. J. Pierik and R. Lill (2011). "Specialized function of yeast Isa1 and Isa2 proteins in the maturation of mitochondrial [4Fe-4S] proteins." J Biol Chem **286**(48): 41205-41216.

Musatov, A. and N. C. Robinson (2012). "Susceptibility of mitochondrial electron-transport complexes to oxidative damage. Focus on cytochrome c oxidase." Free Radic Res **46**(11): 1313-1326.

Nasta, V., A. Giachetti, S. Ciofi-Baffoni and L. Banci (2017). "Structural insights into the molecular function of human [2Fe-2S] BOLA1-GRX5 and [2Fe-2S] BOLA3-GRX5 complexes." Biochimica et Biophysica Acta (BBA) - General Subjects **1861**(8): 2119-2131.

Perez-Gallardo, R. V., L. S. Briones, A. L. Diaz-Perez, S. Gutierrez, J. S. Rodriguez-Zavala and J. Campos-Garcia (2013). "Reactive oxygen species production induced by ethanol in Saccharomyces cerevisiae increases because of a dysfunctional mitochondrial iron-sulfur cluster assembly system." FEMS Yeast Res **13**(8): 804-819.

Rodríguez-Manzaneque, M. T. and J. Tamarit, Bellí G., Ros, J., Herrero, E. (2002). "Grx5 is a mitochondrial glutaredoxin required for the activity of iron/sulfur enzymes." Mol Biol Cell **13**(1059-1524 (Print)): 1109-1121.

Sánchez, L. A., M. Gómez-Gallardo, A. L. Díaz-Pérez, C. Cortés-Rojo and J. Campos-García (2019). "Iba57p participates in maturation of a [2Fe–2S]-cluster Rieske protein and in formation of

supercomplexes III/IV of Saccharomyces cerevisiae electron transport chain." Mitochondrion **44**: 75-84.
Schagger, H. (2006). "Tricine-SDS-PAGE." Nat Protoc **1**(1): 16-22.
Schagger, H. and K. Pfeiffer (2000). "Supercomplexes in the respiratory chains of yeast and mammalian mitochondria." EMBO J **19**(8): 1777-1783.
Schilke, B., B. Williams, H. Knieszner, S. Pukszta, P. D'Silva, E. A. Craig and J. Marszalek (2006). "Evolution of mitochondrial chaperones utilized in Fe-S cluster biogenesis." Curr Biol **16**(16): 1660-1665.
Shaik, I. H. and R. Mehvar (2006). "Rapid determination of reduced and oxidized glutathione levels using a new thiol-masking reagent and the enzymatic recycling method: application to the rat liver and bile samples." Anal Bioanal Chem **385**(1618-2642 (Print)): 105-113.
Sheftel, A. D., C. Wilbrecht, O. Stehling, B. Niggemeyer, H. P. Elsasser, U. Muhlenhoff and R. Lill (2012). "The human mitochondrial ISCA1, ISCA2, and IBA57 proteins are required for [4Fe-4S] protein maturation." Mol Biol Cell **23**(7): 1157-1166.
Smith, P. M., J. L. Fox and D. R. Winge (2012). "Biogenesis of the cytochrome bc(1) complex and role of assembly factors." Biochim Biophys Acta **1817**(2): 276-286.
Snyder, C. H., E. B. Gutierrez-Cirlos and B. L. Trumpower (2000). "Evidence for a concerted mechanism of ubiquinol oxidation by the cytochrome bc1 complex." J Biol Chem **275**(0021-9258 (Print)): 13535-13541.
Stephan, K. and M. Ott "Timing of dimerization of the bc(1) complex during mitochondrial respiratory chain assembly." (1879-2650 (Electronic)).
Vartak, R., C. A. Porras and Y. Bai (2013). "Respiratory supercomplexes: structure, function and assembly." Protein Cell **4**(8): 582-590.
Zara, V., L. Conte and B. L. Trumpower (2009). "Evidence that the assembly of the yeast cytochrome bc1 complex involves the formation of a large core structure in the inner mitochondrial membrane." FEBS J **276**(7): 1900-1914.
Zhang, B., J. C. Crack, S. Subramanian, J. Green, A. J. Thomson, N. E. Le Brun and M. K. Johnson (2012). "Reversible cycling between cysteine persulfide-ligated [2Fe-2S] and cysteine-ligated [4Fe-4S] clusters in the FNR regulatory protein." Proc Natl Acad Sci U S A **109**(39): 15734-15739.

5.4 Capítulo 4

5.4.1 Resultados adicionales no publicados.

El grupo de mutantes *grx5*Δ*, isa1*Δ*, isa2*Δ e *iba57*Δ involucradas en el subsistema [Fe-S]-IBG de la vía ISC, fueron complementados con sus respectivos genes eliminados. En la figura 4C1 se muestran diluciones seriadas de las cepas complementadas y mutantes, crecidas en diferentes concentraciones de etanol, se observa que las cepas complementadas restauran parcialmente el crecimiento en 4% y 8% de etanol. Sin embargo, en 12 % de etanol ocurre una drástica disminución del crecimiento. No obstante, las cepas mutantes se ven afectadas desde concentraciones bajas de etanol. Estos resultados sugieren que las cepas mutantes fueron complementadas, por lo que se procedió a la identificación de las proteínas recombinantes.

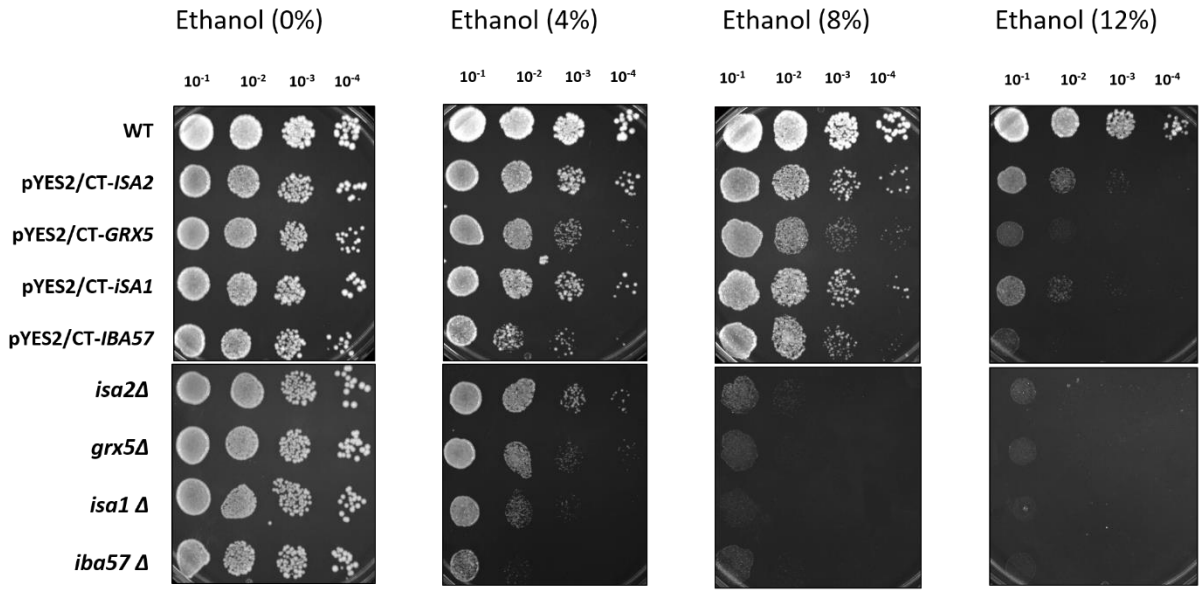

Figura 4C1. Crecimiento en placa de las cepas de *S. cerevisiae* en concentraciones crecientes de etanol 0%, 4%, 8% y 12%. Las imágenes son representativas de 3 experimentos independientes.

5.4.2 Identificación de proteínas recombinantes.

Mediante Western Blot se identificó a las proteínas recombinantes con una etiqueta de histidinas en el extremo carboxilo terminal. En el panel a de la figura 4C2, se muestra un Western blot de mitocondrias aisladas, revelando con un anticuerpo contra histidinas en el que se observa solo el marcador de peso molecular. En el panel b, se observa la presencia de Rip1p solo en la cepa silvestre y la mutante en *GRX5*. En el caso de las cepas complementadas se logró identificar dos proteínas recombinantes con la etiqueta de histidinas, Grx5p e Isa2p, (panel c). Desafortunadamente, no se logró la identificación de Isa1p e Iba57p recombinantes. Se realizó un Western blot contra la proteína Rip1p en mitocondrias de las cepas complementadas (panel d), se muestra que a diferencia de las cepas mutantes, las cepas complementadas recuperan la expresión de esta proteína. Estos resultados junto con los de las pruebas de crecimiento indican que las cepas mutantes se complementaron y que se restauró parcialmente la expresión de Rip1p, aportando mayor evidencia de que las proteínas del subsistema [Fe-S]-IBG están involucradas en el ensamble del centro Fe-S de Rip1p, evitando así su degradación y recuperando la actividad mitocondrial como se muestra en el capítulo 3.

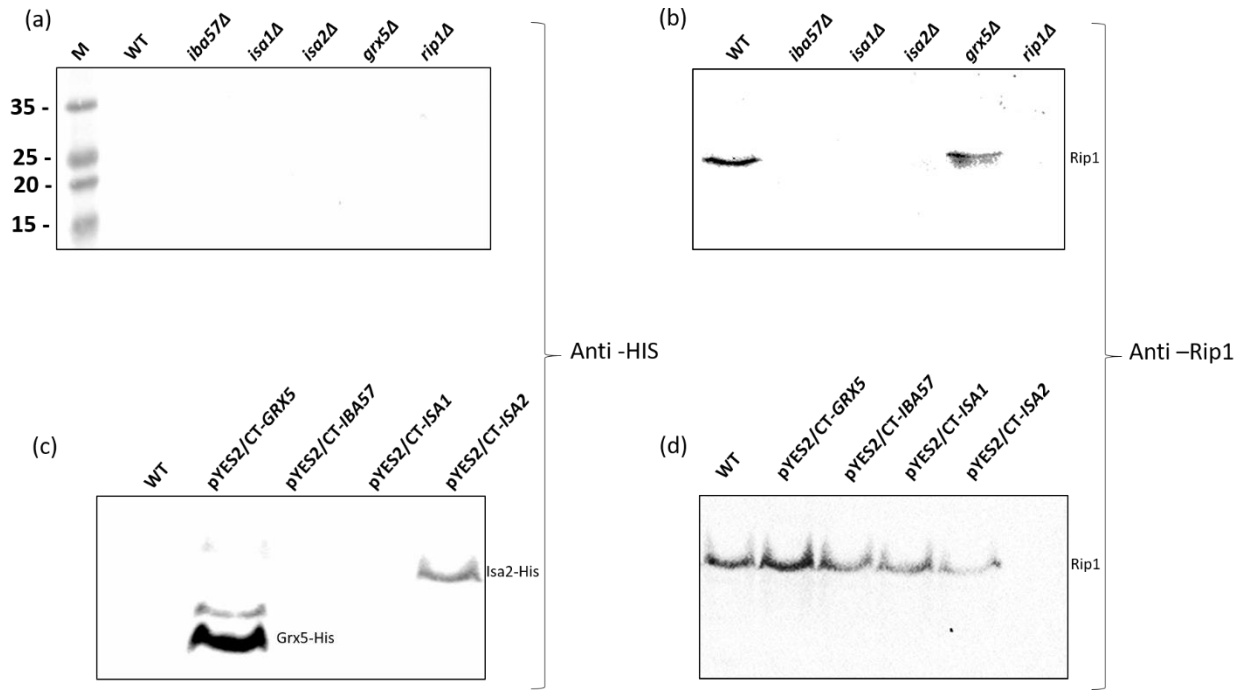

Figura 4C2. Identificación de Rip1p y de las proteínas recombinantes por Western blot utilizando la etiqueta de histidinas

5.4.3 Identificación de las proteínas recombinantes en los supercomplejos respiratorios.

Mitocondrias aisladas de las cepas complementadas fueron solubilizadas con digitonina y los complejos respiratorios fueron separados por BN-PAGE (Blue Native Polyacrylamide Gel Electrophoresis). Luego, el gel fue transferido a una membrana de fluoruro de polivinilideno (PVDF) para la identificación de las proteínas recombinantes con un anticuerpo contra la etiqueta de histidinas. En la figura 4C3 se observa que solo en la cepa complementada *isa2*Δ-*ISA2*-His fue identificada la proteína a la altura donde se encuentra el supercomplejo conformado por un dímero del complejo III y un monómero del complejo IV. Para los casos de la cepa silvestre, *rip1*Δ y *grx5*Δ-*GRX5*-His no se detectó señal alguna.

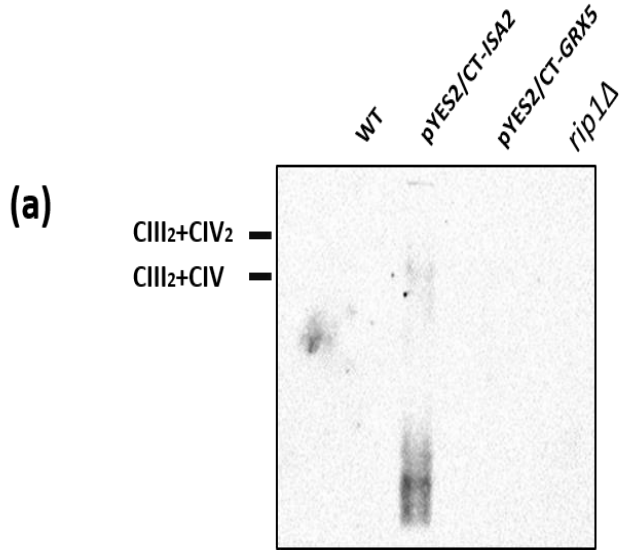

Figura 4C3. Identificación de proteínas recombinantes en BN-PAGE

5.4.4 Evaluación de la F_1F_0-ATPasa mitocondrial de *S. cerevisiae.*

Se evaluó la actividad de la ATPasa mitocondrial en las diferentes cepas utilizadas en este trabajo. Para ello, Mitocondrias aisladas fueron solubilizadas con digitonina, para la separación de los supercomplejos respiratorios y de la ATPasa mediante BN-PAGE. Después de la electroforesis en condiciones no desnaturalizantes los complejos respiratorios así como la ATPasa conservan actividad enzimática, para la evaluación de esta última enzima se monitoreó la hidrolisis de ATP (Suhai *et al*., 2009). La ATPasa mitocondrial forma dímeros, cada monómero está conformado por dos dominios, el dominio F_0 que se ancla a la membrana interna de la mitocondria y el dominio F_1 ubicado hacia la matriz mitocondrial y encargado de la síntesis o hidrolisis de ATP. En el gel nativo es posible detectar el dímero y el monómero de la ATPasa, como se muestra en la siguiente Figura.

Se evaluó la actividad de la F_0F_1-ATPasa mitocondrial de diferentes cepas mutantes en genes involucrados en la vía de biosíntesis de [Fe-S] en geles. En la figura 4C2, paneles a y b, se muestran geles representativos del ensayo de actividad de la ATPasa. En el panel a se observan la cepa nativa (WT) y las diferentes mutantes en los genes que codifican proteínas involucradas en la biogénesis de centros [Fe-S]. En este ensayo también se incluyó una cepa (*rho*$^-$), como control negativo. En el panel b se muestran la cepa silvestre y las cepas mutantes complementadas Δ*grx5*:pYES2/CT-*GRX5* yΔ*isa2:*pYES2/CT-*ISA2.* En el panel c, se muestran los datos de densitometría de la actividad de los dímeros de ATPasa. Se observan diferentes magnitudes de la actividad en las diferentes cepas.La cepa WT y las mutantes Δ*isa1 y* Δ*rip1,* presentan actividad similar en los dímeros de la ATPasa, mientras que las mutantes Δ*ssq1,* Δ*iba57 e* Δ*isa2,* muestran una disminución de la actividad de entre el 55% y 75%, comparadas con la cepa WT. Por otro lado, la mutante Δ*grx5* mostró un incremento del 30 % de actividad respecto a la cepa WT. Como se esperaba, la cepa *rho*^{0} deficiente en ADNmt presenta una drástica disminución de la actividad de más del 90%, comparado con la cepa WT. En el panel d se muestra el análisis densitométrico de la actividad de los dímeros de ATPasa, de las cepas mutantes complementadas con losrespectivos genes eliminados. Se observó que ambas cepas complementadas presentan una disminución en la actividad de los dímeros de ATPasa, con respecto a la cepa WT. Además la actividad de la cepa complementada Δ*grx5*:pYES2/CT-*GRX5* fue menor que la cepa mutante Δ*grx5* sin complementar, mientras que la cepa complementada Δ*isa2:*pYES2/CT-*ISA2* presentó uncomportamiento similar a la cepa mutante sin complementar. Por otro lado, la cepa mutante Δ*isa2* y la complementada Δ*isa2:*pYES2/CT-*ISA2* fueron las únicas que mostraron actividad en las bandas correspondientes a los monómeros de la ATPasa. Como se muestra en el panel e, la actividad del monómero de

ATPasa de la cepa complementada incremento tres veces con respecto a la actividad en la cepa mutante.

Las cepas de levadura mutantes en factores de ensamble que intervienen en el ensamble de los dominios F0 con F1 tienden a acumular el dominio F_1 de la enzima (Lytovchenko *et al*., 2014). En contraste con esto, el dominio F_1 no fue detectado solo, en los ensayos, por lo que es posible inferir que Isa2p está relacionada con la formación de dímeros de la ATPasa mitocondrial. Se conoce muy poco acerca de la secuencia de formación del dímero de ATPasa, así como los factores que influyen en el proceso, por lo que se requieren de una mayor cantidad de estudios para probar la relación entre Isa2p y la dimerización de la enzima.

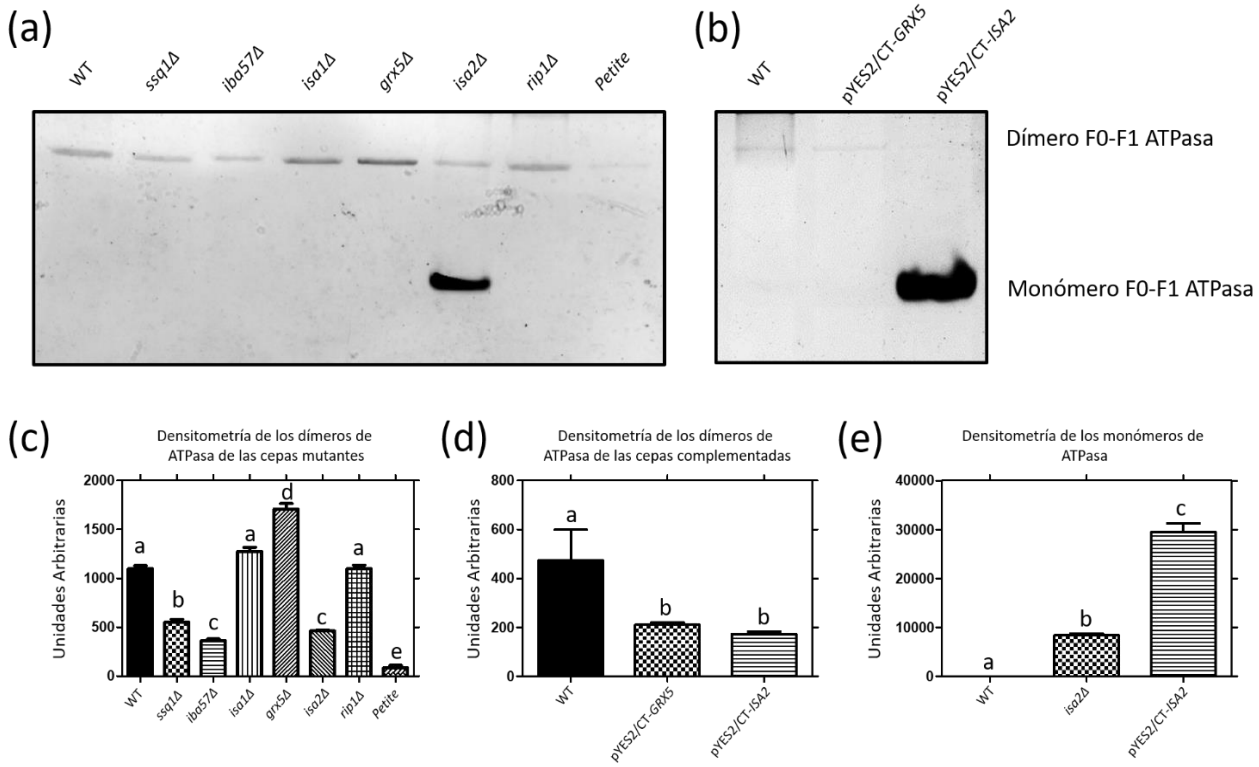

Figura 4C5. Actividad en gel de la F_0F_1-ATPasa mitocondrial. (a) y (b), geles representativos de muestras de mitocondrias solubilizadas, que fueron aisladas de cepas deficientes en la biogénesis de centros [Fe-S], así como de las cepas complementadas Δ*grx5*:pYES2/CT-*GRX5* y Δ*isa2*:pYES2/CT-*ISA2.* (c) y (d), análisis densitométrico de los dímeros de ATPasa de las diferentes cepas. (e), análisis densitométrico de la actividad de los monómeros de ATPasa de las cepas Δ*isa2* y complementada Δ*isa2*:pYES2/CT-*ISA2.* La densitometría se realizó con el programa ImageJ y los datos fueron analizados con el programa estadístico GraphPad Prism 5.0, empleando ANOVA de una vía con una prueba posterior de Tukey, p=0.001, n=3.

5.5 Capítulo 5

5.1Artículo de divulgación.

Participación de las proteínas Grx5p, Isa2p e Iba57p en el ensamble del centro [2Fe-2S] en la subunidad Rip1p y su impacto en la formación de los supercomplejos respiratorios en *Saccharomyces cerevisiae*

La mitocondria es el principal orgánulo celular productor de energía de los eucariontes. La molécula de adenosina trifosfato, más conocida como ATP, es la "moneda de cambio" de la célula; sin embargo, el conseguirla requiere de un trabajo coordinado, exhaustivo y muy complejo.

La mitocondria es como una "empresa" que ofrece diversos servicios a la célula, para ello es requerida una gran diversidad de departamentos bien organizados: seguridad (sistemas antioxidantes), capacitación (ribosomas y chaperonas moleculares), exportación e importación (canales de membrana), inversionistas (moléculas donadoras de electrones), obreros (proteínas de la cadena de transporte de electrones), maquinaria (ATP sintasa), maquiladoras (síntesis de cofactores), etc. Todos estos "departamentos" trabajan en conjunto para lograr hacer de la mitocondria una empresa sustentable.

Los procesos protagonistas

La mitocondria es un orgánulo con dos membranas (externa e interna) que rodean una matriz. Tiene como característica dos procesos protagonistas principales que son: la síntesis de herramientas en la matriz y la cadena transportadora de electrones de la membrana interna, esta última, la conceptualizaremos como los obreros, pues representan a «las proteínas que generarán la fuerza de trabajo que requieren las turbinas de la fábrica generadora de las moléculas de energía, el codiciado ATP».

Parte del gran éxito empresarial radica en que la mitocondria misma es, por una parte, productora de algunas de sus herramientas de trabajo, y por otro lado, coordina el trabajo entre sus obreros. En este sentido, empezaremos describiendo cómo se producen las herramientas que son usadas por éstos para producir el "oro químico" (ATP), en esta empresa celular llamada mitocondria.

Síntesis de herramientas de trabajo

Los cofactores son moléculas de baja masa molecular que se unen a sitios específicos de proteínas (obreros), y para que éstas realicen su función, existen cofactores de naturaleza orgánica e inorgánica. La síntesis de cofactores son procesos muy conservados y complejos entre los organismos. Los principales cofactores o herramientas de la cadena de transporte de electrones son iones de cobre, flavinas, grupos hemo y centros Hierro-Azufre [Fe-S].

Todo obrero requiere de herramientas para realizar su trabajo, y como se mencionó anteriormente, algunas son sintetizadas en la misma mitocondria. La construcción de centros [Fe-S], la lleva

La empresa que sostiene la vida de la célula

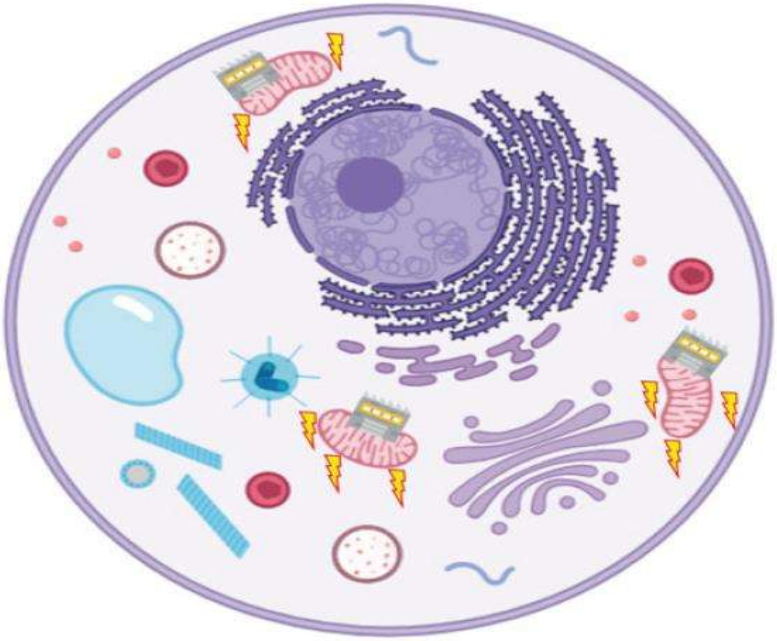

En esta imagen se resaltan las mitocondrias como industrias que producen energía para las demandas energéticas de la célula.

Año 9 /Enero-Febrero/ No. 49 | U.M.S.N.H.

La fábrica de ATP

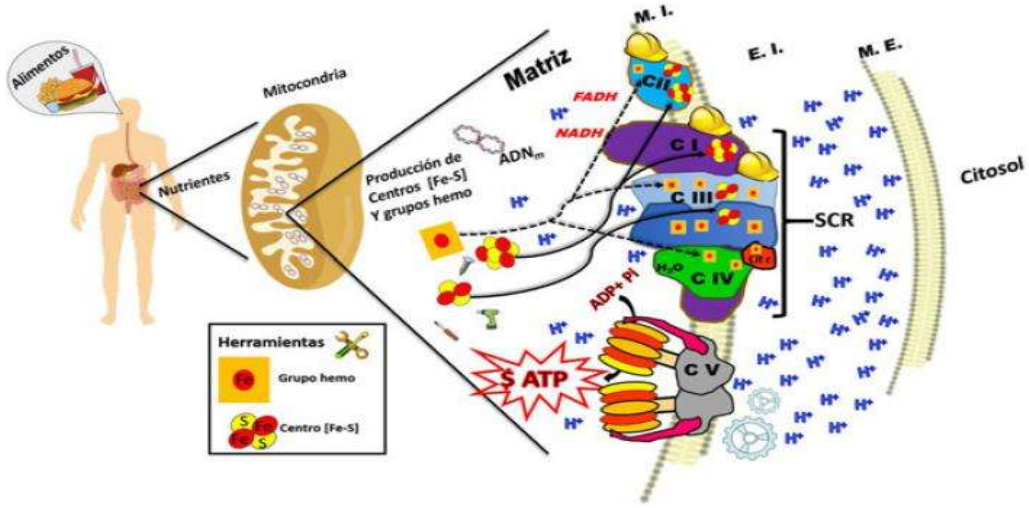

Los alimentos son ingeridos y degradados por el sistema digestivo, los nutrientes son metabolizados hasta obtener ATP principalmente por la fosforilación oxidativa mitocondrial. La imagen representa la organización de la mitocondria, M.I. membrana interna; E.I. espacio intermembranas; M.E. membrana externa; SCR supercomplejos respiratorios, Complejo I, Complejo II, Complejo III y Complejo IV. Se muestran los donadores de electrones NADH y FADH; los cofactores [Fe-S] y grupos hemo, herramientas que utilizan los obreros (SCR) para generar un gradiente electroquímico que se aprovechará en la producción de ATP por la ATP-síntasa (CV).

a cabo principalmente una compleja maquinaria biosintética mitocondrial, nombrada *ISC* por sus siglas en inglés (*Iron Sulfur Cluster*). Las levaduras son el mejor modelo biológico para el estudio de esta vía; se han descrito alrededor de 18 proteínas que trabajan dentro de la mitocondria encargadas de sintetizar los centros [Fe-S] de diferentes configuraciones: centros [2Fe-2S], es decir, dos átomos de hierro unidos a dos átomos de azufre formando un rombo; centros [4Fe-4S], aquellos de cuatro átomos de hierro y cuatro átomos de azufre formando una estructura cúbica, y algunos otros más complejos. El proceso de síntesis comprende dos pasos principales: el ensamblaje del cofactor en proteínas transitorias, y la transferencia de éstos hasta los sitios donde serán usados por otras proteínas.

Otro grupo de herramientas que se sintetizan en la mitocondria son los grupos hemo, a diferencia de los centros [Fe-S], descritos anteriormente, estos cofactores requieren de mano de obra interna y externa, es decir, los precursores de los grupos hemo son enviados al "país vecino" (el citosol) para ser procesados químicamente, los cuales nuevamente se transportarán hacia la mitocondria para completar la síntesis y emplearse como nuevas herramientas.

Exportación, importación y selección de personal

Esta empresa cuenta con tratados de comercio de importación y exportación mediante varios sistemas aduanales que comunican al citosol con la matriz mitocondrial. La mayoría de transportadores mitocondriales no se han identificado, aunque es lógico que se requieren de transportadores de aminoácidos para la construcción de proteínas mitocondriales, transportadores de hierro para la síntesis de cofactores, transportadores de nucleótidos para la síntesis de ácidos nucleicos, y muy importante mencionar, los transportadores de proteínas provenientes del núcleo.

Estos transportadores los podemos encontrar principalmente en la membrana interna mitocondrial, la cual hace las veces de "puentes fronterizos", ya que, no permite el paso de la mayoría de las moléculas. Estos sistemas hacen de la mitocondria una empresa altamente selectiva de materiales de calidad para la producción, así como de personal calificado y especializado.

Producción de ATP

La transformación de los alimentos que consumimos en ATP, se lleva a cabo principalmente por la fosforilación oxidativa ocurrida en la mitocon-

U.M.S.N.H. | Año 9 /Enero-Febrero/ No. 49

dria. Durante la respiración celular, los electrones son "recolectados" de la degradación de azúcares, proteínas y lípidos por ciertas coenzimas que sirven como camiones de carga (NAD y FAD); después, los electrones son entregados a los obreros de la membrana interna mitocondrial para que realicen su trabajo. Los obreros destinados a la producción de energía contratados por la mitocondria, forman cinco equipos denominados complejos respiratorios: complejo I, II, III, IV, y un complejo V (CV). Capacitados con sus respectivas herramientas, estos equipos forman asociaciones nombradas "supercomplejos mitocondriales", lo que hace más eficiente el trabajo en grupo. Cada complejo tiene funciones y formas de trabajo diferentes; sin embargo, actúan ordenadamente para llevar acabo sus propósitos: la transferencia de electrones y la translocación de protones de la matriz mitocondrial al espacio intermembranal.

El flujo de electrones va de un bajo potencial de reducción a un mayor potencial, y se logra gracias a los diferentes potenciales de reducción de los cofactores que utilizan los complejos respiratorios. La energía empleada en la transferencia de electrones, genera fuerza de trabajo para transferir protones al espacio entre membranas mitocondriales, lo que dará lugar a la formación de un gradiente eléctrico que será aprovechado por el complejo V para sintetizar el ATP.

El complejo V o ATP-sintasa, es el último eslabón industrial de producción de ATP, este complejo cuenta con dos módulos operacionales: el módulo *Fo*, el cual se ancla a la membrana y sirve como turbina, y cuyo combustible es la energía almacenada en el gradiente electroquímico de protones; el segundo módulo es el *F1*, que se orienta a la matriz mitocondrial. Estos módulos están conectados por un brazo lateral inmóvil, además de un rotor central que gira conforme pasan los protones en la turbina; este trabajo impulsa cambios conformacionales dentro del módulo *F1* para la síntesis de ATP a partir de la materia prima (ADP y fosfato). Se estima que se producen aproximadamente 100 moléculas de ATP por segundo por cada ATP-sintasa. Esta organización es responsable de proveer el ATP para la "manutención" celular.

Cuando la mitocondria falla

Diversas anomalías pueden causar una disfunción en la producción de ATP mitocondrial: fallas en la síntesis de cofactores, daño a proteínas de la CTE y daño a la ATP-sintasa son las principales causas. No obstante, más de 150 síndromes han sido asociados a fallas en la mitocondria. Los

Banca rota mitocondrial

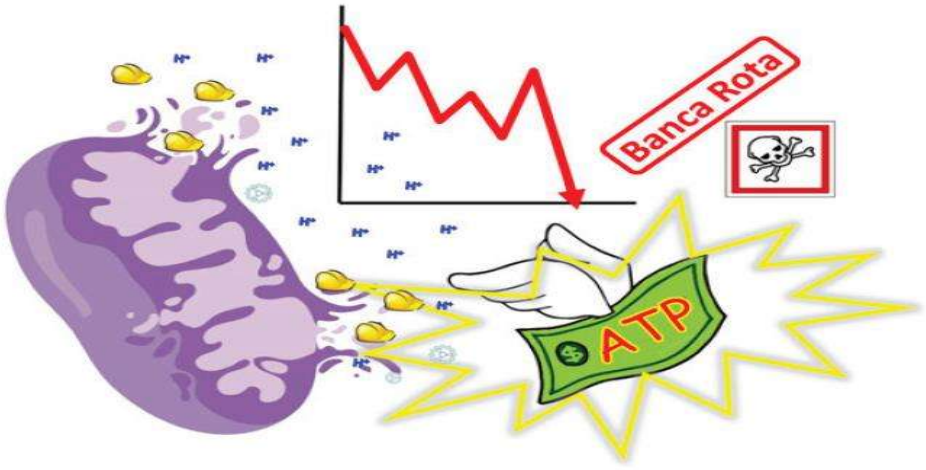

magen representa el fallo de la mitocondria, al romperse las membranas mitocondriales se disip el gradiente electroquímico, los obreros son despedidos por lo que la producción se viene abajo provocando la muerte celular.

casos clínicos incluyen encefalopatías, miopatías, cardiomiopatías, diabetes y enfermedades renales; muchos de los casos se relacionan con el daño al ADN mitocondrial, debido a la sobreproducción de especies reactivas de oxígeno (ERO) por la CTE. La mitocondria soporta cierto umbral de ERO; sin embargo, cuando los sistemas antioxidantes son rebasados, las moléculas de ADN mitocondrial son las de mayor susceptibilidad a los radicales libres, provocando una alta tasa de mutaciones que en consecuencia afectan la síntesis de las proteínas que se requieren dentro de la mitocondria.

Un desequilibrio por la pérdida o malformación de cofactores como los grupos hemo y los centros [Fe-S] de sus respectivas proteínas, causa una sobre carga de hierro mitocondrial, lo que desencadena una excesiva producción de radicales libres mediante "círculos viciosos" entre iones metálicos y ERO. El daño puede ser tan grande que la mitocondria puede declararse en quiebra y venirse abajo, desencadenando la muerte celular.

El éxito empresarial de la mitocondria, radica en un conjunto de asociaciones entre diversos sectores; además de que por sí sola no podría mantener su estatus productivo, también requiere de una gran coordinación con el núcleo y citosol. En los últimos años se han descubierto diversas enfermedades a causa de anomalías mitocondriales. El Diagnóstico temprano y nuevos blancos moleculares para tratamientos específicos, son los objetivos de la investigación de los procesos que ocurren en la mitocondria. Día con día se desarrollan nuevas técnicas moleculares que ayudan a comprender esta compañía, las proyecciones a futuro son el buen funcionamiento de la empresa donde los recursos sean aprovechados en su máxima capacidad sin generar pérdidas que lleven al colapso mitocondrial.

M.C. Luis Alberto Sánchez Briones, es estudiante del Programa Institucional de Doctorado en Ciencias Biológicas en la Opción Biología Experimental, adscrito al Instituto de Investigaciones Químico Biológicas de la Universidad Michoacana de San Nicolás de Hidalgo, donde actualmente realiza su tesis en el laboratorio de Biotecnología Microbiana acerca del funcionamiento de la mitocondria en la levadura *Saccharomyces cerevisiae*. Es de su interés contribuir a la generación y difusión del conocimiento, a la vez que considera que es importante dar a conocer a la sociedad el trabajo que se realiza en los centros de investigación científica.
biol.luis.22@gmail.com

D.B. Jesús Campos García, Profesor-Investigador Titular del Laboratorio de Biotecnología Microbiana del Instituto de Investigaciones Químico Biológicas de la Universidad Michoacana de San Nicolás de Hidalgo (IIQB-UMSNH). Es miembro de la Academia Mexicana de Ciencias A.C. (AMC) y del Sistema Nacional de Investigadores (nivel II). Premio Nacional de Investigación en Ciencias Naturales-2008 por la AMC, Premio Estatal de Investigación Científica y Humanística 2009 (Gob. Edo. Michoacán), Inventor de la primera Patente de la UMSNH (2009), actualmente posee 4 títulos de patentes. Su trabajo de investigación versa sobre los mecanismos de interacción de *Pseudomonas aeruginosa* en el ambiente: mecanismos de degradación, biocombustibles, interacción huésped-patógeno y metabolitos con potencial biotecnológico.

sabermás

Villavicencio-Queijeiro, A. (2012). La mitocondria como fábrica de cofactores: biosíntesis de grupo hemo, centros Fe-S y nucleótidos de flavina (FMN/FAD). *TIP-Revista especializada en ciencias químico-biológicas*, 15(2):116-132. http://www.scielo.org.mx/scielo.php?script=sci_abstract&pid=S1405-888X2012000200005&lng=pt&nrm=iso

Tuena de Gómez-Puyou, M. y García-Trejo, J.J. (2015). La bioenergética, las mitocondrias y la fosforilación oxidativa. *Revista digital universitaria UNAM*, 16(1):1-15. http://www.revista.unam.mx/vol.16/num1/art05/

Boticario-Boticario, C. y Cascales-Angosto, M. (2012). *Digestión y metabolismo energético de los nutrientes*. UNED. Centro de Plasencia. 383 p. https://www2.uned.es/ca-plasencia/DocumentosPDF/libros/Digestion.pdf

6. Discusión:

La biogénesis de centros [Fe-S] es un proceso coordinado y complejo. La importancia de estos cofactores radica tanto en el número de proteínas que requieren un centro [Fe-S] para realizar su función en la célula, como en su participación clave en varios procesos tales como regulación genética, metabolismo de aminoácidos y nucleótidos, generación de ERO, homeostasis del hierro y del azufre, modificación del ADN, reparación de RNAt y respiración aeróbica y anaeróbica (Beinert *et al*., 1999, Netz *et al*.,2014, Andreini *et al.,* 2016). En eucariontes, la síntesis de centros [Fe-S] y su transferencia a apo-proteínas se lleva a cabo en las mitocondrias, también controlan la exportación de precursores para la síntesis de centros [Fe-S] del citosol y del núcleo. En este proceso de síntesis y transferencia están involucradas más de 30 proteínas con funciones establecidas (Stehling y Lill, 2013 y Lill *et al*., 2015). Sin embargo, estudios recientes revelan nuevos indicios de que algunas de las enzimas involucradas en la vía ISC presentan funciones variables, dependiendo del contexto celular (Beilschmidt *et al*., 2017 y Gourdoupis *et al*., 2018).. La biogénesis de centros [Fe-S] presenta tres etapas claves: **1.** La síntesis del cofactor [2Fe-2S] en el sistema transitorio ISU; **2.** La formación de los cofactores [4Fe-4S] por el sistema ISA; **3.** La transferencia de los cofactores a las respectivas apo-proteínas. El objetivo de este trabajo fue investigar si el subsistema [Fe-S]-IBG (Grx5p, Isa2p, Iba57p),está involucrado en la maduración de la proteína Rip1p-[2Fe-2S] del complejo III de la cadena de transporte de electrones mitocondrial.

Se han realizado avances en descifrar el mecanismo de la biogénesis mitocondrial de centros [Fe-S], así como de la transferencia de estos cofactores a apo-proteínas;sin embargo, muchas preguntas permanecen sin contestar. Por ejemplo, existen discrepancias en la comprensión del papel que juega la frataxina en la biogénesis de centros [Fe-S]. Es probable que los transportadores mitocondriales de Fe^{+2} Mrs3p y Mrs4p, tengan un papel

directo en la entrega de Fe^{+2} a la proteína de andamiaje Isu1p (Zhang *et al.*, 2006). También hay controversia en torno al sistema de transferencia de los centros [2Fe-2S]. Se han propuesto dos mecanismos de transferencia, el primero, mediado por la cochaperona Jac1p (homologa de HSC20 en humanos), se ha reportado que el complejo HSC20-HSPA9-ISCU1 (homólogo de Jac1p-Ssq1p-Isu1p) transfiere un centro [Fe-S] a apoproteínas como Rieske, vía la proteína intermediaria LYRM7 (homologa de Mzm1 en levaduras). El complejo Rieske-LYRM7 es reclutado por el complejo de síntesis *de novo* de la maquinaria ISC, HSC20-HSPA9-ISCU1, gracias al reconocimiento del motivo LYR de la proteína LYRM7 por la cochaperona HSC20 (Atkinson *et al*., 2011, Tie-Zhong Cui *et al*., 2012, y Sánchez *et a.,l* 2013). Esta interacción facilita la entrega del grupo [2Fe-2S] a la proteína Rieske (Maio *et al*., 2017).Las proteínas co-chaperonas Jac1p y HSC20 de levadura y humano respectivamente, presentan diferencias principalmente en el amino terminal, que es donde se lleva a cabo el reconocimiento del motivo LYR (Bitto *et al*., 2008), por lo que es probable que el proceso de maduración de la proteína Rieske sea diferente en levaduras.

El otro mecanismo de transferencia de [2Fe-2S] es el mediado por la glutarredoxina mitocondrial Grx5p en conjunto con las proteínas de la familia BolA. Claramente, *in vitro*, se forma un heterodímero híbrido Grx5p-[2Fe-2S]-Bol1p. Sin embargo, no es claro si esta especie existe de manera estable dentro de la matriz mitocondrial y cuál es su función. Además, la función de Bol3p con Nfu1p en la transferencia de centros [4Fe-4S] sigue en cuestión.

Por otro lado, dentro del subcomplejo de ensamble de centros tipo cúbicos, aún no se ha asignado ninguna función específica a Iba57p, mientras que se ha comprobado la condensación de los centros [4Fe-4S] solo con las proteínas Isa1p e Isa2p. Dicha condensación de centros [2Fe-2S] se lleva a cabo por un acoplamiento reductor, por lo que no se conoce el agente reductor para esta reacción. Se sugirió que Iba57p podría participar

en este acoplamiento, pero esto no ha sido demostrado (Brancaccio *et al.*, 2014). Además, el mecanismo de transferencia de centros [Fe-S] de este subsistema no está completamente esclarecido. Por otro lado, dado que los centros [Fe-S] pueden dañarse por la oxidación, se ha reportado una vía de reparación aun indefinida en *Escherichia coli,* con mecanismos de "vigilancia" que también existen en la matriz mitocondrial para identificar los cofactores dañados, por lo que existe la duda de sí existirá una maquinaria similar en la matriz mitocondrial para reparar los centros [Fe-S] dañados (Djaman *et al.,* 2004). Durante la biogénesis de proteínas con centros [Fe-S], las apoproteínas exponen las cadenas laterales de cisteína que coordinan el centro [Fe-S] sin protección, lo que las hace vulnerables a modificaciones oxidativas que podrían interferir con la posterior inserción del centro [Fe-S]. Se han demostrado modificaciones en los grupos sulfidrilo por aductos cíclicos de politiolación en los residuos de cisteína que coordinan el centro [Fe-S] de las apoproteínas, proporcionando resistencia a la oxidación. Estas modificaciones pueden eliminarse por rompimiento reductor, lo que sugiere que sirven como un dispositivo de protección reversible. Estas modificaciones se observan principalmente por defectos en las primeras etapas del sistema de ensamblaje de centros [Fe-S] mitocondrial, en menor grado, también se encuentran en células nativas en condiciones normales de crecimiento. Sin embargo, no se encuentran en las apoproteínas citosólicas (Christ *et al.*, 2016). Se desconoce si los componentes de la maquinaria ISC como el subsistema [Fe-S]-IBG, tienen la capacidad para reparar o reciclar los centros [Fe-S] dañados.

Debido a la versatilidad que han mostrado las enzimas implicadas en el sistema ISC y a los resultados de baja expresión de Rip1p en mutantes de *isa1*Δ (Gómez *et al*., 2014), se sugirió que el subsistema [Fe-S]-IBG está involucrado directamente en el ensamble del centro [Fe-S] de la subunidad Rip1p, la cual aporta estabilidad al complejo III para la formación de supercomplejos respiratorios y evitar que se fuguen electrones para la generación de ERO.

Cepas mutantes en la subunidad Rip1p del complejo III presentan una sobreproducción de ERO (Figura 1 panel d, capítulo 2). De igual manera, mutantes en *ISA1* e *IBA57*, han sido catalogadas como sobre productoras de ERO por Pérez-Gallardo *et al.,* 2013. En este trabajo se evaluaron las cepas *isa2*Δ y *grx5*Δ, así como las cepas complementadas *isa2*Δ-*ISA2*-His y *grx5*Δ-*GRX5*-His, con tres diferentes sondas fluorescentes para detectar ERO como lo son, H_2DCFDA, en la celula y la dihidrorodamina123 y el dihidroetidio, en la mitocondria. Las cepas mutantes generaron altos niveles de ERO (Figura 3, capítulo 3), *isa2*Δ fue la mayor generadora de ERO y al ser complementada con *ISA2*-His, disminuyeron los niveles de ERO, sin llegar a los niveles de las células WT. También se presentan fotografías de microscopia confocal que evidencian altos niveles de ERO en el capítulo 2, figura 2, panel g, para la mutante en *IBA57* y en el panel o para la mutante en *RIP1,* así como en el capítulo 3, figura 4, panel b, para la mutante en *ISA2* y su cepa complementada. Estos resultados concuerdan con la sobreproducción de anión superóxido por parte de la mutante en *ISA1* previamente reportada por Gómez *et al..,*2014. La generación excesiva de ERO por la disfuncionalidad de la vía ISC, aumenta la susceptibilidad de la levadura a agentes estresantes como el etanol, como se demostró en un estudio anterior (Pérez-Gallardo *et al*., 2013) y en la figura 1, paneles a y b, del capítulo 3, donde dichas mutantes no son capaces de crecer en concentraciones mayores a 8 % de etanol.

Entre las causas que aumentan la susceptibilidad a agentes estresantes, es la disminución de la capacidad antioxidante por la deficiencia de centros [Fe-S] que afecta a enzimas involucradas en la biosíntesis de aminoácidos como el glutamato y la cisteína (Patil *et al*., 2013). La aconitasa-[4Fe-4S] cataliza la conversión de citrato a isocitrato, posteriormente, este se descarboxila a α-cetoglutarato por la isocitrato deshidrogenasa. Además, el α-cetoglutarato es sustrato para la síntesis de glutamato (DeLuna *et al*., 2001, Cupp y McAlister., 1991 y 1992). La actividad de la aconitasa se evaluó, en la Figura 8, del capítulo

3, se observa una disminución drástica de la actividad en las mutantes *isa1*Δ, *isa2*Δ e *iba57*Δ, mientras que las cepas *grx5*Δ y *rip1*Δ, la actividad disminuyó 70% y 50%, respectivamente. De esto se puede intuir que solo Isa1p, Isa2p e Iba57p están involucradas en la maduración de la aconitasa.

En la vía del azufre, el sulfato captado del entorno es convertido en sulfito y sulfuro por la sulfito reductasa-[4Fe-4S], mientras que el sulfito es condensado con acetil-homoserina para formar homocisteína, que a su vez, se interconvierte en metionina o cistationina, un intermediario de la cisteína. Las deficiencias en las enzimas con centros [Fe-S] aconitasa y sulfito reductasa conducen a auxotrofía para glutamato, metionina y cisteína (Hansen *et al*., 1994, Thomas y Surdin 1997 y Wen *et al*., 2004). El glutatión, es un tripéptido compuesto por glutamato, cisteína y glicina, es el antioxidante esencial más abundante que mantiene el potencial redox intracelular en la mayoría de los eucariontes incluidas las levaduras. El glutatión actúa como un cofactor de enzimas antioxidantes como la glutatión peroxidasa, que utiliza el glutatión para neutralizar las ERO. La función antioxidante del glutatión depende del grupo tiol activo (-SH) de la cisteína. El glutatión dona los electrones necesarios para reducir las ERO, oxidándose a disulfuro de glutatión (GSSG) (Jamieson, 1998). La disminución de los niveles de glutatión conduce a una mayor sensibilidad a oxidantes como el anión superóxido y el peróxido de hidrogeno. Por lo tanto, para mantener las funciones celulares vitales, deben mantenerse altos niveles de glutatión intracelular. Se han evaluado los niveles de glutatión en cepas mutantes en la maquinaria ISC, se encontró que los niveles de glutatión disminuyeron considerablemente en las mutantes *ssq1*Δ, *isa1*Δ e *iba57*Δ (Pérez-Gallardo et al., 2013). En la figura 5 del capítulo 3, se muestra que en las mutantes *isa2*Δ y *grx5*Δ presentan niveles disminuidos de glutatión mitocondrial. Sin embargo, en la complementación con *isa2*Δ-*ISA2*-His y *grx5*Δ-*GRX5*-His, en dichas mutantes, respectivamente, restaura los niveles de glutatión. Es de esperarse que la

deficiencia de la biogénesis de centros [Fe-S] afecte la síntesis de glutatión y provoque estrés oxidativo mitocondrial.

Con estos resultados se plantearon dos hipótesis: 1) la disminución de la expresión de Rip1p, es el resultado de efectos secundarios como la desregulación del hierro, el exceso de radicales libres que dañan macromoléculas como el ADN mitocondrial y la disminución de los sistemas antioxidantes; 2) El subsistema [Fe-S]-IBG de la maquinaria ISC, está involucrado en el ensamble del centro [2Fe-2S] de la proteína Rip1p. Para comprobar estas hipótesis se plantearon diversas estrategias, una de ellas fue el análisis de presencia o ausencia del ADN mitocondrial, mediante la amplificación de genes mitocondriales por PCR. En la figura 6 del capítulo 1 y la figura suplementaria del capítulo 3, se muestran los productos de PCR de los genes mitocondriales *COX2* y *COX3,* de mitocondrias aisladas de mutantes en *GRX5, ISA2*, e *IBA57*. Si bien las bandas correspondientes a *COX2* y *COX3* tienen menor intensidad que las bandas de la cepa WT, hay presencia del material genético mitocondrial. Esto difiere de un estudio, que reportó que estas mutaciones provocan un fenotipo rho^0 (Jensen y Culotta, 2000). Además, se muestra la identificación de las proteínas Cox2p y Cox3p, en las figura 3, panel g, y figura 4, panel b, del capítulo 1, y figura 9, panel d, del capítulo 3. Cox3p fue identificada como parte de los supercomplejos respiratorios, por lo que además de ser sintetizada, la proteína tiene la capacidad de formar dichas superestructuras proteicas. Estas evidencias sustentan el hecho de que el estrés generado por las mutaciones *per se* no son suficientes para provocar la pérdida de la expresión de las proteínas mitocondriales.

Una vez comprobada la presencia del ADN mitocondrial y la expresión de las proteínas mitocondriales, se analizó la actividad de la cadena de transporte de electrones midiendo el consumo de oxígeno y la actividad de cada uno de los complejos respiratorios. En la figura 1 del capítulo 1 y la figura 6 del capítulo 3, se muestra un consumo de oxígeno nulo

en las mutantes *iba57*Δ*, isa2*Δ y *rip1*Δ. En concordancia con lo anterior, no se detectó actividad de los complejos de las mutantes del subsistema excepto en *grx5*Δ, cuya actividad disminuyó parcialmente en comparación con la cepa WT.

Se evaluó la estabilidad de los supercomplejos respiratorios. Se observó que la formación de supercomplejos se ve afectada en las mutantes en los genes *IBA57, GRX5* y *RIP1*, además se detectó la ausencia de la subunidad Rip1p en las mutantes *iba57*Δ y *rip1*Δ, lo que concuerda con un estudio anterior (Zara *et al.,* 2012), donde se encontró que la ausencia de Rip1p, afectó la formación de los supercomplejos. Con estos resultados se sugiere la participación del subsistema [Fe-S]-IBG en el ensamble de Rip1p-[2Fe-2S].

Las cuatro mutantes de los genes del subsistema [Fe-S]-IBG fueron complementadas. En la figura 1 del capítulo 4, se muestran los resultados de las cepas mutantes *grx5*Δ*, isa1*Δ*, isa2*Δ e *iba57*Δ complementadas con los genes que codifican para sus respectivas proteínas, y se observa una recuperación del crecimiento bajo condiciones estresantes. Solo se pudo demostrar la complementación de las cepas*isa2*Δ-*ISA2*-His y *grx5*Δ-*GRX5*-His por Western blot, por detección de la fusión de la proteína con una etiqueta de histidinas (figura 2, capítulo 4).

Con las cepas *isa2*Δ-*ISA2*-His y *grx5*Δ-*GRX5*-His caracterizadas molecularmente, se analizó la formación de supercomplejos respiratorios en mitocondrias (figura 9 panel b, capítulo 3). Se observó que la complementación de *isa2*Δ-*ISA2*-His restaura parcialmente la presencia de la subunidad Rip1p en las bandas correspondientes a los supercomplejos III_2IV_2 y III_2IV, comparada con la cepa mutante, donde no se detectó dicha subunidad. De manera similar se incrementa la presencia de la subunidad mitocondrial Cox3p en la cepa complementada (figura 9, panel d, capítulo 3), mientras que en el panel c se identificó la etiqueta de histidinas mayormente en la banda correspondiente al supercomplejo III_2IV en

la cepa complementada *isa2*Δ-*ISA2*-His. Asimismo, se demostró que la proteína recombinante Isa2 se encuentra en la misma banda del supercomplejo III_2IV, siendo estos resultados la primera evidencia de interacción proteína-proteína entre el subsistema [Fe-S]-IBG y el complejo respiratorio III. Además, este ensayo también se realizó con la cepa complementada *grx5*Δ-*GRX5*-His (figura 4C3, capítulo 4); sin embargo, no se detectó la proteína recombinante en ninguna banda correspondiente a los complejos respiratorios. Esto sugiere que Isa2p es una proteína específica del ensamble del centro [Fe-S] de Rip1p. Debido a que no se logró identificar las proteínas recombinantes Isa1p e Iba57p, no fue posible detectar la asociación física de estas proteínas con el complejo III. Sin embargo, la complementación con los genes de dichas proteínas se recuperó el crecimiento y la expresión de la subunidad Rip1p (figuras 4C1 y 4C2, capítulo 4), lo que sugiere que todo el subsistema [Fe-S]-IBG está involucrado en la maduración de Rip1p.

Además de la cadena de transporte de electrones, también se evaluó la actividad en gel de la ATP sintasa, con lo cual se logró detectar el dímero de la ATP sintasa en mitocondrias solubilizadas de las mutantes en ISC y las cepas complementadas. Asimismo, solo se detectó acumulación de monómeros en las cepas *isa2*Δ y su contraparte complementada. Estos resultados apoyan la idea de que el ADN mitocondrial en las mutantes es funcional, ya que tres de las subunidades de la ATP sintasa están codificadas en el ADN mitocondrial (Atp6, Atp8 y Atp9) (Macreadie *et al*., 1983). Además, en el ensayo se midió la actividad de hidrolisis del ATP por parte del dominio F_1. Si bien este dominio no cuenta con subunidades mitocondriales, el dominio F_1 en ausencia del dominio F_0 no fue detectado; de otro modo, se asumiría que el dominio F_0 no se formó debido al estrés generado por la disfunción de ISC como se observó en la cepa *rho*$^-$ (figura 4C5).

Los dímeros de ATP sintasa tienen un papel crucial en la formación de las curvatura que caracterizan a las crestas mitocondriales (Baker *et al*., 2012). Fue inesperada la

acumulación de monómeros de ATP sintasa en la mutante *isa2*Δ*,* ya que no se ha reportado una relación directa entre la biogénesis de la ATP sintasa y la biogénesis de centros [Fe-S], por lo que más estudios se requieren para esclarecer el fenómeno, así como la posible participación de Isa2p en la formación de crestas mitocondriales vía la dimerización de la ATP sintasa.

7. Conclusión:

En S. cerevisiae, el subsistema Fe-S-IBG está implicado en la maduración de la subunidad catalítica Rip1p del complejo III, y por consecuencia, en la conformación y funcionalidad de los supercomplejos respiratorios III-IV.

8. Bibliografía

1) Pfeiffer, T., & Morley, A. (2014). An evolutionary perspective on the Crabtree effect. *Frontiers in Molecular Biosciences, 1*. doi:10.3389/fmolb.2014.00017

2) Westermann, B. (2012). Bioenergetic role of mitochondrial fusion and fission. *Biochimica Et Biophysica Acta (BBA) - Bioenergetics, 1817*(10), 1833-1838. doi:10.1016/j.bbabio.2012.02.033

3) Saraste, M. (1999). Oxidative Phosphorylation at the fin de siècle. *Science, 283*(5407), 1488-1493. doi:10.1126/science.283.5407.1488

4) Horvath, S. E., & Daum, G. (2013). Lipids of mitochondria. *Progress in Lipid Research, 52*(4), 590-614. doi:10.1016/j.plipres.2013.07.002

5) Galluzzi, L., Kepp, O., & Kroemer, G. (2012). Mitochondria: Master regulators of danger signalling. *Nature Reviews Molecular Cell Biology, 13*(12), 780-788. doi:10.1038/nrm3479

6) Lill, R., Hoffmann, B., Molik, S., Pierik, A. J., Rietzschel, N., Stehling, O.Mühlenhoff, U. (2012). The role of mitochondria in cellular iron–sulfur protein biogenesis and iron metabolism. *Biochimica Et Biophysica Acta (BBA) - Molecular Cell Research, 1823*(9), 1491-1508. doi:10.1016/j.bbamcr.2012.05.009

7) Claypool, S. (2013). The power of yeast to model diseases of the powerhouse of the cell. *Frontiers in Bioscience, 18*(1), 241. doi:10.2741/4098

8) Chen, X. J., & Clark-Walker, G. D. (1999). The Petite Mutation in Yeasts: 50 Years On. *International Review of Cytology,* 197-238. doi:10.1016/s0074-7696(08)62397-9

9) Bonnefoy, N., & Fox, T. D. (2007). Directed Alteration of Saccharomyces cerevisiae Mitochondrial DNA by Biolistic Transformation and Homologous Recombination. *Methods in Molecular Biology Mitochondria,* 153-166. doi:10.1007/978-1-59745-365-3_11

10) Shibata, T., & Ling, F. (2007). DNA recombination protein-dependent mechanism of homoplasmy and its proposed functions. *Mitochondrion, 7*(1-2), 17-23. doi:10.1016/j.mito.2006.11.024

11) Meunier, B., Fisher, N., Ransac, S., Mazat, J., & Brasseur, G. (2013). Respiratory complex III dysfunction in humans and the use of yeast as a model organism to study mitochondrial myopathy and associated diseases. *Biochimica Et Biophysica Acta (BBA) - Bioenergetics, 1827*(11-12), 1346-1361. doi:10.1016/j.bbabio.2012.11.015

12) Lill, R. (2009). Function and biogenesis of iron–sulphur proteins. *Nature, 460*(7257), 831-838. doi:10.1038/nature08301

13) Fontecilla-Camps, J. C., Amara, P., Cavazza, C., Nicolet, Y., & Volbeda, A. (2009). Structure–function relationships of anaerobic gas-processing metalloenzymes. *Nature, 460*(7257), 814-822. doi:10.1038/nature08299

14) Py, B., & Barras, F. (2010). Building Fe–S proteins: Bacterial strategies. *Nature Reviews Microbiology, 8*(6), 436-446. doi:10.1038/nrmicro2356

15) Johnson, D. C., Dean, D. R., Smith, A. D., & Johnson, M. K. (2005). Structure, Function, and Formation of Biological Iron-Sulfur Clusters. *Annual Review of Biochemistry, 74*(1), 247-281. doi:10.1146/annurev.biochem.74.082803.133518

16) Nanda, V., Senn, S., Pike, D. H., Rodriguez-Granillo, A., Hansen, W. A., Khare, S. D., & Noy, D. (2016). Structural principles for computational and de novo design of 4Fe–4S metalloproteins. *Biochimica Et Biophysica Acta (BBA) - Bioenergetics, 1857*(5), 531-538. doi:10.1016/j.bbabio.2015.10.001

17) Beinert, H. (2000). Iron-sulfur proteins: Ancient structures, still full of surprises. *JBIC Journal of Biological Inorganic Chemistry, 5*(1), 2-15. doi:10.1007/s007750050002

18) Fontecave, M. (2006). Iron-sulfur clusters: Ever-expanding roles. *Nature Chemical Biology, 2*(4), 171-174. doi:10.1038/nchembio0406-171

19) Kiley, P. J., & Beinert, H. (2003). The role of Fe–S proteins in sensing and regulation in bacteria. *Current Opinion in Microbiology, 6*(2), 181-185. doi:10.1016/s1369-5274(03)00039-0

20) Wachnowsky, C., Fidai, I., & Cowan, J. A. (2018). Iron–sulfur cluster biosynthesis and trafficking – impact on human disease conditions. *Metallomics, 10*(1), 9-29. doi:10.1039/c7mt00180k

21) Gomez, M., Pérez-Gallardo, R. V., Sánchez, L. A., Díaz-Pérez, A. L., Cortés-Rojo, C., Carmen, V. M.,. Campos-García, J. (2014). Malfunctioning of the Iron–Sulfur Cluster Assembly Machinery in Saccharomyces cerevisiae Produces Oxidative Stress via an Iron-Dependent Mechanism, Causing Dysfunction in Respiratory Complexes. *PLoS ONE, 9*(10). doi:10.1371/journal.pone.0111585

22) Rao, P. V., & Holm, R. H. (2004). Synthetic Analogues of the Active Sites of Iron—Sulfur Proteins. *ChemInform, 35*(21). doi:10.1002/chin.200421274
23) Leibold, E. A., & Munro, H. N. (1988). Cytoplasmic protein binds in vitro to a highly conserved sequence in the 5' untranslated region of ferritin heavy- and light-subunit mRNAs. *Proceedings of the National Academy of Sciences, 85*(7), 2171-2175. doi:10.1073/pnas.85.7.2171
24) Rouault, T. A., Tang, C. K., Kaptain, S., Burgess, W. H., Haile, D. J., Samaniego, F., Klausner, R. D. (1990). Cloning of the cDNA encoding an RNA regulatory protein--the human iron-responsive element-binding protein. *Proceedings of the National Academy of Sciences, 87*(20), 7958-7962. doi:10.1073/pnas.87.20.7958
25) Kaptain, S., Downey, W. E., Tang, C., Philpott, C., Haile, D., Orloff, D. G., . . . Klausner, R. D. (1991). A regulated RNA binding protein also possesses aconitase activity. *Proceedings of the National Academy of Sciences, 88*(22), 10109-10113. doi:10.1073/pnas.88.22.10109
26) , S., Downey, W. E., Tang, C., Philpott, C., Haile, D., Orloff, D. G., Klausner, R. D. (1991). A regulated RNA binding protein also possesses aconitase activity. *Proceedings of the National Academy of Sciences, 88*(22), 10109-10113. doi:10.1073/pnas.88.22.10109
27) Jacobson, M. R., Brigle, K. E., Bennett, L. T., Setterquist, R. A., Wilson, M. S., Cash, V. L., . . . Dean, D. R. (1989). Physical and genetic map of the major nif gene cluster from Azotobacter vinelandii. *Journal of Bacteriology, 171*(2), 1017-1027. doi:10.1128/jb.171.2.1017-1027.1989
28) Selbach, B. P., Pradhan, P. K., & Santos, P. C. (2013). Protected Sulfur Transfer Reactions by the Escherichia coli Suf System. *Biochemistry, 52*(23), 4089-4096. doi:10.1021/bi4001479
29) Barras, F., Loiseau, L., & Py, B. (2005). How Escherichia coli and Saccharomyces cerevisiae Build Fe/S Proteins. *Advances in Microbial Physiology,* 41-101. doi:10.1016/s0065-2911(05)50002-x
30) Stehling, O., Wilbrecht, C., & Lill, R. (2014). Mitochondrial iron–sulfur protein biogenesis and human disease. *Biochimie, 100*, 61-77. doi:10.1016/j.biochi.2014.01.010
31) Vranken, J. G., Jeong, M., Wei, P., Chen, Y., Gygi, S. P., Winge, D. R., & Rutter, J. (2016). The mitochondrial acyl carrier protein (ACP) coordinates mitochondrial fatty acid synthesis with iron sulfur cluster biogenesis. *ELife, 5*. doi:10.7554/elife.17828
32) Wiedemann, N., Urzica, E., Guiard, B., Müller, H., Lohaus, C., Meyer, H. E., . . . Pfanner, N. (2005). Essential role of Isd11 in mitochondrial iron–sulfur cluster synthesis on Isu scaffold proteins. *The EMBO Journal, 25*(1), 184-195. doi:10.1038/sj.emboj.7600906
33) Schmucker, S., Martelli, A., Colin, F., Page, A., Wattenhofer-Donzé, M., Reutenauer, L., & Puccio, H. (2011). Mammalian Frataxin: An Essential Function for Cellular Viability through an Interaction with a Preformed ISCU/NFS1/ISD11 Iron-Sulfur Assembly Complex. *PLoS ONE, 6*(1). doi:10.1371/journal.pone.0016199
34) Shan, Y., Napoli, E., & Cortopassi, G. (2007). Mitochondrial frataxin interacts with ISD11 of the NFS1/ISCU complex and multiple mitochondrial chaperones. *Human Molecular Genetics, 16*(8), 929-941. doi:10.1093/hmg/ddm038
35) Webert, H., Freibert, S., Gallo, A., Heidenreich, T., Linne, U., Amlacher, S., . . . Lill, R. (2014). Functional reconstitution of mitochondrial Fe/S cluster synthesis on Isu1 reveals the involvement of ferredoxin. *Nature Communications, 5*(1). doi:10.1038/ncomms6013
36) Yan, R., Adinolfi, S., & Pastore, A. (2015). Ferredoxin, in conjunction with NADPH and ferredoxin-NADP reductase, transfers electrons to the IscS/IscU complex to promote iron–sulfur cluster assembly. *Biochimica Et Biophysica Acta (BBA) - Proteins and Proteomics, 1854*(9), 1113-1117. doi:10.1016/j.bbapap.2015.02.002
37) Melber, A., & Winge, D. R. (2018). Steps Toward Understanding Mitochondrial Fe/S Cluster Biogenesis. *Methods in Enzymology Fe-S Cluster Enzymes Part B,* 265-292. doi:10.1016/bs.mie.2017.09.004
38) Babcock, M. (1997). Regulation of Mitochondrial Iron Accumulation by Yfh1p, a Putative Homolog of Frataxin. *Science, 276*(5319), 1709-1712. doi:10.1126/science.276.5319.1709
39) Yoon, T., & Cowan, J. A. (2003). Iron−Sulfur Cluster Biosynthesis. Characterization of Frataxin as an Iron Donor for Assembly of [2Fe-2S] Clusters in ISU-Type Proteins. *Journal of the American Chemical Society, 125*(20), 6078-6084. doi:10.1021/ja027967i
40) Correia, A., Wang, T., Craig, E., & Gomes, C. (2010). Iron-binding activity in yeast frataxin entails a trade off with stability in the α1/β1 acidic ridge region. *Biochemical Journal, 426*(2), 197-203. doi:10.1042/bj20091612

41) Dutkiewicz, R., Schilke, B., Knieszner, H., Walter, W., Craig, E. A., & Marszalek, J. (2003). Ssq1, a Mitochondrial Hsp70 Involved in Iron-Sulfur (Fe/S) Center Biogenesis. *Journal of Biological Chemistry, 278*(32), 29719-29727. doi:10.1074/jbc.m303527200

42) Manicki, M., Majewska, J., Ciesielski, S., Schilke, B., Blenska, A., Kominek, J., Dutkiewicz, R. (2014). Overlapping Binding Sites of the Frataxin Homologue Assembly Factor and the Heat Shock Protein 70 Transfer Factor on the Isu Iron-Sulfur Cluster Scaffold Protein. *Journal of Biological Chemistry, 289*(44), 30268-30278. doi:10.1074/jbc.m114.596726

43) Majewska, J., Ciesielski, S. J., Schilke, B., Kominek, J., Blenska, A., Delewski, W. Dutkiewicz, R. (2013). Binding of the Chaperone Jac1 Protein and Cysteine Desulfurase Nfs1 to the Iron-Sulfur Cluster Scaffold Isu Protein Is Mutually Exclusive. *Journal of Biological Chemistry, 288*(40), 29134-29142. doi:10.1074/jbc.m113.503524

44) Banci, L., Brancaccio, D., Ciofi-Baffoni, S., Conte, R. D., Gadepalli, R., Mikolajczyk, M. Winkelmann, J. (2014). [2Fe-2S] cluster transfer in iron-sulfur protein biogenesis. *Proceedings of the National Academy of Sciences, 111*(17), 6203-6208. doi:10.1073/pnas.1400102111

45) Uzarska, M. A., Dutkiewicz, R., Freibert, S., Lill, R., & Mühlenhoff, U. (2013). The mitochondrial Hsp70 chaperone Ssq1 facilitates Fe/S cluster transfer from Isu1 to Grx5 by complex formation. *Molecular Biology of the Cell, 24*(12), 1830-1841. doi:10.1091/mbc.e12-09-0644

46) Maio, N., & Rouault, T. A. (2015). Iron –sulfur cluster biogenesis in mammalian cells: New insights into the molecular mechanisms of cluster delivery. *Biochimica Et Biophysica Acta (BBA) - Molecular Cell Research, 1853*(6), 1493-1512. doi:10.1016/j.bbamcr.2014.09.009

47) Maio, N., Kim, K. S., Singh, A., & Rouault, T. A. (2017). A Single Adaptable Cochaperone-Scaffold Complex Delivers Nascent Iron-Sulfur Clusters to Mammalian Respiratory Chain Complexes I–III. *Cell Metabolism, 25*(4). doi:10.1016/j.cmet.2017.03.010

48) Uzarska, M. A., Nasta, V., Weiler, B. D., Spantgar, F., Ciofi-Baffoni, S., Saviello, M. R., . . . Lill, R. (2016). Author response: Mitochondrial Bol1 and Bol3 function as assembly factors for specific iron-sulfur proteins. doi:10.7554/elife.16673.030

49) Melber, A., Na, U., Vashisht, A., Weiler, B. D., Lill, R., Wohlschlegel, J. A., & Winge, D. R. (2016). Role of Nfu1 and Bol3 in iron-sulfur cluster transfer to mitochondrial clients. *ELife, 5*. doi:10.7554/elife.15991

50) Gelling, C., Dawes, I. W., Richhardt, N., Lill, R., & Mühlenhoff, U. (2007). Mitochondrial Iba57p Is Required for Fe/S Cluster Formation on Aconitase and Activation of Radical SAM Enzymes. *Molecular and Cellular Biology, 28*(5), 1851-1861. doi:10.1128/mcb.01963-07

51) Mühlenhoff, U., Richter, N., Pines, O., Pierik, A. J., & Lill, R. (2011). Specialized Function of Yeast Isa1 and Isa2 Proteins in the Maturation of Mitochondrial [4Fe-4S] Proteins. *Journal of Biological Chemistry, 286*(48), 41205-41216. doi:10.1074/jbc.m111.296152

52) Lill, R., Dutkiewicz, R., Freibert, S. A., Heidenreich, T., Mascarenhas, J., Netz, D. J., Mühlenhoff, U. (2015). The role of mitochondria and the CIA machinery in the maturation of cytosolic and nuclear iron–sulfur proteins. *European Journal of Cell Biology, 94*(7-9), 280-291. doi:10.1016/j.ejcb.2015.05.002

53) Brancaccio, D., Gallo, A., Mikolajczyk, M., Zovo, K., Palumaa, P., Novellino, E., Banci, L. (2014). Formation of [4Fe-4S] Clusters in the Mitochondrial Iron–Sulfur Cluster Assembly Machinery. *Journal of the American Chemical Society, 136*(46), 16240-16250. doi:10.1021/ja507822j

54) Cai, K., Liu, G., Frederick, R., Xiao, R., Montelione, G., & Markley, J. (2016). Structural/Functional Properties of Human NFU1, an Intermediate [4Fe-4S] Carrier in Human Mitochondrial Iron-Sulfur Cluster Biogenesis. *Structure, 24*(12), 2080-2091. doi:10.1016/j.str.2016.08.020

55) Bych, K., Kerscher, S., Netz, D. J., Pierik, A. J., Zwicker, K., Huynen, M. A., Balk, J. (2008). The iron–sulphur protein Ind1 is required for effective complex I assembly. *The EMBO Journal, 27*(12), 1736-1746. doi:10.1038/emboj.2008.98

56) Sheftel, A. D., Stehling, O., Pierik, A. J., Netz, D. J., Kerscher, S., Elsässer, H., Lill, R. (2009). Human Ind1, an Iron-Sulfur Cluster Assembly Factor for Respiratory Complex I. *Molecular and Cellular Biology, 29*(22), 6059-6073. doi:10.1128/mcb.00817-09

57) Ahting, U., Mayr, J. A., Vanlander, A. V., Hardy, S. A., Santra, S., Makowski, C., Haack, T. B. (2015). Clinical, biochemical, and genetic spectrum of seven patients with NFU1 deficiency. *Frontiers in Genetics, 06*. doi:10.3389/fgene.2015.00123

58) Navarro-Sastre, A., Tort, F., Stehling, O., Uzarska, M., Arranz, J., Del Toro, M., Lill, R. (2011). A Fatal Mitochondrial Disease Is Associated with Defective NFU1 Function in the Maturation of a Subset of Mitochondrial Fe-S Proteins. *The American Journal of Human Genetics, 89*(5), 656-667. doi:10.1016/j.ajhg.2011.10.005

59) Zhang, Y., Lyver, E. R., Knight, S. A., Pain, D., Lesuisse, E., & Dancis, A. (2006). Mrs3p, Mrs4p, and Frataxin Provide Iron for Fe-S Cluster Synthesis in Mitochondria. *Journal of Biological Chemistry, 281*(32), 22493-22502. doi:10.1074/jbc.m604246200

60) Flint, D. H., Tuminello, J. F., & Emptage, M. H. (1993). The inactivation of Fe-S cluster containing hydro-lyases by superoxide. *The Journal of biological chemistry*, *268*(30), 22369–22376.

61) Djaman, O., Outten, F. W., & Imlay, J. A. (2004). Repair of oxidized iron-sulfur clusters in Escherichia coli. *The Journal of biological chemistry*, *279*(43), 44590–44599. https://doi.org/10.1074/jbc.M406487200

62) Christ, S., Leichert, L. I., Willms, A., Lill, R., & Mühlenhoff, U. (2016). Defects in Mitochondrial Iron-Sulfur Cluster Assembly Induce Cysteine S-Polythiolation on Iron-Sulfur Apoproteins. *Antioxidants y redox signaling*, *25*(1), 28–40. doi.org/10.1089/ars.2015.6599

63) Sousa, J. S., D'Imprima, E., & Vonck, J. (2018). Mitochondrial Respiratory Chain Complexes. *Subcellular Biochemistry Membrane Protein Complexes: Structure and Function,* 167-227. doi:10.1007/978-981-10-7757-9_7

64) Kumari, A. (2018). Electron Transport Chain. *Sweet Biochemistry,* 13-16. doi:10.1016/b978-0-12-814453-4.00003-0

65) Wirth, C., Brandt, U., Hunte, C., & Zickermann, V. (2016). Structure and function of mitochondrial complex I. *Biochimica Et Biophysica Acta (BBA) - Bioenergetics, 1857*(7), 902-914. doi:10.1016/j.bbabio.2016.02.013

66) Velázquez, I., & Pardo, J. P. (2001). Kinetic Characterization of the Rotenone-Insensitive Internal NADH: Ubiquinone Oxidoreductase of Mitochondria from Saccharomyces cerevisiae. *Archives of Biochemistry and Biophysics, 389*(1), 7-14. doi:10.1006/abbi.2001.2293

67) Luttik, M. A., Overkamp, K. M., Kötter, P., Vries, S. D., Dijken, J. P., & Pronk, J. T. (1998). TheSaccharomyces cerevisiae NDE1andNDE2Genes Encode Separate Mitochondrial NADH Dehydrogenases Catalyzing the Oxidation of Cytosolic NADH. *Journal of Biological Chemistry, 273*(38), 24529-24534. doi:10.1074/jbc.273.38.24529

68) Trumpower, B. L., & Gennis, R. B. (1994). Energy Transduction by Cytochrome Complexes in Mitochondrial and Bacterial Respiration: The Enzymology of Coupling Electron Transfer Reactions to Transmembrane Proton Translocation. *Annual Review of Biochemistry, 63*(1), 675-716. doi:10.1146/annurev.bi.63.070194.003331

69) Wikstrom, M. K. (1977). Proton pump coupled to cytochrome c oxidase in mitochondria. *Nature, 266*(5599), 271-273. doi:10.1038/266271a0

70) Herrmann, J. M., Woellhaf, M. W., & Bonnefoy, N. (2013). Control of protein synthesis in yeast mitochondria: The concept of translational activators. *Biochimica Et Biophysica Acta (BBA) - Molecular Cell Research, 1833*(2), 286-294. doi:10.1016/j.bbamcr.2012.03.007

71) Vonck, J., & Schäfer, E. (2009). Supramolecular organization of protein complexes in the mitochondrial inner membrane. *Biochimica Et Biophysica Acta (BBA) - Molecular Cell Research, 1793*(1), 117-124. doi:10.1016/j.bbamcr.2008.05.019

72) Schagger, H. and Pfeiffer K. (2000). Supercomplexes in the respiratory chains of yeast and mammalian mitochondria. *The EMBO Journal, 19*(8), 1777-1783. doi:10.1093/emboj/19.8.1777

73) Genova, M., Baracca, A., Biondi, A., Casalena, G., Faccioli, M., Falasca, A., . . . Lenaz, G. (2008). Is supercomplex organization of the respiratory chain required for optimal electron transfer activity? *Biochimica Et Biophysica Acta (BBA) - Bioenergetics, 1777*(7-8), 740-746. doi:10.1016/j.bbabio.2008.04.007

74) Matus-Ortega, M. G., Cárdenas-Monroy, C. A., Flores-Herrera, O., Mendoza-Hernández, G., Miranda, M., González-Pedrajo, B., Pardo, J. P. (2015). New complexes containing the internal alternative NADH dehydrogenase (Ndi1) in mitochondria ofSaccharomyces cerevisiae. *Yeast, 32*(10), 629-641. doi:10.1002/yea.3086

75) Overkamp, K. M., Bakker, B. M., Kötter, P., Tuijl, A. V., Vries, S. D., Dijken, J. P., & Pronk, J. T. (2000). In Vivo Analysis of the Mechanisms for Oxidation of Cytosolic NADH by Saccharomyces cerevisiaeMitochondria. *Journal of Bacteriology, 182*(10), 2823-2830. doi:10.1128/jb.182.10.2823-2830.2000

76) Vries, S. D., & Marres, C. A. (1987). The mitochondrial respiratory chain of yeast. Structure and biosynthesis and the role in cellular metabolism. *Biochimica Et Biophysica Acta (BBA) - Reviews on Bioenergetics, 895*(3), 205-239. doi:10.1016/s0304-4173(87)80003-4

77) Vranken, J. G., Na, U., Winge, D. R., & Rutter, J. (2014). Protein-mediated assembly of succinate dehydrogenase and its cofactors. *Critical Reviews in Biochemistry and Molecular Biology, 50*(2), 168-180. doi:10.3109/10409238.2014.990556

78) Conte, A., Papa, B., Ferramosca, A., & Zara, V. (2015). The dimerization of the yeast cytochrome bc1 complex is an early event and is independent of Rip1. *Biochimica Et Biophysica Acta (BBA) - Molecular Cell Research, 1853*(5), 987-995. doi:10.1016/j.bbamcr.2015.02.006

79) Zara, V., Conte, L., & Trumpower, B. L. (2007). Identification and characterization of cytochrome bc1 subcomplexes in mitochondria from yeast with single and double deletions of genes encoding cytochrome bc1 subunits. *FEBS Journal, 274*(17), 4526-4539. doi:10.1111/j.1742-4658.2007.05982.x

80) Zara, V., Conte, L., & Trumpower, B. L. (2009). Biogenesis of the yeast cytochrome bc1 complex. *Biochimica Et Biophysica Acta (BBA) - Molecular Cell Research, 1793*(1), 89-96. doi:10.1016/j.bbamcr.2008.04.011

81) Wagener, N., Ackermann, M., Funes, S., & Neupert, W. (2011). A Pathway of Protein Translocation in Mitochondria Mediated by the AAA-ATPase Bcs1. *Molecular Cell, 44*(2), 191-202. doi:10.1016/j.molcel.2011.07.036

82) Cui, T., Smith, P. M., Fox, J. L., Khalimonchuk, O., & Winge, D. R. (2012). Late-Stage Maturation of the Rieske Fe/S Protein: Mzm1 Stabilizes Rip1 but Does Not Facilitate Its Translocation by the AAA ATPase Bcs1. *Molecular and Cellular Biology, 32*(21), 4400-4409. doi:10.1128/mcb.00441-12

83) Conte, L., Trumpower, B. L., & Zara, V. (2011). Bcs1p can rescue a large and productive cytochrome bc1 complex assembly intermediate in the inner membrane of yeast mitochondria. *Biochimica Et Biophysica Acta (BBA) - Molecular Cell Research, 1813*(1), 91-101. doi:10.1016/j.bbamcr.2010.08.004

84) Denke, E., Merbitz-Zahradnik, T., Hatzfeld, O. M., Snyder, C. H., Link, T. A., & Trumpower, B. L. (1998). Alteration of the Midpoint Potential and Catalytic Activity of the Rieske Iron-Sulfur Protein by Changes of Amino Acids Forming Hydrogen Bonds to the Iron-Sulfur Cluster. *Journal of Biological Chemistry, 273*(15), 9085-9093. doi:10.1074/jbc.273.15.9085

85) Mcstay, G. P., Su, C. H., & Tzagoloff, A. (2013). Modular assembly of yeast cytochrome oxidase. *Molecular Biology of the Cell, 24*(4), 440-452. doi:10.1091/mbc.e12-10-0749

86) , M., Sharma, V., Kaila, V. R., Hosler, J. P., & Hummer, G. (2015). New Perspectives on Proton Pumping in Cellular Respiration. *Chemical Reviews, 115*(5), 2196-2221. doi:10.1021/cr500448t

87) Ferguson-Miller, S., & Babcock, G. T. (1996). Heme/Copper Terminal Oxidases. *Chemical Reviews, 96*(7), 2889-2908. doi:10.1021/cr950051s

88) Mcstay, G. P., Su, C. H., & Tzagoloff, A. (2013). Modular assembly of yeast cytochrome oxidase. *Molecular Biology of the Cell, 24*(4), 440-452. doi:10.1091/mbc.e12-10-0749

89) Smith, D., Gray, J., Mitchell, L., Antholine, W. E., & Hosler, J. P. (2005). Assembly of Cytochrome-cOxidase in the Absence of Assembly Protein Surf1p Leads to Loss of the Active Site Heme. *Journal of Biological Chemistry, 280*(18), 17652-17656. doi:10.1074/jbc.c500061200

90) Khalimonchuk, O., Bestwick, M., Meunier, B., Watts, T. C., & Winge, D. R. (2009). Formation of the Redox Cofactor Centers during Cox1 Maturation in Yeast Cytochrome Oxidase. *Molecular and Cellular Biology, 30*(4), 1004-1017. doi:10.1128/mcb.00640-09

91) Franco, L. V., Su, C., Mcstay, G. P., Yu, G. J., & Tzagoloff, A. (2018). Cox2p of yeast cytochrome oxidase assembles as a stand-alone subunit with the Cox1p and Cox3p modules. *Journal of Biological Chemistry, 293*(43), 16899-16911. doi:10.1074/jbc.ra118.004138

92) Hell, K., Tzagoloff, A., Neupert, W., & Stuart, R. A. (2000). Identification of Cox20p, a Novel Protein Involved in the Maturation and Assembly of Cytochrome Oxidase Subunit 2. *Journal of Biological Chemistry, 275*(7), 4571-4578. doi:10.1074/jbc.275.7.4571

93) Elliott, L. E., Saracco, S. A., & Fox, T. D. (2011). Multiple Roles of the Cox20 Chaperone in Assembly ofSaccharomyces cerevisiaeCytochromecOxidase. *Genetics, 190*(2), 559-567. doi:10.1534/genetics.111.135665

94) Soto, I. C., Fontanesi, F., Liu, J., & Barrientos, A. (2012). Biogenesis and assembly of eukaryotic cytochrome c oxidase catalytic core. *Biochimica Et Biophysica Acta (BBA) - Bioenergetics, 1817*(6), 883-897. doi:10.1016/j.bbabio.2011.09.005

95) Strogolova, V., Furness, A., Robb-Mcgrath, M., Garlich, J., & Stuart, R. A. (2012). Rcf1 and Rcf2, Members of the Hypoxia-Induced Gene 1 Protein Family, Are Critical Components of the Mitochondrial Cytochrome bc1-Cytochrome c Oxidase Supercomplex. *Molecular and Cellular Biology, 32*(8), 1363-1373. doi:10.1128/mcb.06369-11

96) Strogolova, V., Hoang, N. H., Hosler, J., & Stuart, R. A. (2019). The yeast mitochondrial proteins Rcf1 and Rcf2 support the enzymology of the cytochrome c oxidase complex and generation of the proton motive force. *Journal of Biological Chemistry, 294*(13), 4867-4877. doi:10.1074/jbc.ra118.006888

97) Dawitz, H., Schäfer, J., Schaart, J. M., Magits, W., Brzezinski, P., & Ott, M. (2020). Rcf1 Modulates Cytochrome c Oxidase Activity Especially Under Energy-Demanding Conditions. *Frontiers in Physiology, 10*. doi:10.3389/fphys.2019.01555

98) Franco, L. V., Su, C. H., & Tzagoloff, A. (2020). Modular assembly of yeast mitochondrial ATP synthase and cytochrome oxidase. *Biological Chemistry, 401*(6-7), 835-853. doi:10.1515/hsz-2020-0112

99) Kagawa Y. y Racker, E. (1965). Partial Reactions Of Oxidative Phosphorylation. *Mechanisms in Bioenergetics,* 129-144. doi:10.1016/b978-0-12-574662-5.50016-x

100) Boyer, P. D. (1997). The Atp Synthase—A Splendid Molecular Machine. *Annual Review of Biochemistry, 66*(1), 717-749. doi:10.1146/annurev.biochem.66.1.717

101) Stock, D., Gibbons, C., Arechaga, I., Leslie, A. G., & Walker, J. E. (2000). The rotary mechanism of ATP synthase. *Current Opinion in Structural Biology, 10*(6), 672-679. doi:10.1016/s0959-440x(00)00147-0

102) Macreadie, I. G., Novitski, C. E., Maxwell, R. J., John, U., Ooi, B., Mcmullen, G. L., Nagley, P. (1983). Biogenesis of mitochondria: The mitochondrial gene (aap1) coding for mitochondrial ATPase subunit 8 inSaccharomyces cerevisiae. *Nucleic Acids Research, 11*(13), 4435-4451. doi:10.1093/nar/11.13.4435

103) Fillingame, R. H., & Dmitriev, O. Y. (2002). Structural model of the transmembrane Fo rotary sector of H+-transporting ATP synthase derived by solution NMR and intersubunit cross-linking in situ. *Biochimica Et Biophysica Acta (BBA) - Biomembranes, 1565*(2), 232-245. doi:10.1016/s0005-2736(02)00572-2

104) Stock, D. Andrew G. W. Leslie, John E. Walker (1999). Molecular Architecture of the Rotary Motor in ATP Synthase. *Science, 286*(5445), 1700-1705. doi:10.1126/science.286.5445.1700

105) Walker, J. E., & Dickson, V. K. (2006). The peripheral stalk of the mitochondrial ATP synthase. *Biochimica Et Biophysica Acta (BBA) - Bioenergetics, 1757*(5-6), 286-296. doi:10.1016/j.bbabio.2006.01.001

106) Davies, K. M., Anselmi, C., Wittig, I., Faraldo-Gomez, J. D., & Kuhlbrandt, W. (2012). Structure of the yeast F1Fo-ATP synthase dimer and its role in shaping the mitochondrial cristae. *Proceedings of the National Academy of Sciences, 109*(34), 13602-13607. doi:10.1073/pnas.1204593109

107) Davies, K. M., Strauss, M., Daum, B., Kief, J. H., Osiewacz, H. D., Rycovska, A., Kuhlbrandt, W. (2011). Macromolecular organization of ATP synthase and complex I in whole mitochondria. *Proceedings of the National Academy of Sciences, 108*(34), 14121-14126. doi:10.1073/pnas.1103621108

108) Blum, T. B., Hahn, A., Meier, T., Davies, K. M., & Kühlbrandt, W. (2019). Dimers of mitochondrial ATP synthase induce membrane curvature and self-assemble into rows. *Proceedings of the National Academy of Sciences, 116*(10), 4250-4255. doi:10.1073/pnas.1816556116

109) Netz, D. J., Mascarenhas, J., Stehling, O., Pierik, A. J., & Lill, R. (2014). Maturation of cytosolic and nuclear iron–sulfur proteins. *Trends in Cell Biology, 24*(5), 303-312. doi:10.1016/j.tcb.2013.11.005

110) Andreini, C., Banci, L., Rosato A. (2016). **Exploiting bacterial operons to illuminate human iron-sulfur proteins.** J Proteome Res ;15(4):1308-22. doi: 10.1021/acs.jproteome.6b00045. Epub 2016 Mar 2.

111) Stehling, O., & Lill, R. (2013). The Role of Mitochondria in Cellular Iron-Sulfur Protein Biogenesis: Mechanisms, Connected Processes, and Diseases. *Cold Spring Harbor Perspectives in Biology, 5*(8). doi:10.1101/cshperspect.a011312

112) Beilschmidt, L. K., Choudens, S. O., Fournier, M., Sanakis, I., Hograindleur, M., Clémancey, M., Martelli, A. (2017). ISCA1 is essential for mitochondrial Fe4S4 biogenesis in vivo. *Nature Communications, 8*(1). doi:10.1038/ncomms15124

113) Gourdoupis S, Nasta V, Calderone V, Ciofi-Baffoni S, Banci L. IBA57 Recruits ISCA2 to Form a [2Fe-2S] Cluster-Mediated Complex. J Am Chem Soc. 2018 Oct 31;140(43):14401-14412.

114) Outten, F.W., Djaman, O. and Storz, G. (2004), A *suf* operon requirement for Fe–S cluster assembly during iron starvation in *Escherichia coli*. Molecular Microbiology, 52: 861-872. https://doi.org/10.1111/j.1365-2958.2004.04025.x

115) DeLuna, A., Avendano, A., Riego, L., & Gonzalez, A. (2001). NADP-glutamate dehydrogenase isoenzymes of Saccharomyces cerevisiae. Purification, kinetic properties, and physiological roles. *The Journal of biological chemistry*, *276*(47), 43775–43783.

116) Cupp, J. R., & McAlister-Henn, L. (1991). NAD(+)-dependent isocitrate dehydrogenase. Cloning, nucleotide sequence, and disruption of the IDH2 gene from Saccharomyces cerevisiae. *The Journal of biological chemistry*, *266*(33), 22199–22205.

117) Cupp, J. R., & McAlister-Henn, L. (1992). Cloning and characterization of the gene encoding the IDH1 subunit of NAD(+)-dependent isocitrate dehydrogenase from Saccharomyces cerevisiae. *The Journal of biological chemistry*, *267*(23), 16417–16423.Gisela Storz

118) Hansen T. A. (1994). Metabolism of sulfate-reducing prokaryotes. *Antonie van Leeuwenhoek*, *66*(1-3), 165–185. https://doi.org/10.1007/BF00871638

119) Thomas, D., & Surdin-Kerjan, Y. (1997). Metabolism of sulfur amino acids in Saccharomyces cerevisiae. *Microbiology and molecular biology reviews : MMBR*, *61*(4), 503–532.

120) Wen, Z. H., Gardener, E., & Wang, Y. P. (2004). Nitrates for achalasia. *The Cochrane database of systematic reviews*, *2004*(1), CD002299. https://doi.org/10.1002/14651858.CD002299.pub2

121) Jamieson D. J. (1998). Oxidative stress responses of the yeast Saccharomyces cerevisiae. *Yeast (Chichester, England)*, *14*(16), 1511–1527. https://doi.org/10.1002/(SICI)1097-0061(199812)14:16<1511::AID-YEA356>3.0.CO;2-S

122) Jensen, L. T., & Culotta, V. C. (2000). Role of Saccharomyces cerevisiae ISA1 and ISA2 in iron homeostasis. *Molecular and cellular biology*, *20*(11), 3918–3927. https://doi.org/10.1128/mcb.20.11.3918-3927.2000

123) Reisinger, V., & Eichacker, L. A. (2008). Solubilization of membrane protein complexes for blue native PAGE. *Journal of proteomics*, *71*(3), 277–283. https://doi.org/10.1016/j.jprot.2008.05.004

124) Suhai, T., Heidrich, N. G., Dencher, N. A., & Seelert, H. (2009). Highly sensitive detection of ATPase activity in native gels. *Electrophoresis*, *30*(20), 3622–3625. https://doi.org/10.1002/elps.200900114

125) Macreadie, I. G., Novitski, C. E., Maxwell, R. J., John, U., Ooi, B. G., McMullen, G. L., Lukins, H. B., Linnane, A. W., & Nagley, P. (1983). Biogenesis of mitochondria: the mitochondrial gene (aap1) coding for mitochondrial ATPase subunit 8 in Saccharomyces cerevisiae. *Nucleic acids research*, *11*(13), 4435–4451. https://doi.org/10.1093/nar/11.13.4435

126) Suhai, T., Heidrich, N. G., Dencher, N. A., & Seelert, H. (2009). Highly sensitive detection of ATPase activity in native gels. *Electrophoresis*, *30*(20), 3622–3625. https://doi.org/10.1002/elps.200900114

9. Anexos.

Artículos como coautor dentro del periodo del programa de doctorado 2016-2020.

molecules MDPI

Article

The Antiproliferative Effect of Cyclodipeptides from *Pseudomonas aeruginosa* PAO1 on HeLa Cells Involves Inhibition of Phosphorylation of Akt and S6k Kinases

Laura Hernández-Padilla [1], Dolores Vázquez-Rivera [1], Luis A. Sánchez-Briones [1], Alma L. Díaz-Pérez [1], José Moreno-Rodríguez [2], Mario A. Moreno-Eutimio [2], Victor Meza-Carmen [1], Homero Reyes-De la Cruz [3] and Jesús Campos-García [1,*]

1 Laboratorio de Biotecnología Microbiana, Instituto de Investigaciones Químico-Biológicas, Universidad Michoacana de San Nicolás de Hidalgo, 58030 Morelia, Michoacán, Mexico; laura_190589@hotmail.com (L.H.-P.); dolores_vazquez1001@hotmail.com (D.V.-R.); biol.luis.22@gmail.com (L.A.S.-B.); aldiaz07@yahoo.com (A.L.D.-P.); victor_meza2004@yahoo.com.mx (V.M.-C.)

2 División de Investigación, Hospital Juárez de México, 07760 Ciudad de México, Mexico; jmoreno49@gmail.com (J.M.-R.); marioadan@inmunoquimica.com (M.A.M.-E.)

3 Laboratorio de Control Traduccional, Instituto de Investigaciones Químico-Biológicas, Universidad Michoacana de San Nicolás de Hidalgo, 58030 Morelia, Michoacán, Mexico; delacruz@umich.mx

* Correspondence: jcgarcia@umich.mx; Tel.: +52-443326-5788

Received: 29 May 2017; Accepted: 16 June 2017; Published: 20 June 2017

Abstract: *Pseudomonas aeruginosa* PAO1, a potential pathogen of plants and animals, produces the cyclodipeptides cyclo(L-Pro-L-Tyr), cyclo(L-Pro-L-Phe), and cyclo(L-Pro-L-Val) (PAO1-CDPs), whose effects have been implicated in inhibition of human tumor cell line proliferation. Our purpose was to investigate in depth in the mechanisms of HeLa cell proliferation inhibition by the PAO1-CDPs. The results indicate that PAO1-CDPs, both purified individually and in mixtures, inhibited HeLa cell proliferation by arresting the cell cycle at the G0–G1 transition. The crude PAO1-CDPs mixture promoted cell death in HeLa cells in a dose-dependent manner, showing efficacy similar to that of isolated PAO1-CDPs (LD_{50} of 60–250 µM) and inducing apoptosis with EC_{50} between 0.6 and 3.0 µM. Moreover, PAO1-CDPs showed a higher proapoptotic activity (~10^3–10^5 fold) than their synthetic analogs did. Subsequently, the PAO1-CDPs affected mitochondrial membrane potential and induced apoptosis by caspase-9-dependent pathway. The mechanism of inhibition of cells proliferation in HeLa cells involves inhibition of phosphorylation of both Akt-S473 and S6k-T389 protein kinases, showing a cyclic behavior of their expression and phosphorylation in a time and concentration-dependent fashion. Taken together our findings indicate that PI3K–Akt–mTOR–S6k signaling pathway blockage is involved in the antiproliferative effect of the PAO1-CDPs.

Journal of Industrial Microbiology & Biotechnology
https://doi.org/10.1007/s10295-019-02175-5

SIMB
Society for Industrial Microbiology and Biotechnology

FERMENTATION, CELL CULTURE AND BIOENGINEERING - ORIGINAL PAPER

Over-expression of Isu1p and Jac1p increases the ethanol tolerance and yield by superoxide and iron homeostasis mechanism in an engineered *Saccharomyces cerevisiae* yeast

Lorena Martínez-Alcántar[1] · Alberto Madrigal[1,2] · Luis Sánchez-Briones[1] · Alma L. Díaz-Pérez[1] · Jesús Salvador López-Bucio[3] · Jesús Campos-García[1]

Received: 5 February 2019 / Accepted: 3 April 2019

Abstract

The ethanol stress response in ethanologenic yeast during fermentation involves the swishing of several adaptation mechanisms. In *Saccharomyces cerevisiae*, the Jac1p and Isu1p proteins constitute the scaffold system for the Fe–S cluster assembly. This study was performed using the over-expression of the Jac1p and Isu1p in the industrially utilized *S. cerevisiae* UMArn3 strain, with the objective of improving the Fe–S assembly/recycling, and thus counteracting the toxic effects of ethanol stress during fermentation. The UMArn3 yeast was transformed with both the *JAC1*-His and *ISU1*-His genes-plasmid contained. The Jac1p and Isu1p His-tagged proteins over-expression in the engineered yeasts was confirmed by immunodetection, rendering increases in ethanol tolerance level from a DL_{50} = ~ 4.5% ethanol (v/v) to DL_{50} = ~ 8.2% ethanol (v/v), and survival up 90% at 15% ethanol (v/v) comparing to ~ 50% survival in the control strain. Fermentation by the engineered yeasts showed that the ethanol production was increased, producing 15–20% more ethanol than the control yeast. The decrease of ROS and free-iron accumulation was observed in the engineered yeasts under ethanol stress condition. The results indicate that Jac1p and Isu1p over-expression in the *S. cerevisiae* UMArn3.3 yeast increased its ethanol tolerance level and ethanol production by a mechanism that involves ROS and iron homeostasis related to the biogenesis/recycling of Fe–S clusters dependent proteins.

The Journal of Membrane Biology
https://doi.org/10.1007/s00232-020-00129-y

Nicorandil Affects Mitochondrial Respiratory Chain Function by Increasing Complex III Activity and ROS Production in Skeletal Muscle Mitochondria

E. Sánchez-Duarte[1] · C. Cortés-Rojo[2] · L. A. Sánchez-Briones[2] · J. Campos-García[2] · A. Saavedra-Molina[2] · I. Delgado-Enciso[3] · U. A. López-Lemus[4] · R. Montoya-Pérez[2]

Received: 23 January 2020 / Accepted: 23 June 2020

Abstract

Adenosine triphosphate (ATP)-dependent potassium channels openers (K_{ATP}) protect skeletal muscle against function impairment through the activation of the mitochondrial K_{ATP} channels (mitoK_{ATP}). Previous reports suggest that modulators of the mitochondrial K_{ATP} channels have additional effects on isolated mitochondria. To determine whether the K_{ATP} channel opener nicorandil has non-specific effects that explain its protective effect through the mitochondrial function, chicken muscle mitochondria were isolated, and respiration rate was determined pollarographically. The activity of the electron transport chain (ETC) complexes (I–IV) was measured using a spectrophotometric method. Reactive oxygen species (ROS) levels and lipid peroxidation were assessed using flow cytometry and thiobarbituric acid assay, respectively. Both K_{ATP} channel opener nicorandil and K_{ATP} channel blocker 5-hydroxydecanoate (5-HD) decreased mitochondrial respiration; nicorandil increased complex III activity and decreased complex IV activity. The effects of nicorandil on complex III were antagonized by 5-HD. Nicorandil increased ROS levels, effect reverted by either 5-HD or the antioxidant N-2-mercaptopropionyl glycine (MPG). None of these drugs affected lipid peroxidation levels. These findings suggest that K_{ATP} channel opener nicorandil increases mitochondrial ROS production from complex III. This results by partially blocking electron flow in the complex IV, setting electron carriers in a more reduced state, which is favored by the increase in complex III activity by nicorandil. Overall, our study showed that nicorandil like other mitochondrial K_{ATP} channel openers might not act through mitoK_{ATP} channel activation.

Graphic Abstract

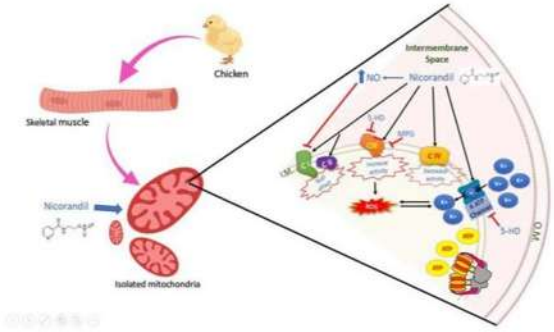

Keywords Mitochondria · mitoK_{ATP} channel · Skeletal muscle · Nicorandil · Reactive oxygen species